

Limiting Factors of Nitrate Removal in Mesoscale
Denitrifying Wood Chip Bioreactors

A Thesis
SUBMITTED TO THE FACULTY OF THE
UNIVERSITY OF MINNESOTA
BY

Nadine Hackshaw

IN PARTIAL FULFILLMENT OF THE
REQUIREMENTS
FOR THE DEGREE OF
MASTER OF SCIENCE

Sebastian Behrens

April 2018

Nadine Hackshaw

Copyright 2018

Acknowledgements

This research was made possible through funding provided by the MnDRIVE initiative. I would like to thank everyone who helped me along the way. In particular, I would like to extend a special thank you to Dr. Lori Krider and Dr. Bruce Wilson who designed and implemented the bioreactor experimental set-up and provided insight and support throughout the length of our collaboration together, Michael Brown for his help with sampling and for completing 400 DNA extractions, Matt Galloway for directing my efforts in data “tidying” and for executing multivariate statistical analysis, and my committee members Dr. Satoshi Ishii, Dr. Paige Novak, and Dr. Sebastian Behrens who had the fortitude to revise this work. I would especially like to thank my advisor, Dr. Sebastian Behrens, for all the help and guidance he has provided along the way. Lastly, thanks to my wonderful wife, Brittany Hackshaw, for her help, support and patience throughout this process. I would not be here today without you. Thank you!



Abstract

The use of woodchip denitrifying bioreactors holds promise as a simple, efficient and cost-effective system to reduce nitrate loads in agricultural runoff through stimulation of microbial denitrification. While bioreactor performance at colder temperatures and under varying hydraulic residence time (HRT) has been investigated, the correlation to functional microbial communities has not been studied in great detail. In this study, we quantified denitrifying functional gene copy numbers throughout the course of a three-month study within mesoscale [1.83m x 0.3m x 0.61m] denitrification bioreactors that were operated at three temperature regimes and two HRT. We found that with increasing temperature and HRT there was a significant increase in percent nitrate removed. Temperature and HRT had little effect on *nirK* and *nosZ* clade I gene copy numbers throughout the length of the bioreactors, however, they had a significant effect on 16S rRNA and *nosZ* clade II gene copy numbers at the inflow locations of the bioreactors. Utilizing a hydraulic flow model developed for the denitrifying bioreactors in this study, a decrease in nitrate concentration along the length of the reactors was calculated. We correlated a decrease in 16S rRNA, *nirK* and *nosZ* clade II gene copy numbers to the decrease in nitrate concentrations predicted by the hydraulic flow model. Our results suggest that at temperatures of 14.5°C and 12-hr HRT, denitrifying bioreactor microbial communities are limited by variables other than temperature and HRT. It is suggested that carbon availability is the most likely limiting factor, indicating a need to further investigate the role of both denitrifying and decomposing communities in denitrifying bioreactors. These findings contribute to a better understanding of the microbial functional

communities in denitrifying wood chip bioreactors, allowing us to optimize the design and performance of these reactors in agricultural midwestern states.

Table of Contents

List of Tables	vii
List of Figures	viii
Introduction.....	1
Methods.....	8
Chemicals	8
Bioreactor Experimental Set Up	8
Experimental Design	8
Construction of Triplicate Bioreactor Troughs	8
Construction of Climate Controlled Chambers	11
Bioreactor Media	12
Plants	14
Bioreactor Media Sampling Bag Design and Construction.....	15
Analytics.....	17
Water Sample Collection from Bioreactors.....	17
Bioreactor Media Sampling Bag Collection.....	18
Nitrite and Ammonia Measurements.....	19
DOC Measurements	20
Sulfide Measurements	20
Nitrate Measurements.....	21
pH, DO and ORP Measurements.....	21
Phosphate Measurements	22
Nitrous Oxide and Methane Collection and Analysis	22
Bromide Tracer Tests and Hydraulic Modeling	23
DNA Extractions	23
Qubit	24
Primers.....	24
gBlock Standards.....	25
Real-time Polymerase Chain Reaction (qPCR).....	26
Statistics	27
Results.....	28
Chemical Data	28
Percent Nitrate Removed (Nitrate Removal Efficiency).....	28
Nitrate Removal Rate	30

Dissolved Organic Carbon (DOC)	32
Dissolved Oxygen (DO)	34
Oxidative-Reductive Potential (ORP)	35
Nitrous Oxide	36
Percent Phosphate Removed	38
pH	39
Ammonia	40
Nitrite.....	41
Sulfide.....	41
Methane	41
Nitrate Concentration Along Bioreactor Length	42
Biological Data.....	43
16S rRNA	46
nirK (Nitrite Reductase)	51
nirS (Nitrite Reductase)	56
nosZ Clade I (Typical Nitrous Oxide Reductase)	59
nosZ Clade II (Atypical Nitrous Oxide Reductase).....	61
Multivariate Analysis	66
Discussion	70
Chemical Data	70
Percent Nitrate Removed (Nitrate Removal Efficiency)	70
Nitrate Removal Rate ($\text{g-N m}^{-3}\text{d}^{-1}$).....	71
Dissolved Organic Carbon (DOC)	73
Dissolved Oxygen (DO)	75
Nitrous Oxide Emissions	76
Phosphate Removal Efficiency.....	77
pH	78
Ammonia and Nitrite	79
Sulfide and Methane.....	80
Nitrate Concentrations Along Bioreactor Length.....	81
Biological Data.....	82
16S rRNA	82
Nitrite Reductase (nirK and nirS).....	84
Nitrous Oxide Reductase (nosZ clade I and clade II).....	87

Linking the Bacterial Community and Bioreactor Performance.....	91
Nitrate Removal Efficiency and Nitrate Removal Rate	91
Nitrate Concentration	92
DOC/C Availability.....	94
Dissolved Oxygen (DO)	96
Biochar.....	97
Outlook	101
Conclusion	105
References.....	108
Appendix A: Walnut Shell Biochar Characterization.....	114
Appendix B: Additional Chemical Parameters of Bioreactor Troughs	116
Appendix C: Additional Biological Data for Bioreactor Troughs.....	122

List of Tables

Table 1: Artificial agricultural runoff composition and concentrations used as bioreactor influent media	10
Table 2: Genes, primers, sequences and references used to quantify total bacteria and functional denitrifying gene copy numbers using qPCR.	24
Table 3: gBlock standard sequences and sources used to quantify gene copy numbers of bioreactor samples by qPCR.	25
Table 4: Reaction mixtures and thermal profile of qPCR reactions performed for each target gene. Total volume for each reaction mixture was 10 µL.	26
Table 5: p-values of comparisons to show the effect of cool (6°C, weeks 1-4) and warm (14.5°C, weeks 9-12) temperature regimes, and 12-hour and 4-hour hydraulic residence time (HRT) on 16S rRNA, nirK, nirS, nosZ clade I (1) and nosZ clade II (2) gene copy numbers at inflow (I), middle (M) and outflow (O) sampling locations (post-hoc t-tests). Highlighted values indicate a significant correlation.	43
Table 6: p-values showing the effect of location between inflow, middle and outflow sampling locations for 16S rRNA, nirK, nirS, nosZ clade I (1) and nosZ clade II (2) under cool (6°C, weeks 1-4) and warm (14.5°C, weeks 9-12) temperature regimes and 12-hour and 4-hour hydraulic residence time (HRT) (post hoc, t-tests). Highlighted values indicate a significant correlation.	45
Table 7: Walnut shell biochar physical and chemical properties along with recommendations from the International Biochar Initiative (IBI) and the European Biochar Certificate (EBC).	114

List of Figures

Figure 1: Schematic of experimental design. Three replicate bioreactor troughs in climate controlled chambers operated under 12 and 4-hour hydraulic residence time (HRT) and under three temperature regimes.....	9
Figure 2: Diagram of a climate controlled chamber containing triplicate bioreactor troughs. Each chamber had an air conditioning unit, growth lights, air holes, and flow meters for each replicate bioreactor trough.	11
Figure 3: Profile view of one trough of the triplicate bioreactor troughs. Three rigid mesh sampling tubes were placed in each trough to allow microbial sampling throughout the experiment. Sampling tubes were filled with twelve sampling bags and one soil bag. One sampling bag from each sampling tube was removed and replaced each week for microbial analysis. An aluminum gas sampling container was placed on top of the soil at the end of each bioreactor trough. Gas samples were collected from this container each week. Grasses were planted in the soil along the remaining length of each bioreactor trough.	12
Figure 4: Picture of triplicate bioreactor troughs inside a climate controlled chamber. Six grasses were planted along the length of each bioreactor trough. Each replicate bioreactor trough had three sampling tubes placed along its length and an aluminum gas collection container at the end of its length. An air conditioner was installed in each climate controlled chamber and the water was chilled in a nearby tank to maintain accurate water and ambient temperatures.	13
Figure 5: Schematic of a rigid mesh sampling tube containing twelve sampling bags attached to a string. Sampling bags were used to obtain bioreactor media samples throughout the length of the experiment. The top-most bag was a sampling bag filled with soil.....	16
Figure 6: Picture from inside one replicate bioreactor trough showing three sampling tubes along the length of the reactor. The picture was taken while bioreactor troughs were still being filled with the bioreactor media mix. Sampling bags can be seen inside the sampling tubes.	17
Figure 7: Percent nitrate removed over time for 12-hour and 4-hour hydraulic residence time (HRT). Temperature regime is indicated by background color. Blue indicates cool (6°C weeks 1-4), purple designates warming (+2.1°C each week, weeks 5-8) and red denotes warm (14.5°C, weeks 9-12) temperature regime.	28
Figure 8: Effect of temperature and hydraulic residence time (HRT) on the percent nitrate removed for 12-hour and 4-hour HRT for both cool (6°C, weeks 1-4) and warm (14.5°C, weeks 9-12) temperature regimes. Identical letters indicate no significant difference, while different letters denote a significant difference (two-way ANOVA; $p < 0.05$).	29
Figure 9: Nitrogen removed over time ($\text{gm}^{-3}\text{d}^{-1}$) for 12-hour and 4-hour hydraulic residence time (HRT). Temperature regime is indicated by background color. Blue indicates cool (6°C weeks 1-4), purple designates warming (+2.1°C each week, weeks 5-8) and red denotes warm (14.5°C, weeks 9-12) temperature regime.....	30
Figure 10: Effect of temperature and hydraulic residence time (HRT) on $\text{g-N m}^{-3} \text{d}^{-1}$ removed for 12-hour and 4-hour HRT for both cool (6°C, weeks 1-4) and warm (14.5°C, weeks 9-12) temperature regimes. Identical letters indicate no statistically significant difference, different letters denote statistical significance (two-way ANOVA; $p < 0.05$).	31

Figure 11: Dissolved organic carbon (DOC) over time for 12-hour and 4-hour hydraulic residence time (HRT) and influent. Temperature regime is indicated by background color. Blue indicates cool (6°C weeks 1-4), purple designates warming (+2.1°C each week, weeks 5-8) and red denotes warm (14.5°C, weeks 9-12) temperature regime.	32
Figure 12: Effect of temperature and hydraulic residence time (HRT) on the dissolved organic carbon (DOC) produced for cool (6°C, weeks 1-4) and warm (14.5°C, weeks 9-12) temperature regimes. Produced DOC was calculated by subtracting the weekly influent values from the weekly effluent values of the corresponding bioreactor trough at the same time point and averaging these values across HRT and temperature treatments. Identical letters indicate no significant difference, different letters denote a significant difference (two-way ANOVA; $p < 0.05$).	33
Figure 13: Dissolved oxygen (DO) concentration over time for 12-hour and 4-hour hydraulic residence time (HRT) and influent. Temperature regime is indicated by background color. Blue indicates cool (6°C weeks 1-4), purple designates warming (+2.1°C each week, weeks 5-8) and red denotes warm (14.5°C, weeks 9-12) temperature regime.	34
Figure 14: Nitrous oxide emissions over time for 12-hour and 4-hour hydraulic residence time (HRT). Temperature regime is indicated by background color. Blue indicates cool (6°C weeks 1-4), purple designates warming (+2.1°C each week, weeks 5-8) and red denotes warm (14.5°C, weeks 9-12) temperature regime.	36
Figure 15: Effect of temperature and hydraulic residence time (HRT) on nitrous oxide emissions for 12-hour and 4-hour HRT for both cool (6°C, weeks 1-4) and warm (14.5°C, weeks 9-12) temperature regimes. Identical letters indicate no statistically significant difference, different letters denote statistical significance (two-way ANOVA; $p < 0.05$).	37
Figure 16: Percent phosphate removed over time for 12-hour and 4-hour hydraulic residence time (HRT). Temperature regime is indicated by background color. Blue indicates cool (6°C weeks 1-4), purple designates warming (+2.1°C each week, weeks 5-8) and red denotes warm (14.5°C, weeks 9-12) temperature regime.	38
Figure 17: Effect of temperature and hydraulic residence time (HRT) on percent phosphate removed for 12-hour and 4-hour HRT and for both cool (6°C, weeks 1-4) and warm (14.5°C, weeks 9-12) temperature regimes. Identical letters indicate no statistically significant difference, different letters denote statistical significance (two-way ANOVA; $p < 0.05$).	39
Figure 18: Concentration of nitrate by sampling port along the length of the reactor for 12-hour and 4-hour HRT under cool (6°C, weeks 1-4) and warm (14.5°C, weeks 9-12) temperature regimes. Nitrate concentrations were modeled using the hydraulic model developed by (Krider, 2018). Identical letters indicate a significant difference, while similar letters indicate no difference (three-way ANOVA; $p < 0.05$).	42
Figure 19: 16S rRNA gene copy number per gram of wet bioreactor media over time for 12-hour hydraulic residence time (HRT) and 4-hour HRT inflow, middle and outflow sampling locations. Temperature regime is indicated by background color. Blue indicates cool (6°C weeks 1-4), purple designates warming (+2.1°C each week, weeks 5-8) and red denotes warm (14.5°C, weeks 9-12) temperature regime.	46
Figure 20: Effect of location and hydraulic residence time (HRT) on 16S rRNA gene copy numbers during the cool (6°C, weeks 1-4) temperature regime for 12-hour and 4-	

hour HRT and for inflow, middle and outflow sampling locations. Identical letters indicate no statistically significant difference, different letters denote statistical significance (two-way ANOVA; $p < 0.05$).....	47
Figure 21: Effect of location and hydraulic residence time (HRT) on 16S rRNA gene copy numbers during the warm (14.5°C, weeks 9-12) temperature regime for 12-hour and 4-hour HRT and for inflow, middle and outflow sampling locations. Identical letters indicate no statistically significant difference, different letters denote statistical significance (two-way ANOVA; $p < 0.05$).....	48
Figure 22: Effect of location and temperature regime on 16S rRNA gene copy numbers during 12-hour hydraulic residence time (HRT) for cool (6°C, weeks 1-4) and warm (14.5°C, weeks 9-12) temperature regimes and for inflow, middle and outflow sampling locations. Identical letters indicate no statistically significant difference, different letters denote statistical significance (two-way ANOVA; $p < 0.05$).....	49
Figure 23: Effect of location and temperature regime on 16S rRNA gene copy numbers during 4-hour hydraulic residence time (HRT) for cool (6°C, weeks 1-4) and warm (14.5°C, weeks 9-12) temperature regimes and for inflow, middle and outflow sampling locations. Identical letters indicate no statistically significant difference, different letters denote statistical significance (two-way ANOVA; $p < 0.05$).....	50
Figure 24: nirK gene copy number per gram of wet bioreactor media over time for 12-hour hydraulic residence time (HRT) and 4-hour HRT inflow, middle and outflow sampling locations. Temperature regime is indicated by background color. Blue indicates cool (6°C weeks 1-4), purple designates warming (+2.1°C each week, weeks 5-8) and red denotes warm (14.5°C, weeks 9-12) temperature regime.	51
Figure 25: Effect of location and hydraulic residence time (HRT) on nirK gene copy numbers during the cool temperature regime (6°C, weeks 1-4) for 12-hour and 4-hour HRT and for inflow, middle and outflow sampling locations. Identical letters indicate no statistically significant difference, different letters denote statistical significance (two-way ANOVA; $p < 0.05$).....	52
Figure 26: Effect of location and hydraulic residence time (HRT) on nirK gene copy numbers during the warm temperature regime (14.5°C, weeks 9-12) for 12-hour and 4-hour HRT and for inflow, middle and outflow sampling locations. Identical letters indicate no statistically significant difference, different letters denote statistical significance (two-way ANOVA; $p < 0.05$).....	53
Figure 27: Effect of location and temperature regime on nirK gene copy numbers during 12-hour hydraulic residence time (HRT) for cool (6°C, weeks 1-4) and warm (14.5°C, weeks 9-12) temperature regimes and for inflow, middle and outflow sampling locations. Identical letters indicate no statistically significant difference, different letters denote statistical significance (two-way ANOVA; $p < 0.05$).....	54
Figure 28: Effect of location and temperature regime on nirK gene copy numbers during 4-hour hydraulic residence time (HRT) for cool (6°C, weeks 1-4) and warm (14.5°C, weeks 9-12) temperature regimes and for inflow, middle and outflow sampling locations. Identical letters indicate no statistically significant difference, different letters denote statistical significance (two-way ANOVA; $p < 0.05$).....	55
Figure 29: nirS gene copy number per gram of wet bioreactor media over time for 12-hour hydraulic residence time (HRT) and 4-hour HRT inflow, middle and outflow sampling locations. Temperature regime is indicated by background color. Blue indicates	

cool (6°C weeks 1-4), purple designates warming (+2.1°C each week, weeks 5-8) and red denotes warm (14.5°C, weeks 9-12) temperature regime.	56
Figure 30: Effect of location and hydraulic residence time (HRT) on nirS gene copy numbers during the cool (6°C, weeks 1-4) temperature regime for 12-hour and 4-hour HRT and for inflow, middle and outflow sampling locations. Identical letters indicate no statistically significant difference, different letters denote statistical significance (two-way ANOVA; $p < 0.05$).	57
Figure 31: Effect of location and temperature regime on nirS gene copy numbers during 4-hour hydraulic residence time (HRT) for cool (6°C, weeks 1-4) and warm (14.5°C, weeks 9-12) temperature regimes and for inflow, middle and outflow sampling locations. Identical letters indicate no statistically significant difference, different letters denote statistical significance (two-way ANOVA; $p < 0.05$).	58
Figure 32: nosZ clade I gene copy number per gram of wet bioreactor media over time for 12-hour hydraulic residence time (HRT) and 4-hour HRT inflow, middle and outflow sampling locations. Temperature regime is indicated by background color. Blue indicates cool (6°C weeks 1-4), purple designates warming (+2.1°C each week, weeks 5-8) and red denotes warm (14.5°C, weeks 9-12) temperature regime.	59
Figure 33: Effect of location and temperature regime on nosZ clade I gene copy numbers during 4-hour hydraulic residence time (HRT) for cool (6°C, weeks 1-4) and warm (14.5°C, weeks 9-12) temperature regimes and for inflow, middle and outflow sampling locations. Identical letters indicate no statistically significant difference, different letters denote statistical significance (two-way ANOVA; $p < 0.05$).	60
Figure 34: nosZ clade II gene copy number per gram of wet bioreactor media over time for 12-hour hydraulic residence time (HRT) and 4-hour HRT inflow, middle and outflow sampling locations. Temperature regime is indicated by background color. Blue indicates cool (6°C weeks 1-4), purple designates warming (+2.1°C each week, weeks 5-8) and red denotes warm (14.5°C, weeks 9-12) temperature regime.	61
Figure 35: Effect of location and hydraulic residence time (HRT) on nosZ clade II gene copy numbers during the cool (6°C, weeks 1-4) temperature regime for 12-hour and 4-hour HRT and for inflow, middle and outflow sampling locations. Identical letters indicate no statistically significant difference, different letters denote statistical significance (two-way ANOVA; $p < 0.05$).	62
Figure 36: Effect of location and hydraulic residence time (HRT) on nosZ clade II gene copy numbers during the warm (14.5°C, weeks 9-12) temperature regime for 12-hour and 4-hour HRT and for inflow, middle and outflow sampling locations. Identical letters indicate no statistically significant difference, different letters denote statistical significance (two-way ANOVA; $p < 0.05$).	63
Figure 37: Effect of location and temperature regime on nosZ clade II gene copy numbers during 12-hour hydraulic residence time (HRT) for cool (6°C, weeks 1-4) and warm (14.5°C, weeks 9-12) temperature regimes and for inflow, middle and outflow sampling locations. Identical letters indicate no statistically significant difference, different letters denote statistical significance (two-way ANOVA; $p < 0.05$).	64
Figure 38: Effect of location and temperature regime on nosZ clade II gene copy numbers during 4-hour hydraulic residence time (HRT) for cool (6°C, weeks 1-4) and warm (14.5°C, weeks 9-12) temperature regimes and for inflow, middle and outflow sampling	

locations. Identical letters indicate no statistically significant difference, different letters denote statistical significance (two-way ANOVA; $p < 0.05$).	65
Figure 39: Principle component analysis (PCA) plot of the chemical and biological parameters measured in this study. Points in close proximity to one another indicate a strong correlation, points at a great distance from one another denote a low correlation. 66	
Figure 40: Whisker plot of percent nitrate removed by 12-hour and 4-hour hydraulic residence times (HRT).	67
Figure 41: Effect of temperature ($^{\circ}\text{C}$) on percent nitrate removal for 12-hour and 4-hour hydraulic residence times (HRT) using a linear mixed effects model ($p < 0.05$).	68
Figure 42: Percent nitrate removed over time for 12-hour and 4-hour hydraulic residence time (HRT) using a linear mixed effects model ($p < 0.05$).	69
Figure 43: Effect of temperature and hydraulic residence time (HRT) on the change in dissolved oxygen (DO). Change in DO saturation was calculated by subtracting daily influent values from daily effluent values for each bioreactor trough and obtaining the average of these values across the different temperature and HRT treatments. Identical letters indicate no significant difference, while different letters denote a significant difference (two-way ANOVA; $p < 0.05$).	116
Figure 44: Oxidative-reductive potential (ORP) over time for inflow, 12-hour and 4-hour hydraulic residence time (HRT). Temperature regime is indicated by background color. Blue indicates cool (6°C weeks 1-4), purple designates warming ($+2.1^{\circ}\text{C}$ each week, weeks 5-8) and red denotes warm (14.5°C , weeks 9-12) temperature regime.	117
Figure 45: Effect of temperature and hydraulic residence time (HRT) on the change in oxidative-reductive potential (ORP) for 12-hour and 4-hour HRT for both cool (6°C , weeks 1-4) and warm (14.5°C , weeks 9-12) temperature regimes. Change in ORP was calculated by subtracting daily influent values from daily effluent values for each bioreactor trough and obtaining the average of these values across the different temperature and HRT treatments. Identical letters indicate no statistically significant difference, different letters denote statistical significance (two-way ANOVA; $p < 0.05$).	117
Figure 46: pH over time for 12-hour and 4-hour hydraulic residence time (HRT) and influent. Temperature regime is indicated by background color. Blue indicates cool (6°C weeks 1-4), purple designates warming ($+2.1^{\circ}\text{C}$ each week, weeks 5-8) and red denotes warm (14.5°C , weeks 9-12) temperature regime.	118
Figure 47: Effect of temperature and hydraulic residence time (HRT) on the change of pH for 12-hour and 4-hour HRT for cool (6°C , weeks 1-4) and warm (14.5°C , weeks 9-12) temperature regimes. Change in pH was calculated by subtracting daily influent values from daily effluent values for each bioreactor trough and obtaining the average of these values across the different temperature and HRT treatments. Different letters indicate a significant difference; identical letters do not (two-way ANOVA; $p < 0.05$).	119
Figure 48: Ammonia concentration over time for inflow, 12-hour HRT and 4-hour hydraulic residence time (HRT). Temperature regime is indicated by background color. Blue indicates cool (6°C weeks 1-4), purple designates warming ($+2.1^{\circ}\text{C}$ each week, weeks 5-8) and red denotes warm (14.5°C , weeks 9-12) temperature regime.	119
Figure 49: Nitrite concentration over time for inflow, 12-hour and 4-hour hydraulic residence time (HRT). Background color indicates temperature regime. Blue indicates	

cool (6°C weeks 1-4), purple designates warming (+2.1°C each week, weeks 5-8) and red denotes warm (14.5°C, weeks 9-12) temperature regime.	120
Figure 50: Sulfide concentration over time for inflow, 12-hour and 4-hour hydraulic residence time (HRT). Temperature regime is indicated by background color. Blue indicates cool (6°C weeks 1-4), purple designates warming (+2.1°C each week, weeks 5-8) and red denotes warm (14.5°C, weeks 9-12) temperature regime.	121
Figure 51: Methane concentration over time for 12-hour and 4-hour hydraulic residence time (HRT). Temperature regime is indicated by background color. Blue indicates cool (6°C weeks 1-4), purple designates warming (+2.1°C each week, weeks 5-8) and red denotes warm (14.5°C, weeks 9-12) temperature regime.	121
Figure 52: Effect of location and hydraulic residence time (HRT) on nirS gene copy numbers during the warm (14.5°C, weeks 9-12) temperature regime for 12-hour and 4-hour HRT and for inflow, middle and outflow sampling locations. Identical letters indicate no statistically significant difference, different letters denote statistical significance (two-way ANOVA; $p < 0.05$).	122
Figure 53: Effect of location and temperature regime on nirS gene copy numbers during 12-hour hydraulic residence time (HRT) for cool (6°C, weeks 1-4) and warm (14.5°C, weeks 9-12) temperature regimes and for inflow, middle and outflow sampling locations. Identical letters indicate no statistically significant difference, different letters denote statistical significance (two-way ANOVA; $p < 0.05$).	122
Figure 54: Effect of location and hydraulic residence time (HRT) on nosZ clade I gene copy numbers during the cool (6°C, weeks 1-4) temperature regime for 12-hour and 4-hour HRT and for inflow, middle and outflow sampling locations. Identical letters indicate no statistically significant difference, different letters denote statistical significance (two-way ANOVA; $p < 0.05$).	123
Figure 55: Effect of location and hydraulic residence time (HRT) on nosZ clade I gene copy numbers during the warm (14.5°C, weeks 9-12) temperature regime for 12-hour and 4-hour HRT and for inflow, middle and outflow sampling locations. Identical letters indicate no statistically significant difference, different letters denote statistical significance (two-way ANOVA; $p < 0.05$).	124
Figure 56: Effect of location and temperature regime on nosZ clade I gene copy numbers during 12-hour hydraulic residence time (HRT) for cool (6°C, weeks 1-4) and warm (14.5°C, weeks 9-12) temperature regimes and for inflow, middle and outflow sampling locations. Identical letters indicate no statistically significant difference, different letters denote statistical significance (two-way ANOVA; $p < 0.05$).	124

Introduction

With the advent of the Haber-Bosch method, the contribution of anthropogenic sources of nitrogen to the environment has dramatically increased. Specifically, agricultural fertilizer application is the largest source of anthropogenic nitrate-nitrogen into our watersheds (Galloway et al., 2008). While the Haber-Bosch method has increased the productivity of agricultural fields four-fold since 1909, fertilizer application has also led to the demise of water quality by eutrophication. When excess amounts of limiting nutrients, such as nitrate, leach out of agricultural soils into our waterways, aquatic plants, like algae and duckweed, thrive (Schindler, 1974). Algae blooms lead to an increase in organic matter available for decomposition, which depletes oxygen in the water, resulting in fish kills and the formation of hypoxic zones (when DO concentrations are below 2 mg/L). Minnesota lakes, streams and rivers feed into three large water basins, most notably the Mississippi River. The MPCA (2013) has reported that 95 million kilograms of total nitrogen exits Minnesota via the Mississippi River every year, with over three quarters of the 95 million kilograms originating from Minnesota. As of 2008, Minnesota was the 6th highest contributor of nitrogen loading into the Mississippi River (MPCA, 2013), which significantly contributes to the formation of the hypoxic “dead” zone in the Gulf of Mexico (MPCA, 2014). Besides environmental issues, there are also public health concerns regarding the consumption of nitrate-laden water, which has been demonstrated to cause methemoglobinemia in infants (more commonly known as “Blue Baby Syndrome”) at concentrations of 22.9 to 27.4 mg/L nitrate-N, and can lead to death (US EPA, 2017; Knobeloch et al., 2000). In an attempt to mitigate these problems, the EPA has issued a

maximum contaminant level (MCL) of 10 mg/L of nitrate-N in drinking water, however, further regulation is at the discretion of each individual state.

Concentrations of nitrate in agricultural drainage ditches adjacent to fertilizer applied fields in southern Minnesota frequently exceed 10 mg/L of nitrate-N (Krider, 2018), despite this, nitrogen has not yet been included in the state's water quality standards (Office of the Revisor of Statutes, 2017). Minnesota state legislature has directed the MPCA to issue a draft for water quality standards that include regulations for nitrogen loading into class 2A (cold) and class 2B (cool/warm) surface waters. The draft limits chronic nitrogen loading to 4.9 mg/L nitrate-N for 2B waters and 3.1 mg/L for 2A waters within a 4-day period, and permits a maximum standard of 41 mg/L nitrate-N within a 24-hour period (MPCA, 2010). In lieu of stringent regulations, the USDA, and several midwestern states, including Minnesota, have more recently issued nutrient reduction plans to reduce the amount of nutrient loading into watersheds (USDA-NRCS, 2015; IL EPA, 2015; Iowa Nutrient Reduction Strategy, 2016; MPCA, 2014). Along with 11 other states, Minnesota is also a part of the Gulf of Mexico Hypoxia Task Force that is committed to developing nutrient reduction strategy plans and technologies that can decrease nitrate loading into major river basins and watersheds (MPCA, 2014).

The Minnesota Nutrient Reduction Strategy identifies agricultural tile drainage and other pathways from cropland as a priority nitrogen source to be mitigated (MPCA, 2014). It sets state nitrogen loading reduction goals of 20% by 2025 and of 45% by 2040 and recommends best management practices (BMPs) and technology options to achieve these goals. BMPs are conventional methods that are utilized on a small-scale to achieve local enhancement of desired processes, such as denitrification, to mitigate water quality

degradation from non-point sources. Current BMPs have only reduced nitrate loading by 2% since 2000, demonstrating the need for further research and implementation of BMPs at a greater scale (MPCA, 2014). Four general categories of BMPs are recommended in the Minnesota Nutrient Reduction Strategy; increasing efficiency of fertilizer application, increasing living cover on fields, decreasing erosion and treating sub-surface tile drainage. While more efficient fertilizer application can greatly prevent nitrate loading into watersheds, it will need to be paired with other technologies to achieve significant water quality improvement that the state is endeavoring to achieve (Randall & Sawyer, 2008). Specific emphasis is placed on the need to treat tile-drainage with the use of constructed wetlands, two-stage ditches and bioreactors (MPCA, 2014). The MPCA expressly identifies a need for an increase in accessibility and knowledge of processes within bioreactors to aid in optimal design and ease of installation for farmers.

Due to the lack of more stringent environmental regulations and enforcement of nitrate in our waterways, along with the ubiquitous nature of nitrogen loss from agricultural fields, there is little incentive for farmers to invest in these nitrate mitigation strategies. Subsequently, there is also a distinct need not only for effective, but also cost-effective solutions. A technology that has low installation costs (or is simple enough for a farmer to install him or herself), that requires little maintenance, has a small footprint and is capable of removing sufficient amounts of nitrate from agricultural runoff is ideal. Woodchip denitrifying bioreactors fulfill these requirements and are becoming an accepted technology for nitrate reduction mitigation strategies (Christianson & Schipper, 2016; Schipper et al., 2010). Bioreactors typically comprise of a trench that is filled with a solid carbon source, typically woodchips, and is placed adjacent to an agricultural field to

intercept and treat sub-surface tile drainage. Because of the simplicity of the design, installation and maintenance costs of denitrifying woodchip bioreactors are low (Christianson et al., 2012; Schipper et al., 2010). As noted in Schipper et al. (2010) installation costs can be mostly eliminated if the farmer has access to a backhoe, as the farmer could install the bioreactor by him or herself due to the simple design. Furthermore, the footprints of denitrifying bioreactors are much smaller than other passive technologies, such as constructed wetlands, which require the use of land that could otherwise be profitable cropland. For these reasons, woodchip denitrifying bioreactors have been included in the United States Department of Agriculture, Iowa, Illinois and Minnesota nutrient reduction strategy plans (USDA-NRCS, 2015; IL EPA, 2015; Iowa Nutrient Reduction Strategy, 2016; MPCA, 2014).

Woodchip denitrifying bioreactors operate as nitrogen sinks by promoting the microbial process of denitrification. This is done by maintaining anoxic conditions and providing a solid carbon source (woodchips); a simple and passive method for treatment that has also proven to be successful (Addy et al., 2016). Microbial denitrification is a natural process that removes dissolved forms of nitrogen from water and reduces it to a gaseous product. When microbial denitrification is complete, nitrogen is completely reduced to nitrogen gas (N_2), an inert, harmless gas that contributes to over 75% of our atmosphere. When microbial denitrification is incomplete, nitrogen reduction ceases after the formation of nitrous oxide, a potent greenhouse gas. Consequently, complete denitrification is desired because nitrous oxide is not only a potent greenhouse gas, but it is also the third most abundant greenhouse gas contributing to climate change (Thomson et al., 2012).

Despite the inclusion of denitrifying bioreactors in these nutrient reduction strategy plans, there are still concerns regarding the application of woodchip denitrifying bioreactors in midwestern states (Christianson & Schipper, 2016). This is because of the wide, and extreme, fluctuations in weather that occur in the Midwest. Due to snow melt coinciding with fertilizer application in the early spring, there are specific concerns with high nitrogen loading rates occurring at low temperatures and high flow rates (Feyereisen et al., 2016). High nitrogen loading rates paired with cool temperatures could alter bioreactor performance in extreme and unexpected ways. Some studies have shown that with decreased temperatures and increased flow rates there is a decrease in bioreactor performance, while others have shown that it does not influence performance significantly (Christianson & Schipper, 2016; Schipper et al., 2010). Furthermore, very little is known about the community of microorganisms that are responsible for performing nitrate removal in woodchip denitrifying bioreactors and how it is influenced by changes in hydraulic residence time (HRT), temperature and location within the bioreactor. There is a need to understand the microbial dynamics in denitrifying bioreactors not only to further our knowledge, but also to optimize the design of these bioreactors for conditions found in midwestern agricultural states.

Denitrification is the step-wise reduction of nitrate (NO_3^-) or nitrite (NO_2^-) to nitrogen gas (N_2) that can be performed by many anaerobic microorganisms (both obligate and facultative). The enzymes that catalyze the reduction of nitrate are encoded by the functional genes nitrate reductase (*narG* and *napA*), nitrite reductase (*nirK* and *nirS*), nitric oxide reductase (*norB*) and nitrous oxide reductase (*nosZ* clade I and clade II) (Philippot et al., 2007; Henry et al., 2006). The intermediate nitrous oxide, a potent greenhouse gas,

is a common byproduct that can be produced if denitrification is incomplete, stopping prior to the reduction of nitrous oxide to nitrogen gas by means of *nosZ* clade I or clade II functional genes.

The two genes that encode for nitrite reductase, *nirK* and *nirS*, are the key enzymes for most “real”, complete denitrifiers and have been demonstrated to contribute significantly to denitrifying community abundance in agricultural soils (Veraart et al., 2017; Wallenstein et al., 2006). Although both *nirK* and *nirS* correspond to the production of nitrite reductase, the structure of the enzyme is determined by which gene is encoded (Henry et al., 2004). Nitrite reductase that is encoded by the *nirK* gene contains a copper cofactor, while those encoded by *nirS* do not. There has also been indication that niche differentiation between the two nitrite reductase genes might occur in agricultural soils (Hallin et al., 2009). Unfortunately, few studies on denitrifying bioreactors have incorporated both *nirK* and *nirS* functional genes into their analysis and, thus, very little is known about the presence of nitrite reductase carrying organisms in these bioreactors, let alone the effect that changes in HRT, temperature and location within the reactor might have.

The final step in denitrification is the reduction of nitrous oxide (N_2O) to nitrogen gas (N_2), which is catalyzed by nitrous oxide reductase. The presence and abundance of nitrous oxide reductase is of particular interest because it indicates the genetic potential in the bacterial community to perform complete denitrification, thereby reducing the production of nitrous oxide. Nitrous oxide reductase is encoded by two different genes, *nosZ* clade I and *nosZ* clade II, also referred to as typical *nosZ* and atypical *nosZ*, respectively. Organisms that carry the *nosZ* clade I gene are considered “classical” denitrifiers, have the genetic capability to perform the other previous steps in denitrification and typically belong

to the Proteobacteria (Harter et al., 2016). Conversely, *nosZ* clade II carrying organisms are from a variety of Phyla and about half of the organisms in this clade do not have the genetic ability to perform the other steps in denitrification. Accordingly, *nosZ* clade II carrying organisms are frequently called “incomplete” denitrifiers, because they only have the genetic potential to reduce nitrous oxide to nitrogen gas (Jones et al., 2013). Only a few studies on denitrifying bioreactors have incorporated microbial analysis on *nosZ* carrying organisms, moreover, only one of these has included both *nosZ* clade I and clade II (Andrus et al., 2014; Porter et al., 2015; Feyereisen et al., 2016). Subsequently, little is known about the effect of temperature, HRT and location within the bioreactor on both *nosZ* clade I and clade II carrying organisms.

Microbial denitrification is known to be the main mechanism for nitrate removal in denitrification bioreactors, typically accounting for upwards of 95% of nitrate removal, particularly when nitrogen is in excess (Kraft et al., 2014; Warneke et al., 2011c; Warneke et al., 2011a; Greenan et al., 2006). Because microbial denitrification is known to be responsible for nitrate removal in denitrifying bioreactors, our study focuses on nitrogen-cycling functional genes and the effect of temperature, HRT and location along the length of the bioreactor and how this compares to bioreactor performance. The main objectives of this mesoscale denitrifying bioreactor study were to establish basic trends of the total bacterial and denitrifying functional gene copy numbers under varying HRT, temperatures and at varying locations within the denitrifying bioreactors and to link any trends to bioreactor performance.

Methods

Chemicals

All chemicals used were of at least reagent grade (Sigma Aldrich, unless otherwise indicated).

Bioreactor Experimental Set Up

Experimental Design

The experiment was designed to allow for the testing of two different hydraulic residence times (HRT), 4 and 12 hours, concurrently for three months in a mesoscale laboratory setting. Temperature was tested by maintaining a “cool” temperature regime for the first month (weeks 1-4) at 6°C, slowly increasing the temperature by 2.1°C per week during the second, “warming” month (weeks 5-8), and maintaining a “warm” temperature regime for the last month (weeks 9-12) of the experiment at 14.5°C. During the length of the experiment both chemical and biological samples were collected at different time intervals and analyzed as described below.

Construction of Triplicate Bioreactor Troughs

Bioreactor troughs were constructed out of sheets of 1.27 cm-thick polypropylene (Seelye Plastics). For each experimental HRT condition, three replicate bioreactor troughs were constructed. The replicate bioreactor troughs were enclosed in climate controlled chambers (*Figure 1*). Two individual climate controlled chambers with three replicate bioreactors were used in this experiment, one chamber for each HRT condition. Each bioreactor trough measured 1.83 m long, 0.30 m wide and 0.61 m deep. Each bioreactor trough was sealed using a waterproof silicone caulking (Ultima Window, Door and Roof).

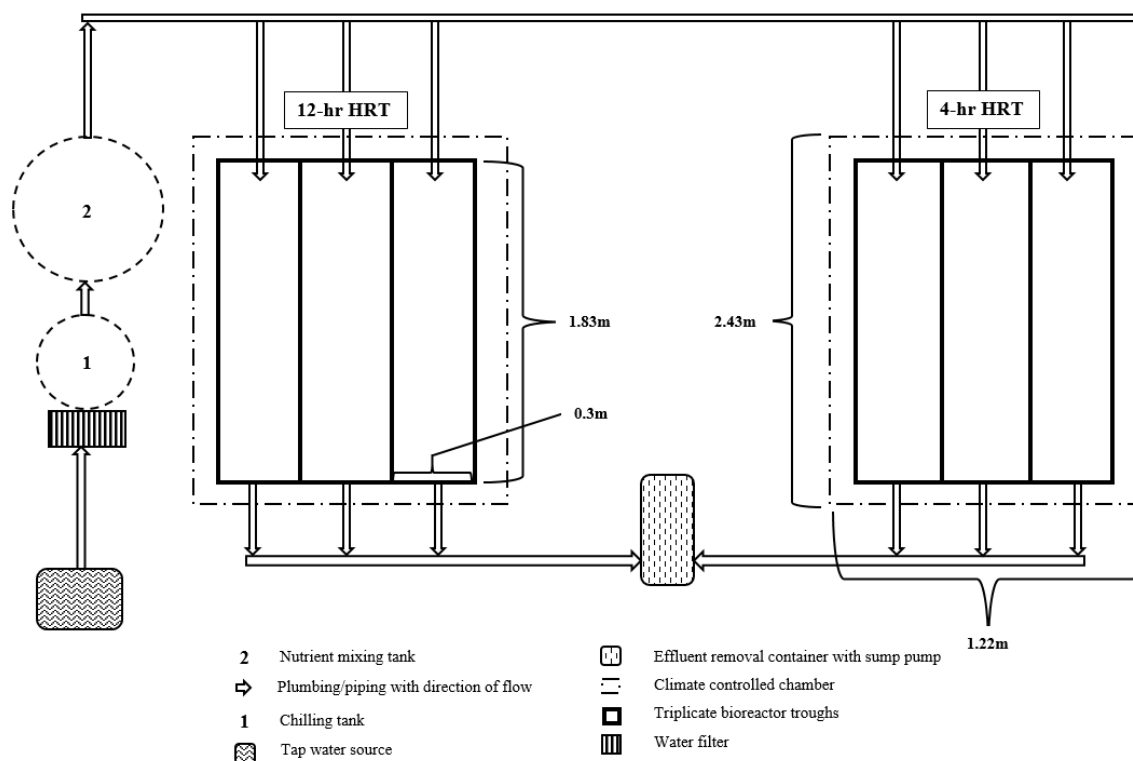


Figure 1: Schematic of experimental design. Three replicate bioreactor troughs in climate controlled chambers operated under 12 and 4-hour hydraulic residence time (HRT) and under three temperature regimes.

Inlet and outlet plumbing, as well as sampling spouts and tubing, were made of PVC pipes (Seelye Plastics). All PVC plumbing was assembled together using PVC primer and cement (Oatey Purple Primer and Regular Clear PVC Cement) and sealed using waterproof silicone caulking (Ultima Window, Door and Roof). All inlet plumbing, and chilling and nutrient mixing tanks were insulated to help maintain desired water temperature using reflective insulation (Reflectix).

Water was obtained from a nearby tap. To reduce variability and effects from chemicals in the water (i.e.: chlorine, fluoride and heavy metals) the tap water was passed through a whole house 2-stage water filtration system with multi-gradient sediment and catalytic carbon (Home Master, model 205612083) prior to being chilled in the first tank (Figure 1). A 189.3 L tank served as the chilling tank, where a drop-in aquarium chiller

(TradeWind Drop-in Chiller 1/5 HP) was used to lower the water to the desired temperature. Using a centrifugal pump, the chilled water was then passed to a 378.5 L tank where nutrients were added in 3.79 L mixtures to produce a representative artificial agricultural runoff (Table 1). The water, now chilled and containing the right concentration of nutrients, was pumped further to the experimental troughs. There, a flow meter further regulated the flow rate of the water to achieve the desired HRT (Figure 2). Once the water passed through the bioreactors, it emerged from the outlet piping and was collected in a 113.6 L PVC bin where a sump pump (Hydromatic HP33 Submersible Sump Pump) removed the effluent into overhead piping and down a drain.

Table 1: Artificial agricultural runoff composition and concentrations used as bioreactor influent media

Nutrient/Chemical	Form	Final concentrations of (mg/L)
Calcium Nitrate	$\text{Ca}(\text{NO}_3)_2 \cdot 4\text{H}_2\text{O}$	Nitrate 30
Magnesium Chloride	MgCl_2	Magnesium 20
Calcium Chloride	$\text{CaCl}_2 \cdot 2\text{H}_2\text{O}$ and $\text{Ca}(\text{NO}_3)_2 \cdot 4\text{H}_2\text{O}$	Chloride 150 Calcium 55
Potassium Phosphate and Potassium Bromide	KH_2PO_4 and KBr	Phosphate 0.5 Potassium 5
Sodium Acetate*	$\text{C}_2\text{H}_3\text{NaO}_2$	Sodium 28 Acetate 72

*sodium acetate dose was only used up to two weeks prior to the experiment start date

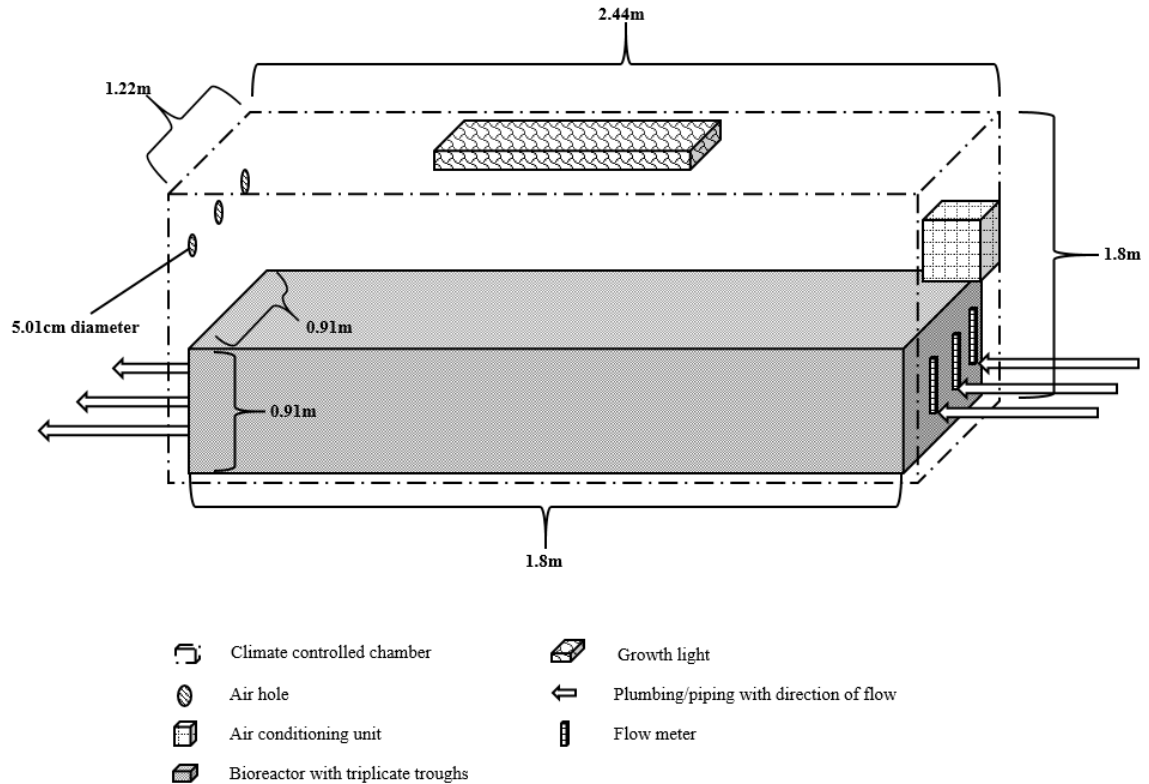


Figure 2: Diagram of a climate controlled chamber containing triplicate bioreactor troughs. Each chamber had an air conditioning unit, growth lights, air holes, and flow meters for each replicate bioreactor trough.

Construction of Climate Controlled Chambers

Climate controlled chambers were constructed out of wood and insulated (Owens Corning Foamular). One panel of each chamber had hinges to allow it to serve as a door for getting into the chambers and collecting samples. Each chamber contained triplicate bioreactor troughs which were operated under the same flow conditions (Figure 2). Each chamber also had its own air conditioning unit (GE 6,050 BTU) and growth lights to maintain the desired air temperature and to provide enough light for plant growth in the bioreactors. To allow for adequate air circulation, three air holes, all 5.01 cm in diameter, were placed 1.22 m above the ground on the rear wall of each climate controlled chamber.

Bioreactor Media

A vertical gravel inlet was constructed by filling the first 12.7 cm along the length of the trough with gravel (Figure 3). The gravel was washed in tap water prior to installation in the troughs to remove dust. The remainder of each trough was filled with alternating horizontal layers of woodchips (mixed hard-wood, The Mulch Store) and a walnut shell biochar. The woodchips comprised of 90% (v/v) of the trough reactor volume, and the biochar constituted the remaining 10% (v/v) of the total reactor volume. Layering of the two materials was done to prevent the separation of the smaller biochar from the larger woodchips and thus maintain as much of a consistent ratio of biochar to woodchip as possible throughout the entire volume of each bioreactor trough. There were three layers of woodchips and two layers of biochar. Each trough had 80 mL of soil sprinkled over the biochar layers to aid in inoculation of microbes in the bioreactors.

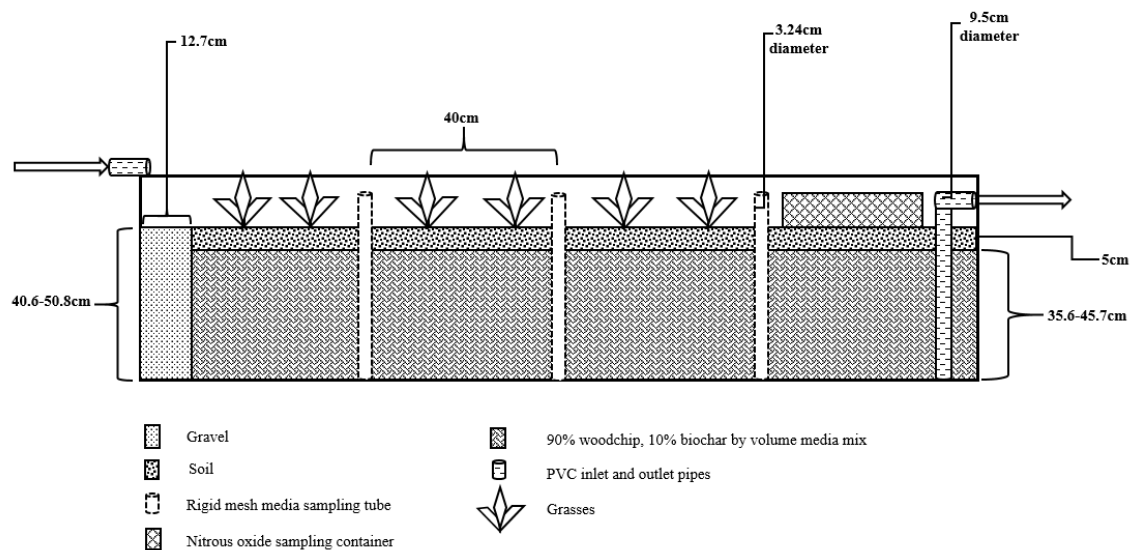


Figure 3: Profile view of one trough of the triplicate bioreactor troughs. Three rigid mesh sampling tubes were placed in each trough to allow microbial sampling throughout the experiment. Sampling tubes were filled with twelve sampling bags and one soil bag. One

sampling bag from each sampling tube was removed and replaced each week for microbial analysis. An aluminum gas sampling container was placed on top of the soil at the end of each bioreactor trough. Gas samples were collected from this container each week. Grasses were planted in the soil along the remaining length of each bioreactor trough.



Figure 4: Picture of triplicate bioreactor troughs inside a climate controlled chamber. Six grasses were planted along the length of each bioreactor trough. Each replicate bioreactor trough had three sampling tubes placed along its length and an aluminum gas collection container at the end of its length. An air conditioner was installed in each climate controlled chamber and the water was chilled in a nearby tank to maintain accurate water and ambient temperatures.

The walnut shell biochar was produced by Char Energy (Ada, Minnesota) using a feedstock of extra coarse walnut shells (Harbor Freight, 12 grit). The walnut shells were gasified in a mechanically fed baked gasifier at 510°C for one hour. The biochar was sent to Eurofins (Germany) for chemical and physical analysis (Appendix A: Walnut Shell Biochar Characterization).

A rigid mesh net (Industrial Netting Inc., XN2950-37.5P) was placed over the biochar and woodchip media mix to aid in maintaining a stable layer of soil for plants (Figure 3). Soil was collected from a sloped ditch adjacent to cropland in Mower County, Minnesota. Soil was dried for two weeks on tarps at 16.7°C, and was turned once after a week of drying. Soil was then mixed using an auger to break up larger masses of soil. Large rocks and pieces of hard clay were also picked out. The resulting soil was then stored in the dark at -12.2°C for 8 months until troughs were ready to be filled. Prior to placing soil in the reactors and on top of the rigid mesh netting, it was thawed at 16.7°C.

Plants

Six grass plants were planted in each triplicate trough. As indicated in Figure 3 and in Figure 4, grasses were planted in groups of two, with the last 40 cm along the reactor length being left free of plants. This open soil had an aluminum gas collection contraption placed on it where nitrous oxide and methane gas collection was performed. Each trough had two plants of three different grass species planted; fox sedge, dark green bulrush and fowl manna grass (Cardno Native Plant Nursery, Walkerton, Indiana). These grasses were selected because they are representative of grasses that grow naturally in ditches and around farmland in southern Minnesota.

Bioreactor Media Sampling Bag Design and Construction

To obtain bioreactor media samples to analyze the bacterial community throughout the course of the experiment, a sampling tube was designed and constructed to be placed in the bioreactor troughs. Each bioreactor trough had three sampling tubes placed along its length as shown in Figure 3, above. The distance between each sampling tube and from sampling tubes to the gravel inlet and outlet piping of the trough was 40 cm. Sampling tubes were made of rigid mesh polypropylene, had an inner diameter of 3.24 cm, a thickness of 0.236 cm, were approximately 53.98 cm tall and had an open area of 40% (Industrial Netting Inc., RN2540). Sampling bags attached to a string were placed inside of each sampling tube and were removed once a week to acquire media samples (Figure 5 and Figure 6). Each sampling string comprised of 12 sampling bags attached to a polyester string (diamond braided, KingCord) with cable-ties on the top and bottom of each bag. Sampling bags were made of a double layer of fine polyester (Drain Sleeve, Carriff Corporation Inc.) and were filled with 90% woodchip (v/v), and 10% walnut shell biochar (v/v). Each end of the sampling bag was closed with a cable tie and attached to the sampling string using another cable tie. Sampling bags measured approximately 3.24 cm in length and in diameter. Placed on top of the sampling string was a sampling bag filled with soil, it measured 5.08 cm long and approximately 3.24 cm diameter. The soil bag had a separate polyester string that it was attached to. The soil bag served to maintain the soil layer across the length of the trough as well as to ensure that the sampling tubes had the same conditions as the entire trough.

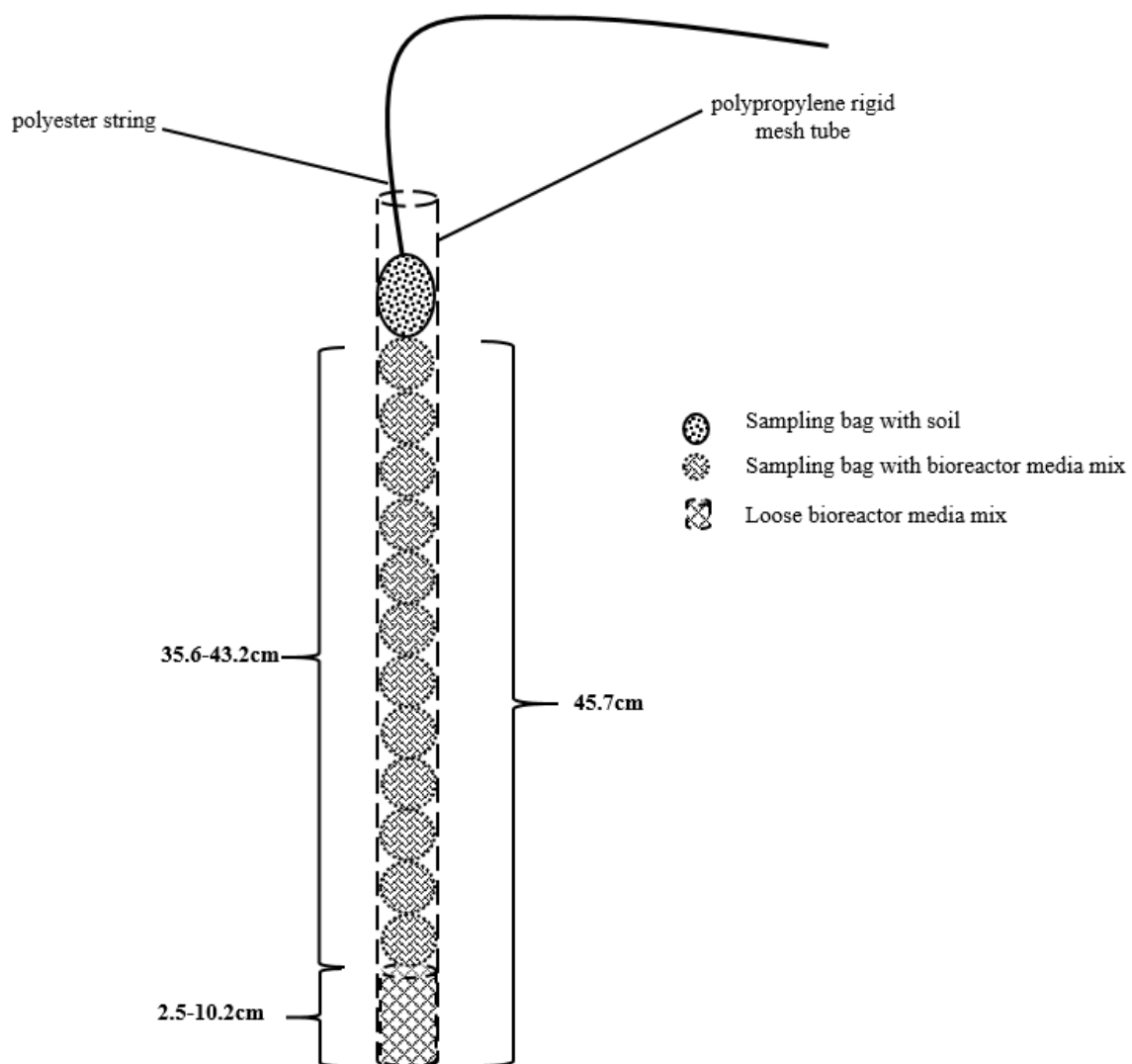


Figure 5: Schematic of a rigid mesh sampling tube containing twelve sampling bags attached to a string. Sampling bags were used to obtain bioreactor media samples throughout the length of the experiment. The top-most bag was a sampling bag filled with soil.



Figure 6: Picture from inside one replicate bioreactor trough showing three sampling tubes along the length of the reactor. The picture was taken while bioreactor troughs were still being filled with the bioreactor media mix. Sampling bags can be seen inside the sampling tubes.

Analytics

Water Sample Collection from Bioreactors

To ensure no cross contamination between water samples of triplicate bioreactor troughs, all outflow ports attached to the same effluent pipe as the outflow port being

sampled were closed (see Figure 1, above). Water in the effluent pipe was allowed to drain out for 1 minute before the sampling port for the trough of interest was opened and allowed to drain into a bucket for another minute. Thus, ensured of no cross contamination, water samples were then collected in acid washed and baked sample vials (Fisher Scientific) or in autoclaved and acid washed glass bottles (Fisher Scientific), as determined by the chemical analysis to be performed. Once sampling was complete, all outlet ports were opened and bioreactors were permitted to drain for two minutes prior to the next sampling. This was to avoid altering the HRT and to prevent the troughs from overflowing. Water samples undergoing dissolved organic carbon (DOC), nitrite, ammonia and sulfide analysis were immediately placed on ice after collection. Water samples used to measure nitrate, phosphate, pH, dissolved oxygen (DO) and oxidative reductive potential (ORP) were processed immediately. All samples that were put on ice were brought directly to the lab. Water samples to be analyzed for DOC were acidified with the addition of 100 μ L of 2M HCl. Water samples used for ammonia, nitrate and sulfide analysis were filtered through 0.2- μ m syringe filters (Acrodisc syringe filters, Pall Corporation). Half of each sample was acidified to a pH of two using 1M H₂SO₄ (sulfuric acid) and stored in 50-mL sterile centrifuge tubes (Fisherbrand). The other half was not altered after filtration and simply stored in 50-mL sterile centrifuge tubes. All water samples were kept at 4°C until analysis.

Bioreactor Media Sampling Bag Collection

All materials used for media sampling were washed with ethanol prior to use and again between sampling reactors. First, the soil bag was removed and placed aside, then the string with the sampling bags attached was removed and placed in a sterile bin. Using wire clippers dipped in ethanol, the cable ties attaching the sampling bag to the string were

removed and the desired sampling bag was placed into an ethanol-washed plastic organizer. An unused replacement sampling bag was then attached to the sampling string using cable ties and the sampling bags were re-inserted into the sampling tube with the aid of an ethanol-washed wooden rod. The soil bag was replaced, materials were washed with ethanol and the process repeated for the following sampling tube. The sampling bag to be removed was randomly determined using a random number generator (random.org) to avoid any sampling bias resulting from sampling bag depth. Immediately after sampling, all sampling bags were brought to the lab. Using ethanol dipped wire clippers and working over a Bunsen burner, one cable tie on each sampling bag was removed and each sampling bag was placed, intact, into a sterile 50-mL centrifuge tube (Fisherbrand). All surfaces and materials were washed with ethanol between each sampling bag. The centrifuge tubes containing the sampling bags were stored in two Ziploc bags at -80°C until further analysis.

Nitrite and Ammonia Measurements

Nitrite and ammonia measurements were performed on a Segmented Flow Analyzer (AA3, Seal Analytical) following manufacturer's instructions (ISO/DIS 13395 and ISO/DIS 11732, respectively). Water samples that were used for this analysis were filtered using a 0.2- μ m syringe filter (Acrodisc syringe filter, Pall Corporation) and acidified using 1M sulfuric acid until a pH of two was achieved, following EPA standard procedures on sample preservation (U.S. Environmental Protection Agency, 1982) All water samples were kept at 4°C until analysis and were measured within 30 days of collection. Milli-Q water was used for making all solutions and served as baseline/blank readings.

DOC Measurements

All sample vials (Fisher Scientific) used for DOC sampling were acid washed in a 10% HCl acid bath overnight, rinsed six times and baked in a muffle furnace at 600°C for four hours. 20 mL of water samples were collected from each trough and DI water was used as a blank. DOC samples were acidified by adding 100µL of 2M HCl and all samples were kept at 4°C until analysis. All DOC measurements were taken within 14 days of sample collection with a TOC analyzer (TOC-L, Shimadzu Scientific Instruments) following manufacturer's instructions.

Sulfide Measurements

Samples that were filtered, but not acidified, were used for all sulfide measurements. Sulfide analysis of all water samples was performed within 24 hours of water sample collection. Sulfide was measured using the spectrophotometric method described by Cord-Ruwisch (Cord-Ruwisch, 1985). A copper reagent solution of 50 mM HCl and 5 mM CuSO₄ was made with Milli-Q water. A second solution of sodium sulfide was also made by anoxically dissolving Na₂S*9H₂O into a graduated cylinder containing Milli-Q water. The concentration of sulfide in the solution was determined by weighing the graduated cylinder before and after the addition of Na₂S*9H₂O. The copper reagent solution was then aliquoted in 0.975 mL volumes into 2-mL centrifuge tubes (Eppendorf). The sodium sulfide solution was then serially diluted in separate 2-mL centrifuge tubes to develop a standard curve. The concentrations of sulfide used to produce the standard curve were 20 mM, 10 mM, 5.0 mM, 2.5 mM, and 1.25 mM.

Following this, 0.25 mL of the standard curve solution was pipetted into a 2-mL centrifuge tube containing the copper reagent solution. This mixture was then degassed, shaken vigorously by hand for 20 seconds and poured into a 1.5-mL cuvette. The cuvettes were inserted into a spectrophotometer (Spectronic 20 Genesys, Spectronic Instruments) and the absorbance was measured at 480 nm. This method was repeated for each standard curve solution. Utilizing the absorbance readings for the standard solutions, a linear plot of the absorbance versus concentration was generated and used to correlate absorbance to sulfide concentration in bioreactor water samples. Milli-Q water served as the blank for all sulfide measuring.

Nitrate Measurements

Nitrate concentrations were measured twice a day using a nitrate probe (Hoch Nitratax Plus). The probe and water collection cup were rinsed with DI water prior to use and between samplings. Immediately after sample collection in the water collection cup, the probe was fully submerged. Nitrate concentration was measured after 1.5 minutes, when the front sensor had completed 6 wipes. Drift was tested once daily with DI water. The nitrate probe was calibrated each week with DI and a 50 mg/L $\text{NO}_3\text{-N}$ standard or as needed when drift exceeded 0.2 mg/L $\text{NO}_3\text{-N}$.

pH, DO and ORP Measurements

Dissolved oxygen (DO), pH and oxidative reductive potential (ORP) were all measured using a Multi-Parameter Water Quality Sonde with ROX Optical DO (YSI, 6 Series) following manufacturer's instructions. Probe and water collection cup were rinsed with DI water prior to use and between samplings. Directly after sample collection, the

probe was fully submerged in the sample and readings were measured. The Sonde probe DO and pH were calibrated once each day, while the ORP was calibrated once every two weeks. At the initial installation of the Sonde probe, the pH was calibrated using 4, 7 and 10 pH standards. Daily pH calibration was performed using only a 7-pH standard. DO calibration was completed at barometric atmospheric pressure and ORP calibration was accomplished using a Zobell Solution composed of potassium chloride and potassium ferrocyanide of 231 mV at 25°C.

Phosphate Measurements

Phosphate measurements were obtained using the PhosVer 3 Absorbic Acid Method using Colorimeter for Reactive Phosphorous (Hach DR890). Water samples were collected in 1M HCl acid-washed colorimeter vials, stored at 4°C, and were used within 48 hours of collection. Measurements were obtained using manufacturer's instructions and the colorimeter was calibrated once a week using DI water and a 1 mg/L PO_4^{-3} standard solution.

Nitrous Oxide and Methane Collection and Analysis

Glass vials closed with rubber septa that had previously been flushed with helium gas were used to collect nitrous oxide and methane samples. All gas samples were collected once a week and included a blank sample that was obtained from the air in the bioreactor room. Empty syringes were inserted into a rubber septum located on the gas sampling container, which remained on top of the soil for each bioreactor trough for the entirety of the experiment (see Figure 3), and flushed three times using the gas collected before removing 5 mL of a gas sample. Syringes were inserted into the flushed glass vials and the

gas samples were deposited inside. Gas samplings were taken three times from each bioreactor trough, with 15 minutes allowed to pass between samplings. Nitrous oxide and methane were quantified using a gas chromatographer (HP 5890 GC/FID/TCD/ECD) according to manufacturer's instructions. All rubber septa on the gas sampling containers were replaced each week following sampling.

Bromide Tracer Tests and Hydraulic Modeling

Bromide tracer tests were performed to ascertain hydraulic residence time and to model the hydraulic flow of each replicate bioreactor trough. Methods used for the bromide tracer test and the application of these results to create a hydraulic model for the reactors is detailed in (Krider, 2018). The resulting hydraulic models were used to obtain more accurate results for nitrate removal for each trough, as well as to accurately predict the nitrate concentration at each sampling tube location.

DNA Extractions

DNA extractions were performed using the DNeasy PowerSoil Kit (2-mL size, Qiagen) following the manufacturer's directions with the following amendments. Bioreactor sampling bags were stored whole in 50-mL sterile centrifuge tubes (Fisherbrand) and two Ziploc bags. Sampling bags were removed from the freezer and thawed on ice 45 minutes prior to the DNA extraction procedure. Once thawed, 1.5 g of wet media that was composed of approximately 10% biochar (v/v) and 90% (v/v) woodchips was weighed and placed into a 15-mL sterile centrifuge tube (Fisherbrand). The contents of one 2-mL PowerBead Tube was emptied into the 15-mL centrifuge tube and 60 μ L of Solution C1 was added to the 15-mL centrifuge tube as well. A 15-mL vortex

adapter (Mo Bio) was used to centrifuge the centrifuge tubes for 10 minutes. After vortexing, the 15-mL tubes were centrifuged at 4,000 rpm for 3 minutes. The supernatant was removed and placed into a sterile 2-mL collection tube. The collection tube was vortexed at 10,000 g for 30 seconds, and the supernatant was removed and transferred to another 2-mL collection tube. Procedure continued as outlined in manufacturer's instructions and DNase and RNase-free water (Sigma Life Sciences) was used in place of Solution C6. Extractions were stored at -20 °C until further use.

Qubit

To ensure that DNA extractions were successful, DNA concentrations were measured using Qubit 3.0 Fluorometer (Life Technologies). Manufacturer's procedure was followed, with 2 µL of sample being used to test the DNA concentration. All reagents used were High Sensitivity (Invitrogen by Thermo Fisher Scientific) according to manufacturer's specifications.

Primers

Primers used for functional denitrifying genes are listed in Table 2. Primers were obtained from Integrated DNA Technologies and manufacturer's instructions were followed for preparation.

Table 2: Genes, primers, sequences and references used to quantify total bacteria and functional denitrifying gene copy numbers using qPCR.

Gene	Primer Name	Sequence (5'→3')	Reference
16S rRNA V3 gene	338F	CCTACGGGAGGCAGCAG	Muyzer et al 1993
16S rRNA V3 gene	518R	ATTACCGCGGCTGCTGG	Muyzer et al 1993
<i>nirK</i> F	nirK876c	ATYGGCGGVCA YGGCGA	Henry et al. (2004) (modified)
<i>nirK</i> R	nirK1040	GCCTCGATCAGRTTTRTGG	Henry et al. (2004)

			(modified)
<i>nirS</i> F	nirSCd3aF	AACGYSAAGGARACSGG	Kandeler et al. (2006)
<i>nirS</i> R	nirSR3cd	GASTTCGGRTGSGTCTTSA YGAA	Kandeler et al. (2006)
<i>nosZ</i> clade I F	nosZ2F	CGCRACGGCAASAAGGTS MSSGT	Henry et al. (2006)
<i>nosZ</i> clade I R	nosZ2R	CAKRTGCAKSGCRTGGCA GAA	Henry et al. (2006)
<i>nosZ</i> clade II F	nosZ-II-F	CTNGGNCCNYTKCAYAC	Jones et al. (2013), modified as in Harter et al. (2016)
<i>nosZ</i> clade II R	nosZ-II-R	GCNGARCARAANTCBGTR C	Jones et al. (2013) modified as in Harter et al. (2016)

gBlock Standards

DNA standards were made using gBlocks from Integrated DNA Technologies. Standards were prepared using manufacturer's instructions. gBlock sequences for each denitrifying gene of interest are listed in Table 3.

Table 3: gBlock standard sequences and sources used to quantify gene copy numbers of bioreactor samples by qPCR.

Gene	Sequence	Source of gene
16S rRNA V3 gene	cgggccagactcctacgggaggcagcagtgagggaatattgc acaatgggcgcaagcctgatgcagccatgccgcgtgtatgaa gaaggccttcgggttgtaaagtactttcagcggggaggaagg gagtaaagttaatacctttgctcattgacgttaccgcagaaga agcaccggctaactccgtgccagcagccgcggtataacgga gggtgcaagcgta	Thiobacillus sp.
<i>nirK</i>	cccgcacctgatcggcggccatggcgactatgtctgggctac cggcaagttccgaatgctccggacgtcgatcaggagacctg gttcataccggcggcacggcgggcgctgccttctacacctt cgagcagcccggcatctatgcctacgtcaaccataacctgatc gaggcattcgagctt	Ensifer meliloti 1021
<i>nirS</i>	gttcgtgatcaacgccaaggagaccggcaagatcctgatggt caactactcggacttgccaacctgaagaccaccaccatcgat tcggccaagttcctgcatgacggcggttcgacgccaccggc cgctacttctggtggccgccaatgcgtccgacaagattgcc gtggtcgacaccaaggaagacaagctggccgcgctgatcga cgtgggcaagaccccgcatccggggcgcgccgccaacttc atgcatccgaagttgggcccgtctgggccaccagccacctt	Ralstonia eutropha H16

	ggcgacgagaccatcagcctgatcggcaccgacccggccg gacacccggcgagggcgtggaaggtggtgcagaccatcaa gggccagggcggggtcactcttcatcaagaccacccga agtcgtccaacctg	
<i>nosZ</i> clade I	ggaagtcacccgcgacggcaacaaggtccgcgtctacatga cgtccgcccggccttcgggtctggacgacttcaccgtca agcagggcgacgaggttacggtctatgtgacgaatcgcag aggtcgaggatctcacgcatggattctgcatcgtcaactacgg catcaacatggaggtgcaccgcaagcgaccgttcggtcac cttaaggcgagcagaccggcggtctactggtactactgcac ctggttctgcatgcgatgcacatggagatgaagg	Ensifer meliloti 1021
<i>nosZ</i> clade II	gttctttcttaggtccgttcacacatgctgatcttcgcggct tcgatcgcgttgccgtagtgcggttcgccgtggtcgggaagt cgagcagcagcttgcgcccagatgtcgtagctgcgcc gactgcgtgagctccggaccgtgggcaggtaccgatccttc gtgatctgttgagcggcagcagatacttccccggcggttg tggtggcgccggcgggaatcatcaggtgaccgatcgagtagt acgtcggcaccgatcgacgatctccacgtaccagcttc acttcacgatctcgtggagatgaacagcgacgttaggcgt agcccttgccatcgaactcgggtgtgcagggggccgaggcca ggatccttcacttcgcgtacggactttgtcagccggcca	Gemmatimonas aurantiaca

Real-time Polymerase Chain Reaction (qPCR)

Quantification of gene copy numbers for 16S rRNA, *nirK*, *nirS*, *nosZ* clade I and *nosZ* clade II were completed using a Bio Rad CFX Connect Real-Time System. The temperature protocol and reaction mixture used was modified from (Harter et al., 2016) and is stated in Table 4.

Table 4: Reaction mixtures and thermal profile of qPCR reactions performed for each target gene. Total volume for each reaction mixture was 10 μ L.

Gene	Reaction Mixture	Volume Used (μ L)	Thermocycler Protocol
16S rRNA gene	2X Sso Advanced Universal SYBR 338F (25 μ M) 338R (25 μ M) PCR Water Sample	5 0.1 0.1 3.8 1	98°C for 10 s 58°C for 20 s X 40 cycles
<i>nirK</i>	2X Sso Advanced Universal SYBR <i>nirK</i> 876c (25 μ M) <i>nirK</i> 1040 (25 μ M)	5 0.1 0.1	98°C for 10 s 58°C for 20 s X 40 cycles

	PCR Water Sample	3.8 1	
<i>nirS</i>	2X Sso Advanced Universal SYBR <i>nirSCd3Af</i> (25 μ M) <i>nirSR3cd</i> (25 μ M) PCR Water Sample	5 0.2 0.2 3.6 1	98°C for 30 s 57°C for 30 s 72°C for 30 s X 40 cycles
<i>nosZ</i> clade I	2X Sso Advanced Universal SYBR <i>nosZ2F</i> (25 μ M) <i>nosZ2r</i> (25 μ M) PCR Water Sample	5 0.1 0.1 3.8 1	98°C for 15 s 60°C for 25 s X 40 cycles
<i>nosZ</i> clade II	2X iTaq Universal SYBR <i>nosZ-II-F</i> (25 μ M) <i>nosZ-II-R</i> (25 μ M) PCR Water Sample	5 0.4 0.4 3.2 1	98°C for 30 s 54°C for 30 s 72°C for 45 s 80°C for 30 s X 40 cycles

SYBR Green Supermixes purchased from Bio-Rad

Statistics

Multi-factor analysis of variance (ANOVA) statistics tests were performed in Excel with XLSTAT add-on (Microsoft). Post-hoc analyses of two-way and three-way ANOVA for multiple pairwise comparisons were performed using the Tukey Honest Significant Difference (HSD) procedure. To illustrate the effects of all parameters on the bioreactor performance and on the bacterial community, principal components analysis (PCA) was performed in R. Average values of gene copy numbers of each functional gene and total bacterial gene for each replicate trough was utilized to assess the correlation of the microbial community with the chemical parameters tested in this study. To test which parameters had the greatest effect on percent nitrate removal, a linear mixed effects model was developed. A random intercept was added in the model to compensate for the lack of independence in samples, due to repeated samplings of the same sampling tubes through

the course of the experiment. The linear mixed effects model was created and analyzed in R. A confidence interval of 95% was utilized for all statistical analyses.

Results

Chemical Data

Percent Nitrate Removed (Nitrate Removal Efficiency)

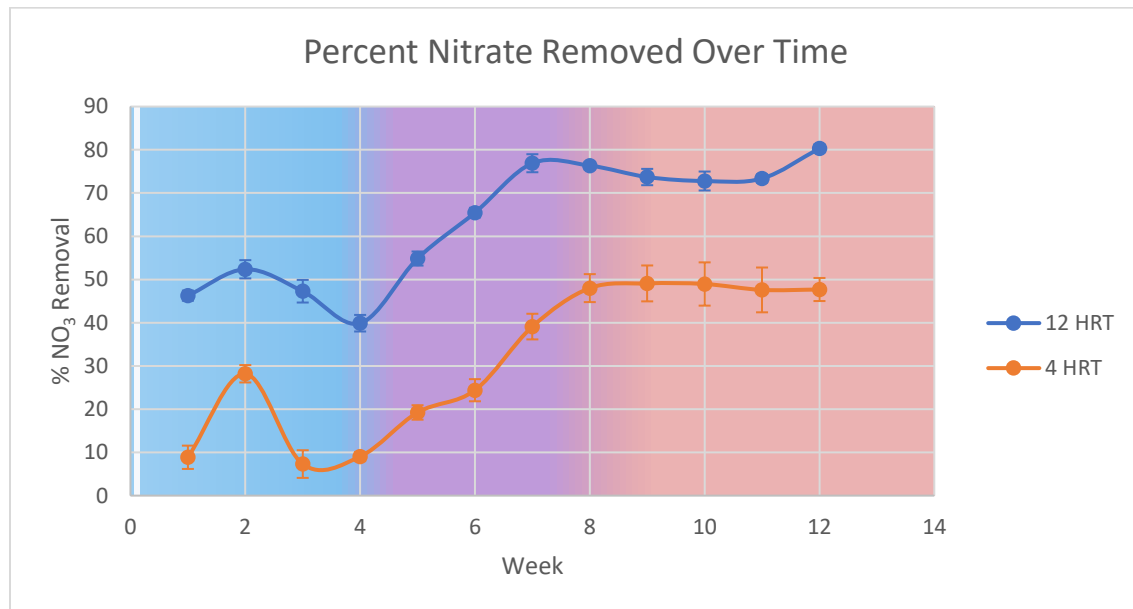


Figure 7: Percent nitrate removed over time for 12-hour and 4-hour hydraulic residence time (HRT). Temperature regime is indicated by background color. Blue indicates cool (6°C weeks 1-4), purple designates warming (+2.1°C each week, weeks 5-8) and red denotes warm (14.5°C, weeks 9-12) temperature regime.

During the course of the study, it was found that there was an increase in nitrate removal (Figure 7) over time. The greatest increase in nitrate removal was during the warming temperature regime, when the water temperature was increased by 2.1°C each week (weeks 5-8). The percent of nitrate removal during the cool (6°C, weeks 1-4) and the warm (14.5°C, weeks 9-12) temperature regimes remained fairly constant, with the warm temperature regime having a higher percent nitrate removed.

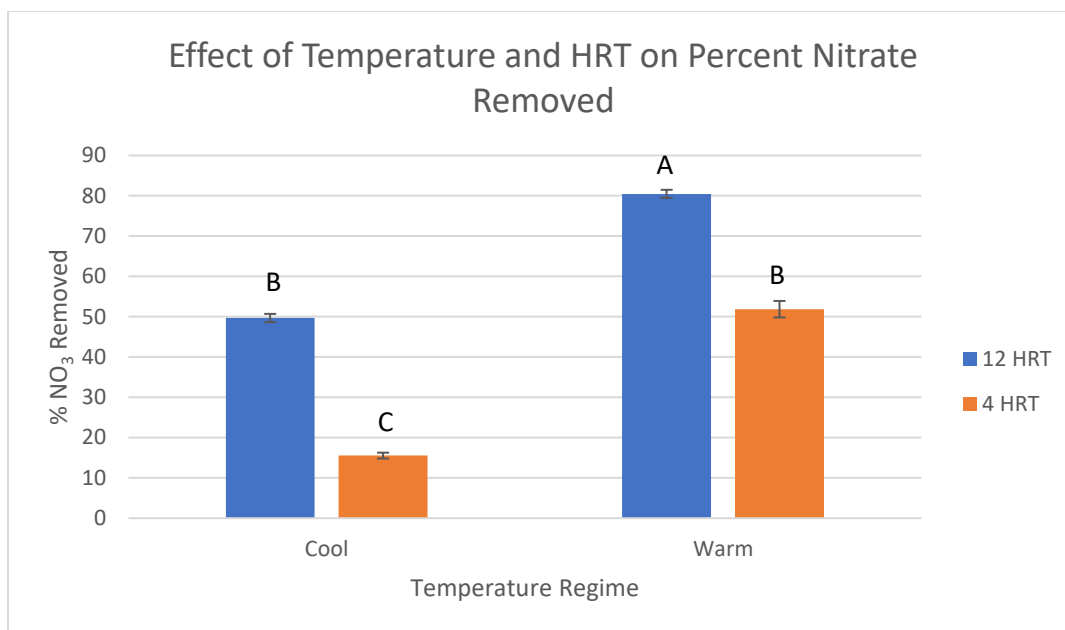


Figure 8: Effect of temperature and hydraulic residence time (HRT) on the percent nitrate removed for 12-hour and 4-hour HRT for both cool (6°C, weeks 1-4) and warm (14.5°C, weeks 9-12) temperature regimes. Identical letters indicate no significant difference, while different letters denote a significant difference (two-way ANOVA; $p < 0.05$).

There was significantly higher percent nitrate removal during the warm temperature regime than the cool temperature regime (Figure 8; $p < 0.0001$). Similarly, there was also a significantly higher percent nitrate removal in bioreactors with 12-hour HRT than 4-hour HRT (Figure 8; $p < 0.0001$). A significant interaction was also found between temperature regime and HRT ($p = 0.016$).

Nitrate Removal Rate

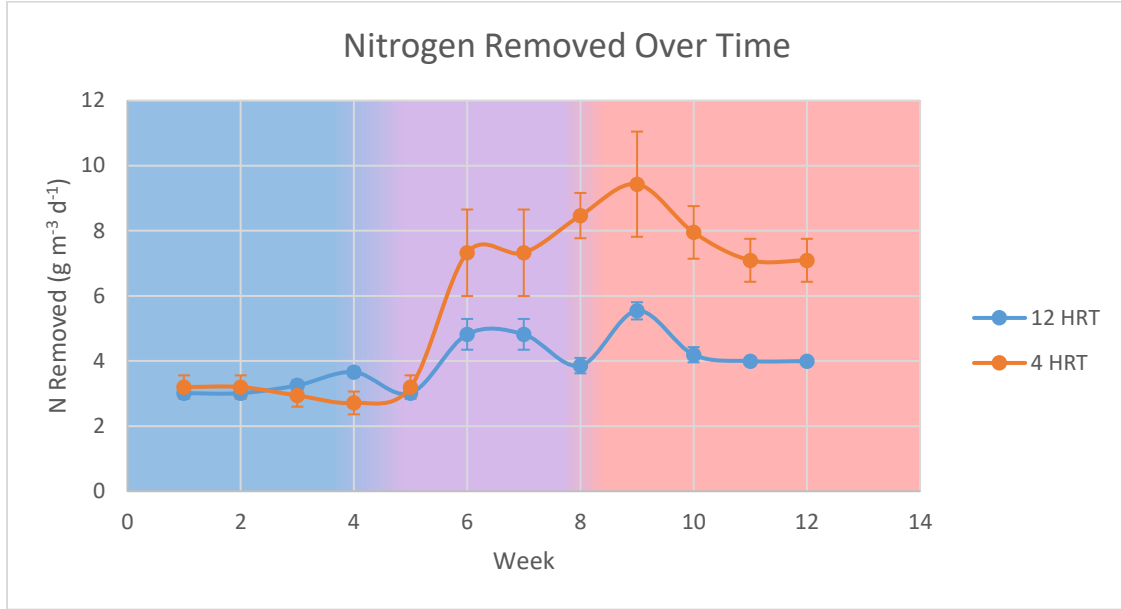


Figure 9: Nitrogen removed over time ($\text{g m}^{-3} \text{d}^{-1}$) for 12-hour and 4-hour hydraulic residence time (HRT). Temperature regime is indicated by background color. Blue indicates cool (6°C weeks 1-4), purple designates warming ($+2.1^{\circ}\text{C}$ each week, weeks 5-8) and red denotes warm (14.5°C , weeks 9-12) temperature regime.

The 12-hour and 4-hour HRT reactors removed approximately $3 \text{ g-N m}^{-3} \text{d}^{-1}$ during the cool temperature regime (6°C , weeks 1-4) (Figure 9). During the warming temperature regime ($+2.1^{\circ}\text{C}$ each week, weeks 5-8), there was an increase in $\text{g-N m}^{-3} \text{d}^{-1}$ removed for both the 12-hour and 4-hour HRT reactors, with peak removal demonstrated at week nine, during the warm temperature regime (14.5°C , weeks 9-12). Following week five, the 4-hour HRT reactors removed more $\text{g-N m}^{-3} \text{d}^{-1}$ than the 12-hour reactors, with the maximum rates during week nine being $9 \text{ g-N m}^{-3} \text{d}^{-1}$ and $5.5 \text{ g-N m}^{-3} \text{d}^{-1}$, respectively (Figure 9).

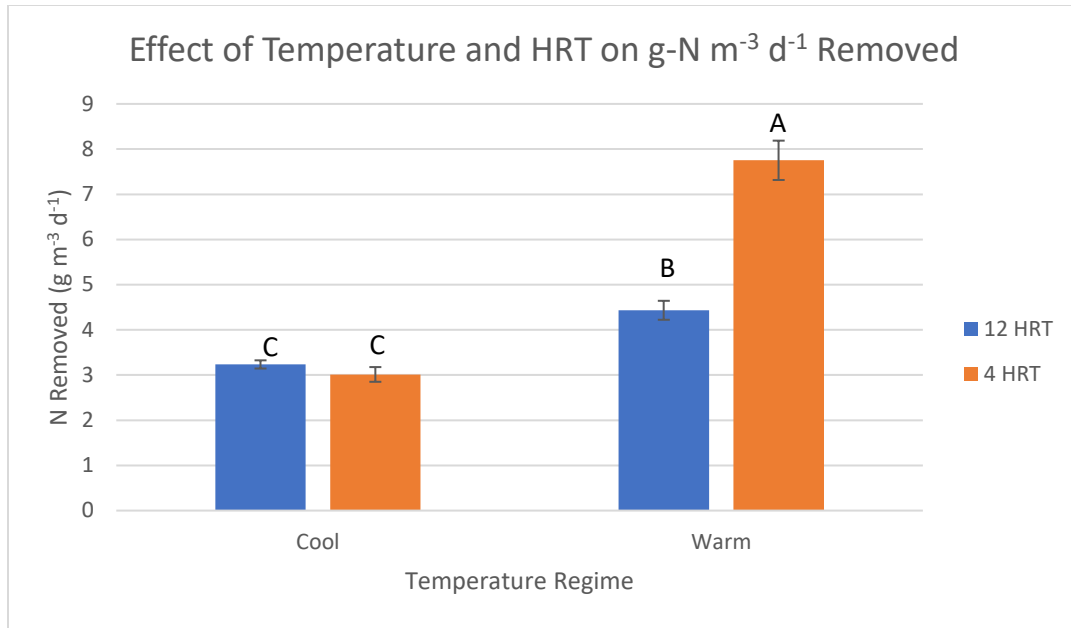


Figure 10: Effect of temperature and hydraulic residence time (HRT) on $\text{g-N m}^{-3} \text{d}^{-1}$ removed for 12-hour and 4-hour HRT for both cool (6°C , weeks 1-4) and warm (14.5°C , weeks 9-12) temperature regimes. Identical letters indicate no statistically significant difference, different letters denote statistical significance (two-way ANOVA; $p < 0.05$).

There were no statistically significant differences found for $\text{g-N m}^{-3} \text{d}^{-1}$ removed between the two HRT during the cool temperature regime (6°C , weeks 1-4) (Figure 10; $p = 0.926$). In contrast, there was significantly higher $\text{g-N m}^{-3} \text{d}^{-1}$ removed for the 4-hour than the 12-hour HRT during the warm temperature regime (14.5°C , weeks 9-12) (Figure 10; $p < 0.001$). There was also significantly higher $\text{g-N m}^{-3} \text{d}^{-1}$ removed for the warm than the cool temperature regime for both the 12-hour and 4-hour HRT (Figure 10; $p < 0.001$). A significant interaction was also found between temperature regime and HRT ($p < 0.001$).

Dissolved Organic Carbon (DOC)

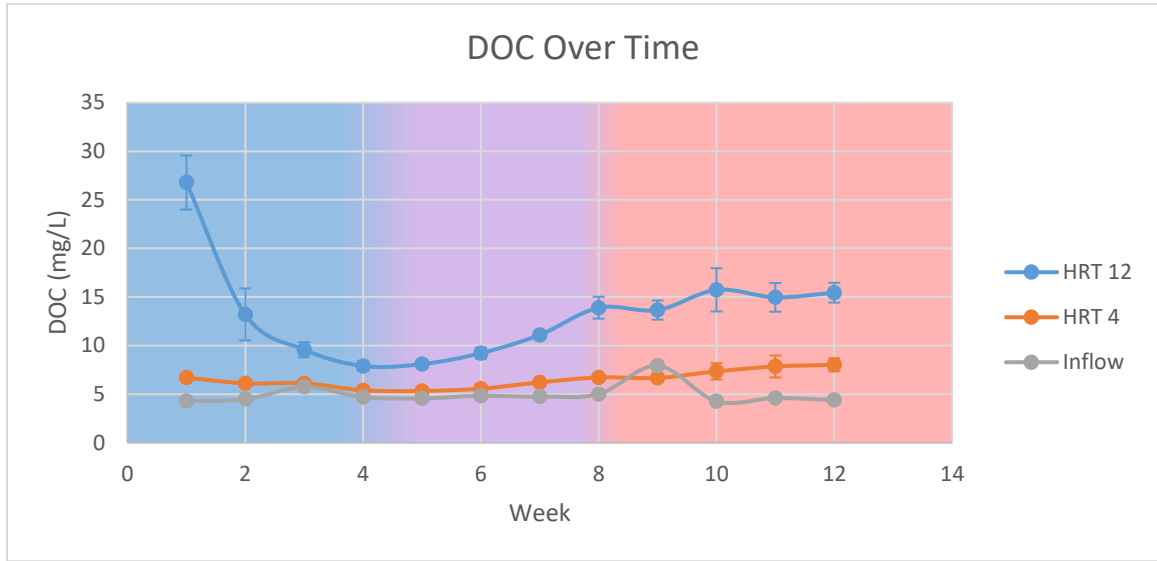


Figure 11: Dissolved organic carbon (DOC) over time for 12-hour and 4-hour hydraulic residence time (HRT) and influent. Temperature regime is indicated by background color. Blue indicates cool (6°C weeks 1-4), purple designates warming (+2.1°C each week, weeks 5-8) and red denotes warm (14.5°C, weeks 9-12) temperature regime.

The dissolved organic carbon (DOC) content had an initial high startup concentration for the 12-hour HRT, which decreased rapidly through the cool temperature regime (6°C, weeks 1-4) (Figure 11). During the warming (+2.1°C each week, weeks 5-8) and warm (14.5°C, weeks 9-12) temperature regime, the DOC increased each week. The 12-hour HRT reactors had higher effluent DOC concentrations throughout the course of the entire experiment than the influent and the 4-hour HRT. The influent remained relatively constant throughout the length of the experiment, with the exception of a small peak during week 9 when the concentration reached approximately 8 mg/L, which was 1 mg/L higher than the effluent of the 4-hour HRT reactors (Figure 11).

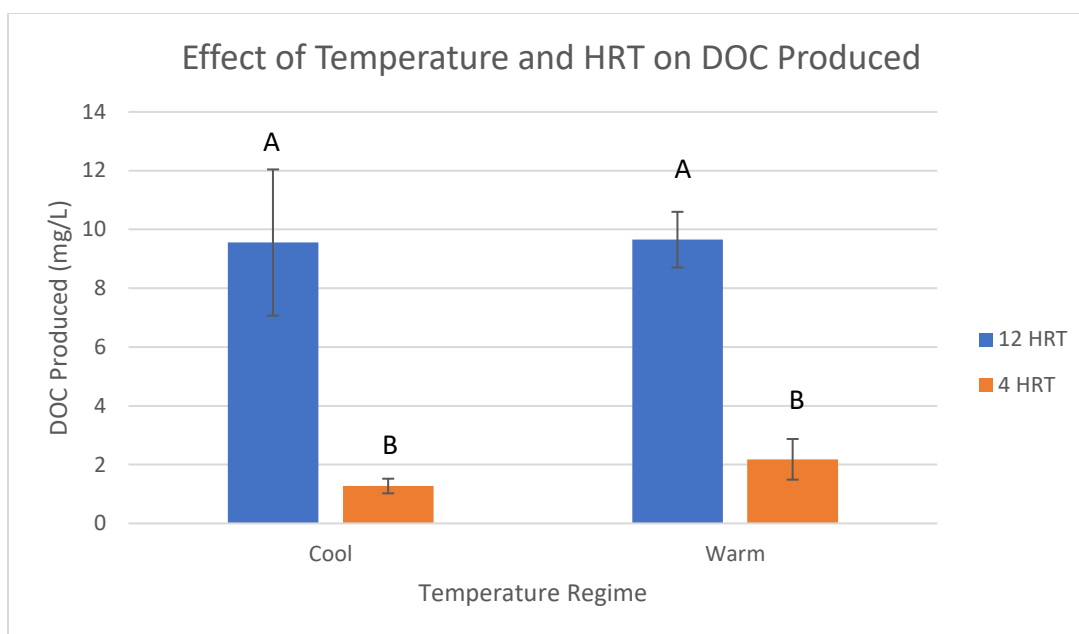


Figure 12: Effect of temperature and hydraulic residence time (HRT) on the dissolved organic carbon (DOC) produced for cool (6°C, weeks 1-4) and warm (14.5°C, weeks 9-12) temperature regimes. Produced DOC was calculated by subtracting the weekly influent values from the weekly effluent values of the corresponding bioreactor trough at the same time point and averaging these values across HRT and temperature treatments. Identical letters indicate no significant difference, different letters denote a significant difference (two-way ANOVA; $p < 0.05$).

Produced DOC was calculated by subtracting the weekly influent values from the weekly effluent values of the corresponding bioreactor trough at the same time point and averaging these values across HRT and temperature treatments. There was a significant difference between the dissolved organic carbon (DOC) produced between 12-hour and 4-hour HRT, however, no significant difference between the two temperature regimes was found (Figure 12; $p < 0.001$). The 12-hour HRT reactors produced approximately 9.5 mg/L of DOC, while the 4-hour produced nearly 2 mg/L for both cool (6°C, weeks 1-4) and warm (14.5°C, weeks 9-12) temperature regimes.

Dissolved Oxygen (DO)

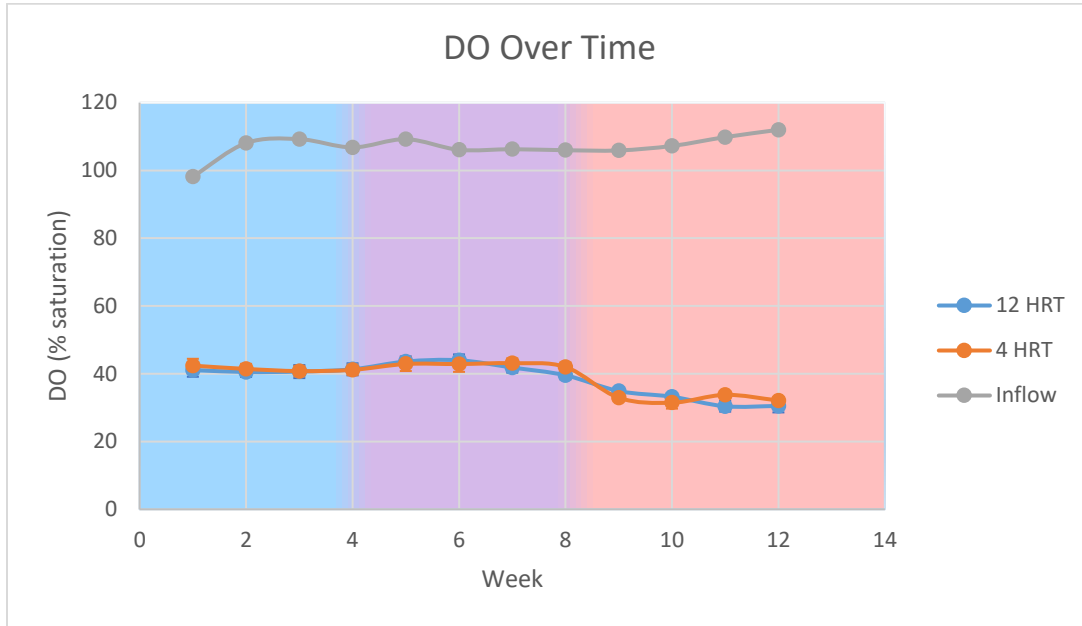


Figure 13: Dissolved oxygen (DO) concentration over time for 12-hour and 4-hour hydraulic residence time (HRT) and influent. Temperature regime is indicated by background color. Blue indicates cool (6°C weeks 1-4), purple designates warming (+2.1°C each week, weeks 5-8) and red denotes warm (14.5°C, weeks 9-12) temperature regime.

Over the course of the experiment the DO of the influent remained fairly constant with a slight increase during the warm temperature regime (14.5°C, weeks 9-12) (Figure 13.) Despite this, the effluent DO concentrations for both the 12-hour and 4-hour HRT decreased slightly during the warm temperature regime (14.5°C, weeks 9-12).

Changes in DO saturation were calculated by subtracting daily influent values from daily effluent values for each bioreactor trough and obtaining the average of these values across the different temperature and HRT treatments. Significantly more decreased DO concentrations were observed for both 4-hour and 12-hour HRT reactors under a warm temperature regime (14.5°C, weeks 9-12) than their corresponding cool temperature regimes (6°C, weeks 1-4) (Appendix B: Additional Chemical Parameters of Bioreactor

Troughs; Figure 43; $p < 0.0001$). In contrast, there was no significant difference observed between 12-hour and 4-hour HRT of the same temperature regime. Accordingly, no interaction effect was demonstrated to occur between temperature and HRT (Appendix B: Additional Chemical Parameters of Bioreactor Troughs; Figure 43; $p > 0.05$).

Oxidative-Reductive Potential (ORP)

Throughout the length of the experiment, the ORP decreased for the influent, 12-hour and 4-hour HRT (Appendix B: Additional Chemical Parameters of Bioreactor Troughs; Figure 44). The decrease in ORP for the influent was less distinctive due to the cyclical increase and decrease in ORP, nevertheless, it slowly decreased throughout the course of the experiment. The decrease in ORP for the 12-hour and 4-hour HRT was clearly noticeable throughout the warming (weeks 5-8) and warm (weeks 9-12) temperature regimes, but was not as distinctive during the cool (weeks 1-4) temperature regime, where there was even a slight increase at week four. The ORP for both the 12-hour and 4-hour HRT were consistently below zero after reaching week six, whereas the inflow concentration remained positive, cycling above and below between 300 to 150 mV (Appendix B: Additional Chemical Parameters of Bioreactor Troughs; Figure 44). The ORP of the 12-hour HRT reactors remained considerably lower than that of the 4-hour HRT reactors for the entirety of the experiment.

Change in ORP was calculated by subtracting daily influent values from daily effluent values for each bioreactor trough and obtaining the average of these values across the different temperature and HRT treatments. A significantly greater decrease in ORP was noted for the 12-hour than the 4-hour HRT for both the cool and warm temperature regimes (Appendix B: Additional Chemical Parameters of Bioreactor Troughs; Figure 45; $p < 0.001$

and $p=0.018$, respectively). There was no statistically significant difference found between cool (6°C , weeks 1-4) and warm (14.5°C , weeks 9-12) temperature regimes for the 12-hour HRT, however, there was for the 4-hour HRT. There was a significantly greater decrease in ORP during the warm temperature regime than the cool temperature regime for 4-hour HRT (Appendix B: Additional Chemical Parameters of Bioreactor Troughs; Figure 45; $p<0.001$). A significant interaction was also found between temperature regime and HRT ($p<0.001$).

Nitrous Oxide

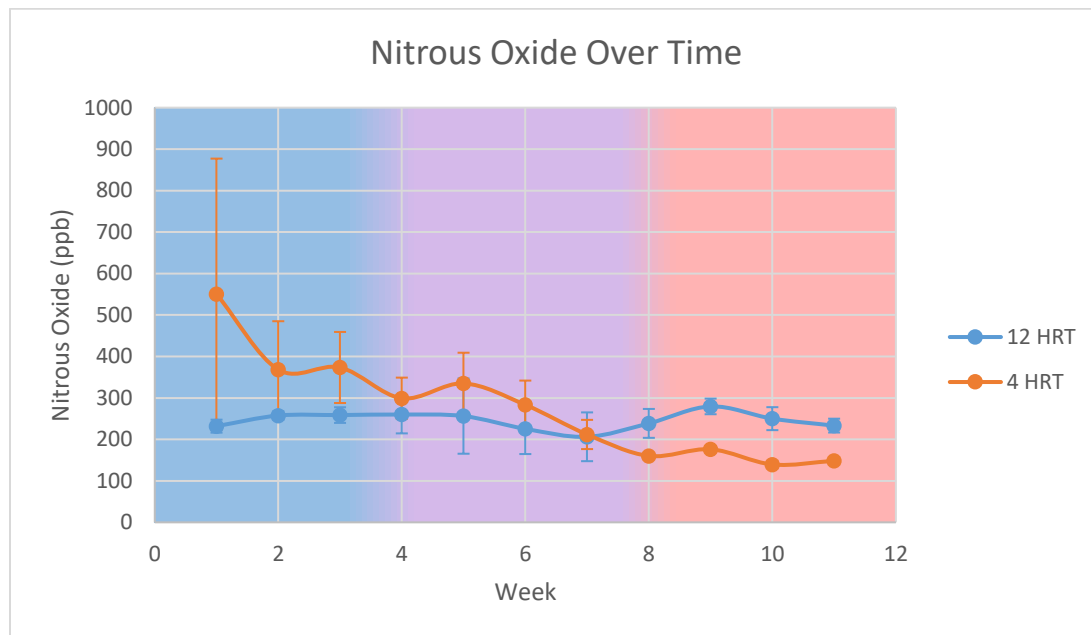


Figure 14: Nitrous oxide emissions over time for 12-hour and 4-hour hydraulic residence time (HRT). Temperature regime is indicated by background color. Blue indicates cool (6°C weeks 1-4), purple designates warming ($+2.1^{\circ}\text{C}$ each week, weeks 5-8) and red denotes warm (14.5°C , weeks 9-12) temperature regime.

Throughout the course of the experiment the nitrous oxide emissions from the 4-hour HRT reactors decreased steadily (Figure 14). This contrasts with the nitrous oxide emissions from the 12-hour HRT reactors, which remained relatively stable at about 250

ppb, except for a slight increase between weeks eight through ten. For the first seven weeks, the emissions from the 4-hour HRT treatments were higher than those of the 12-hour HRT treatments. Following week seven, the 12-hour HRT emissions were higher than those of the 4-hour HRT reactors (Figure 14).

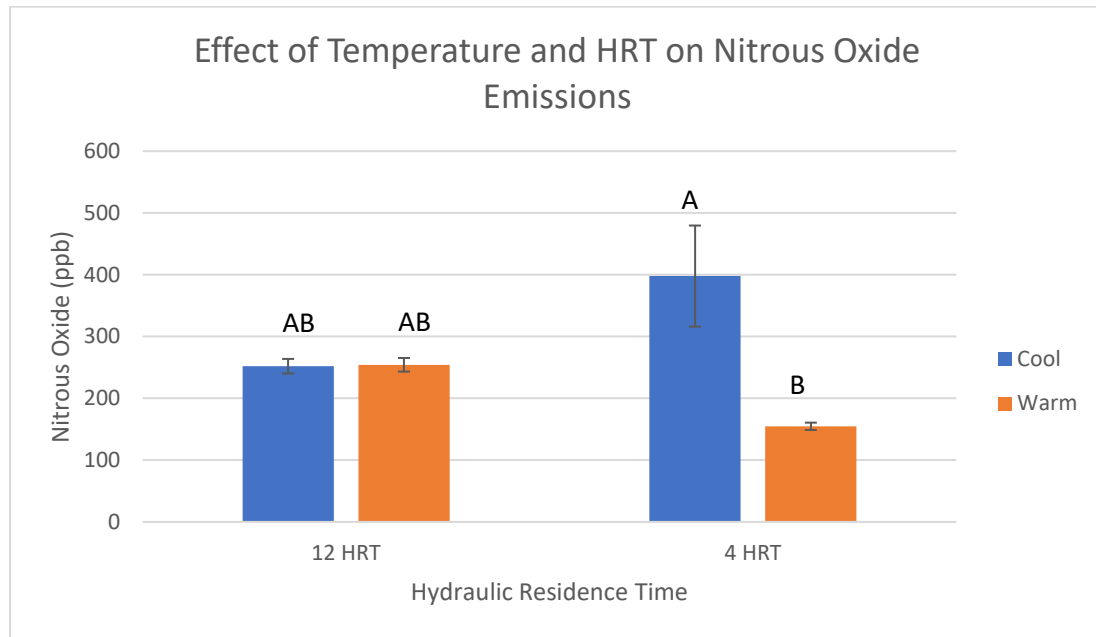


Figure 15: Effect of temperature and hydraulic residence time (HRT) on nitrous oxide emissions for 12-hour and 4-hour HRT for both cool (6°C, weeks 1-4) and warm (14.5°C, weeks 9-12) temperature regimes. Identical letters indicate no statistically significant difference, different letters denote statistical significance (two-way ANOVA; $p < 0.05$).

A significant effect of temperature on nitrous oxide emissions was observed for 4-hour HRT, with the cool temperature regime (6°C, weeks 1-4) having significantly higher emissions than the warm temperature regime (14.5°C, weeks 9-12) (Figure 15; $p < 0.006$). Conversely, there were no observed significant differences between cool and warm temperature regime nitrous oxide emissions for the 12-hour HRT reactors. No significant differences between 12-hour and 4-hour HRT for the two temperature regimes were

perceived, however, there was a significant interaction between HRT and temperature (Figure 15; $p=0.016$).

Percent Phosphate Removed

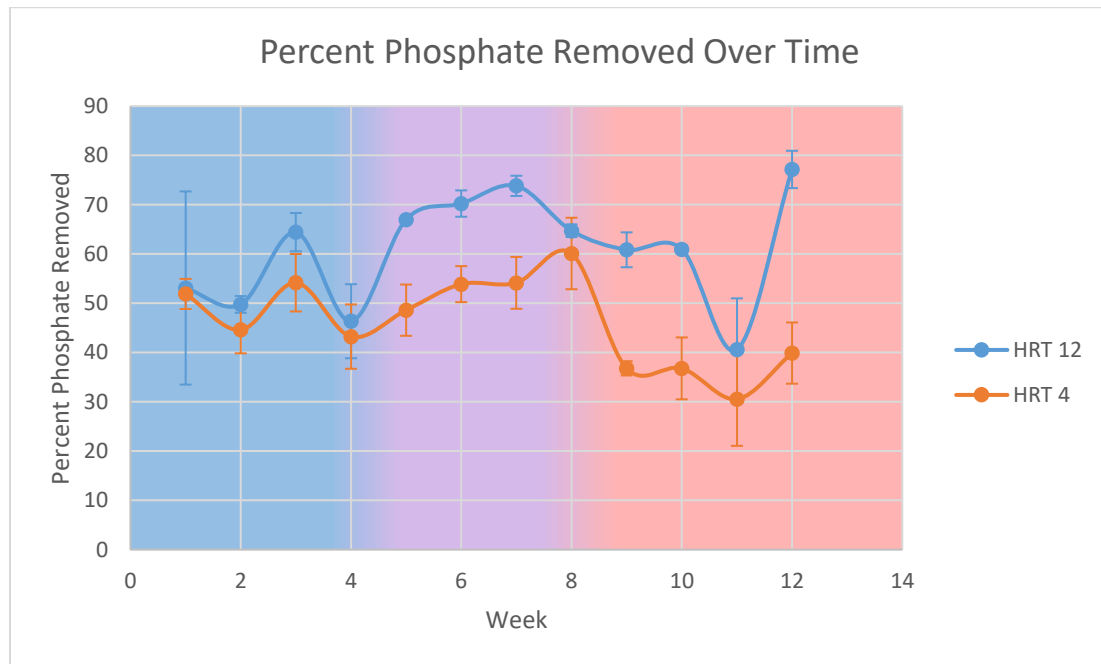


Figure 16: Percent phosphate removed over time for 12-hour and 4-hour hydraulic residence time (HRT). Temperature regime is indicated by background color. Blue indicates cool (6°C weeks 1-4), purple designates warming (+2.1°C each week, weeks 5-8) and red denotes warm (14.5°C, weeks 9-12) temperature regime.

Percent phosphate removed was higher for the 12-hour HRT reactors than the 4-hour HRT reactors for the entirety of the experiment (Figure 16). Both HRTs demonstrated an increase in percent phosphate removed during the warming temperature regime (+2.1°C each week, weeks 5-8), followed by decreasing percent phosphate removed during the warm temperature regime (14.5°C, weeks 9-12), except for an increase during week twelve.

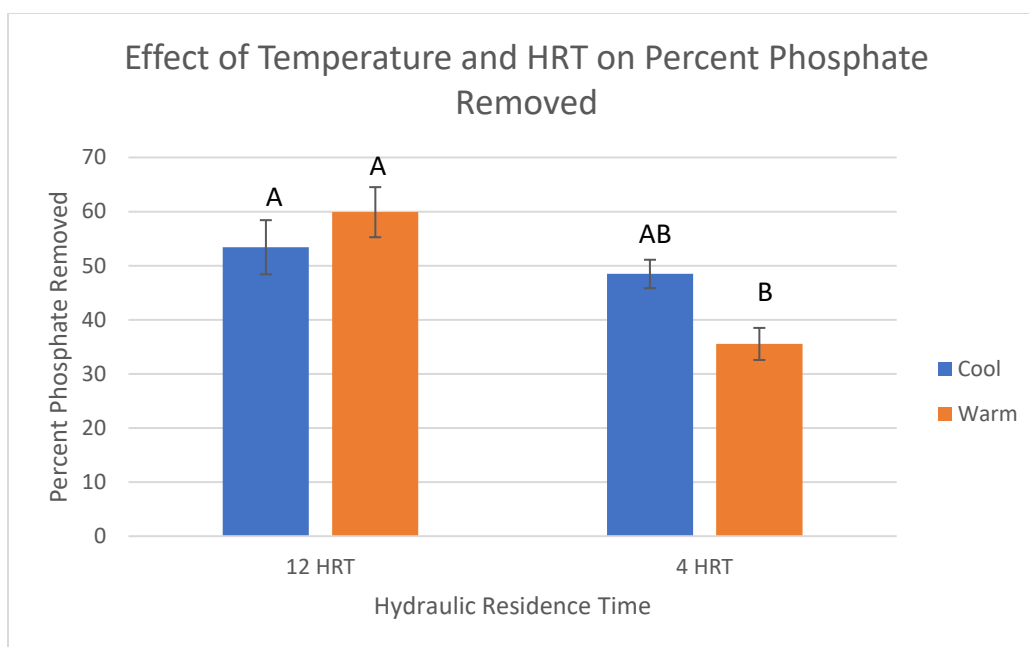


Figure 17: Effect of temperature and hydraulic residence time (HRT) on percent phosphate removed for 12-hour and 4-hour HRT and for both cool (6°C, weeks 1-4) and warm (14.5°C, weeks 9-12) temperature regimes. Identical letters indicate no statistically significant difference, different letters denote statistical significance (two-way ANOVA; $p < 0.05$).

During the warm temperature regime (14.5°C, weeks 9-12), the 12-hour HRT reactors had significantly higher percent phosphate removed than the 4-hour HRT reactors (Figure 17; $p < 0.001$). There were no other statistically significant differences between the different residence times during the cold temperature regime (6°C, weeks 1-4). Furthermore, no statistically significant differences were observed between the two temperature regimes. Overall percent phosphate removed values ranged from approximately 35%-60% throughout the length of the experiment (Figure 17).

pH

The pH of the influent remained around 8.2 through the extent of the experiment (Appendix B: Additional Chemical Parameters of Bioreactor Troughs; Figure 46). The pH of the effluent for both the 12-hour and the 4-hour HRT were considerably lower than the

pH of the influent and remained constant through the cold (6°C, weeks 1-4) and warming (+2.1°C each week, weeks 5-8) temperature regime, but showed a gradual decrease during the warm (14.5°C, weeks 9-12) temperature regime. Furthermore, the pH of the 12-hour HRT reactor effluent was lower than that of the 4-hour HRT reactors (Appendix B: Additional Chemical Parameters of Bioreactor Troughs; Figure 46).

Change in pH was calculated by subtracting daily influent values from daily effluent values for each bioreactor trough and obtaining the average of these values across the different temperature and HRT treatments. It was found that there was a significantly larger decrease in pH for 12-hour HRT than 4-hour HRT for both cool (6°C, weeks 1-4) and warm (14.5°C, weeks 9-12) temperature regimes (Appendix B: Additional Chemical Parameters of Bioreactor Troughs; Figure 47; $p < 0.001$). The 12-hour HRT treatment decreased the pH by 1.4 throughout the cool and warm temperature regimes, while the 4-hour HRT decreased the pH by about 1.2 for both temperature regimes.

Ammonia

After an initial increase in inflow concentration of ammonia, the inflow concentration remained between 0.6 mg/L and 0.8 mg/L for the remainder of the experiment (Appendix B: Additional Chemical Parameters of Bioreactor Troughs; Figure 48). Both the 12-hour and 4-hour HRT had an increase in ammonia concentration during week three, but then decreased throughout the rest of the experiment. Overall ammonia concentrations for inflow, 12-hour and 4-hour HRT never exceeded 0.9 mg/L (Appendix B: Additional Chemical Parameters of Bioreactor Troughs; Figure 48).

Nitrite

Throughout the course of the experiment the inflow concentration of nitrite remained at 0 mg/L (Appendix B: Additional Chemical Parameters of Bioreactor Troughs; Figure 49). The 12-hour and 4-hour HRT effluent concentrations of nitrite demonstrated an increase at weeks four and five, followed with a decrease for the following three weeks. For the last four weeks of the experiment the nitrite concentration remained at about 0 mg/L for both the 12-hour and 4-hour HRT. Nitrite concentrations for the inflow, 12-hour and 4-hour HRT never exceeded 0.5 mg/L (Appendix B: Additional Chemical Parameters of Bioreactor Troughs; Figure 49).

Sulfide

Concentrations of sulfide in the bioreactors varied throughout the experiment for both 12-hour and 4-hour HRT, but remained at 0 mM for the influent from week 5 onward (Appendix B: Additional Chemical Parameters of Bioreactor Troughs; Figure 50). Both 12-hour and 4-hour HRT showed a slight decrease in sulfide during the cold temperature regime (6°C, weeks 1-4) and a slight increase during the warm temperature regime (14.5°C, weeks 9-12), however, there was variance between the replicate reactors. The overall concentrations of sulfide for 12-hour, 4-hour HRT and inflow were consistently less than 0.6 mM throughout the experiment (Appendix B: Additional Chemical Parameters of Bioreactor Troughs; Figure 50).

Methane

Methane emissions never exceeded 82 ppm, and remained under 20 ppm until week 4 for the 4-hour HRT and until week 8 for the 12-hour HRT (Appendix B: Additional

Chemical Parameters of Bioreactor Troughs; Figure 51). At week 4, the 4-hour HRT reactors had increasing methane emissions, when temperatures began increasing. At week 8, the 12-hour HRT reactors also had increasing methane emissions, when temperatures were maintained at 14.5°C. From weeks 4 until week 11, the 4-hour HRT reactors had higher methane emissions than the 12-hour HRT reactors, however the difference in emissions were not statistically significant.

Nitrate Concentration Along Bioreactor Length

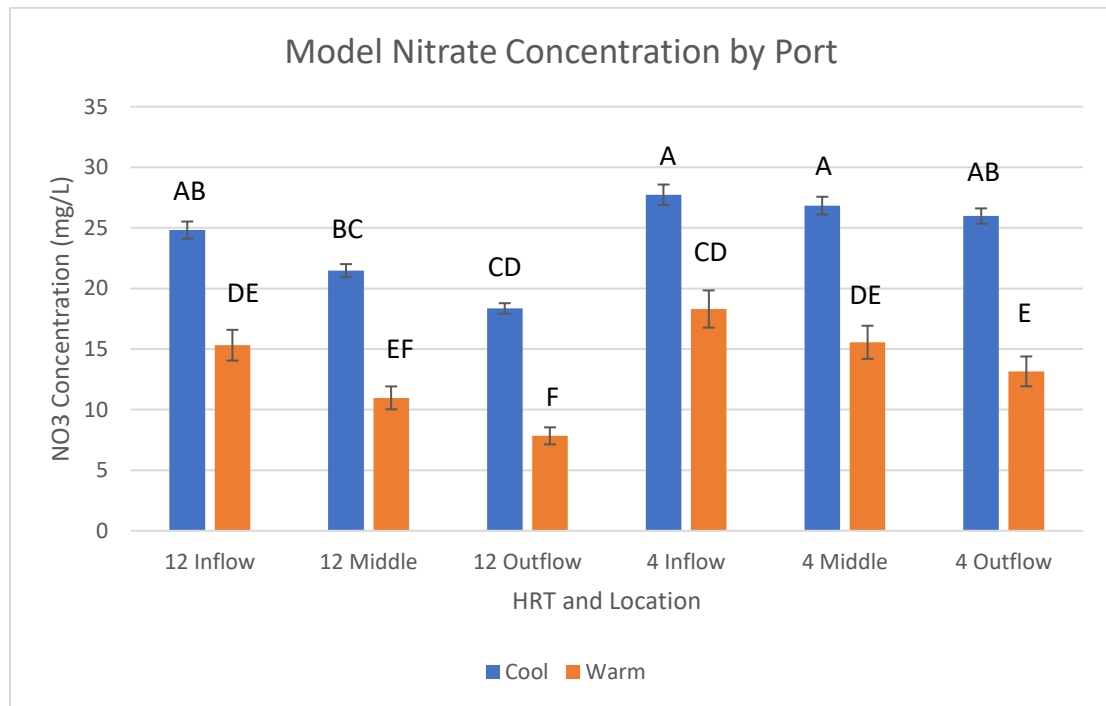


Figure 18: Concentration of nitrate by sampling port along the length of the reactor for 12-hour and 4-hour HRT under cool (6°C, weeks 1-4) and warm (14.5°C, weeks 9-12) temperature regimes. Nitrate concentrations were modeled using the hydraulic model developed by (Krider, 2018). Identical letters indicate a significant difference, while similar letters indicate no difference (three-way ANOVA; $p < 0.05$).

Using the numerical hydraulic model developed by (Krider, 2018), nitrate concentrations were modeled along the length of the bioreactor to obtain values for nitrate

concentrations at each sampling port for each separate reactor. There were significantly lower concentrations between the inflow sampling port and the outflow sampling port for the 12-hour HRT cool (6°C, weeks 1-4) and warm (14.5°C, weeks 9-12) temperature regimes, as well as the 4-hour HRT warm temperature regime (Figure 18; $p < 0.05$). There were no significant differences found for nitrate concentrations along the length of the 4-hour HRT reactors under cool temperatures, however, all reactors followed a similar trend of decreasing nitrate concentrations along the length of the bioreactors. Furthermore, the nitrate concentrations at each port were significantly lower during warm temperatures than cool temperatures for both 4-hour and 12-hour HRT (Figure 18; $p < 0.001$).

Biological Data

Table 5: p-values of comparisons to show the effect of cool (6°C, weeks 1-4) and warm (14.5°C, weeks 9-12) temperature regimes, and 12-hour and 4-hour hydraulic residence time (HRT) on 16S rRNA, *nirK*, *nirS*, *nosZ* clade I (1) and *nosZ* clade II (2) gene copy numbers at inflow (I), middle (M) and outflow (O) sampling locations (post-hoc t-tests). Highlighted values indicate a significant correlation.

	Effect of HRT (Cool)	Effect of HRT (Warm)	Effect of Temp (12-hr)	Effect of Temp (4-hr)
16S I	0.01	0.02	0.005	0.005
16S M	0.994	0.997	1	0.949
16S O	1	0.98	1	0.895
<i>nirK</i> I	0.975	1	0.013	0.877
<i>nirK</i> M	0.999	1	1	1
<i>nirK</i> O	1	1	1	1
<i>nirS</i> I	0.001	0.178	0.977	0.055
<i>nirS</i> M	0.998	0.428	0.997	0.003
<i>nirS</i> O	0.999	0.396	0.992	0.002
<i>nosZ</i> (1) I	0.537	0.225	0.988	0.02
<i>nosZ</i> (1) M	0.877	0.077	0.818	0.089
<i>nosZ</i> (1) O	1	0.491	0.796	0.763
<i>nosZ</i> (2) I	0.001	0.002	0.008	0.003
<i>nosZ</i> (2) M	0.994	0.083	1	0.003
<i>nosZ</i> (2) O	0.998	0.647	1	0.277

A significant effect of HRT and temperature was noted for total bacteria gene copy numbers only at the inflow sampling location (Table 5). Significantly higher gene copy numbers were found with longer HRT for both cool (6°C, weeks 1-4) and warm (14.5°C, weeks 9-12) temperature regimes for 16S rRNA, similarly, significantly higher 16S rRNA gene copy numbers were also observed at the warm temperature regime than the cool temperature regime for both 12-hour and 4-hour HRT at the inflow sampling location. Significantly higher *nirK* gene copy numbers were only observed at the inflow sampling location during warm temperatures than cool temperatures, however this was only under the 12-hour HRT (Table 5). Significantly higher *nirS* gene copy numbers were noted during warm temperature regimes under the 4-hour HRT at the middle and outflow sampling locations. There was also a significant effect of HRT observed on *nirS* gene copy numbers during the cool temperature regime at the inflow sampling location. Only one significant effect was found for *nosZ* clade I, there were significantly higher *nosZ* clade I gene copy numbers during the warm temperature regime than the cool under the 4-hour HRT at the inflow sampling locations. A significant effect of HRT and temperature was noted for *nosZ* clade II gene copy numbers at the inflow sampling location (Table 5). Significantly higher gene copy numbers were found with longer HRT for both cool and warm temperature regimes for *nosZ* clade II, similarly, significantly higher *nosZ* clade II gene copy numbers were also observed at the warm temperature regime than the cool temperature regime for both 12-hour and 4-hour HRT. A significant effect of temperature on *nosZ* clade II gene copy numbers was also noted at the middle sampling location for the 4-hour HRT (Table 5).

Table 6: p-values showing the effect of location between inflow, middle and outflow sampling locations for 16S rRNA, *nirK*, *nirS*, *nosZ* clade I (1) and *nosZ* clade II (2) under cool (6°C, weeks 1-4) and warm (14.5°C, weeks 9-12) temperature regimes and 12-hour and 4-hour hydraulic residence time (HRT) (post hoc, t-tests). Highlighted values indicate a significant correlation.

	Inflow & Middle	Inflow & Outflow	Middle & Outflow
16S 12&warm	0.001	0.001	1
16S 4&warm	0.002	0.005	1
16S 12&cool	0.001	0.001	1
16S 4&cool	0.057	0.073	1
<i>nirK</i> 12&warm	0.087	0.04	1
<i>nirK</i> 4&warm	0.028	0.029	1
<i>nirK</i> 12&cool	0.067	0.025	0.999
<i>nirK</i> 4&cool	0.148	0.156	1
<i>nirS</i> 12&warm	0.088	0.098	1
<i>nirS</i> 4&warm	0.637	0.571	1
<i>nirS</i> 12&cool	0.026	0.022	1
<i>nirS</i> 4&cool	0.882	0.867	1
<i>nosZ</i> (1) 12&warm	0.986	0.832	0.994
<i>nosZ</i> (1) 4&warm	1	0.54	0.638
<i>nosZ</i> (1) 12&cool	1	0.97	0.883
<i>nosZ</i> (1) 4&cool	0.943	0.99	1
<i>nosZ</i> (2) 12&warm	0.001	0.001	0.997
<i>nosZ</i> (2) 4&warm	0.911	0.091	0.553
<i>nosZ</i> (2) 12&cool	0.001	0.001	0.998
<i>nosZ</i> (2) 4&cool	0.689	0.498	1

No significant differences in gene copy numbers for all target genes were noted between middle and outflow locations for all temperature regime and HRT combinations (Table 6). Significantly higher gene copy numbers for 16S rRNA at the inflow location than the middle and outflow sampling locations were noted for 12-hour HRT and warm (14.5°C, weeks 9-12), 4-hour HRT and warm, and 12-hour HRT and cool (6°C, weeks 1-4) temperature regime (Table 6). Significantly higher *nirK* gene copy numbers were observed at the inflow than the outflow sampling location for 12-hour HRT and warm and cool temperature regimes as well as the 4-hour HRT and warm temperature regime. A

significant effect of location on *nirK* gene copy numbers was also observed between the inflow and middle sampling locations during the 4-hour HRT and warm temperature regime. Significantly higher *nirS* gene copy numbers were only observed during the 12-hour HRT and cool temperature regime between the inflow and middle, and inflow and outflow sampling locations. No significant effect of location was perceived on *nosZ* clade I gene copy numbers. In contrast, *nosZ* clade II gene copy numbers were significantly higher at the inflow than the middle and outflow sampling locations for the 12-hour HRT and warm and cool temperature regimes. This finding was not replicated for the 4-hour HRT (Table 6).

16S rRNA

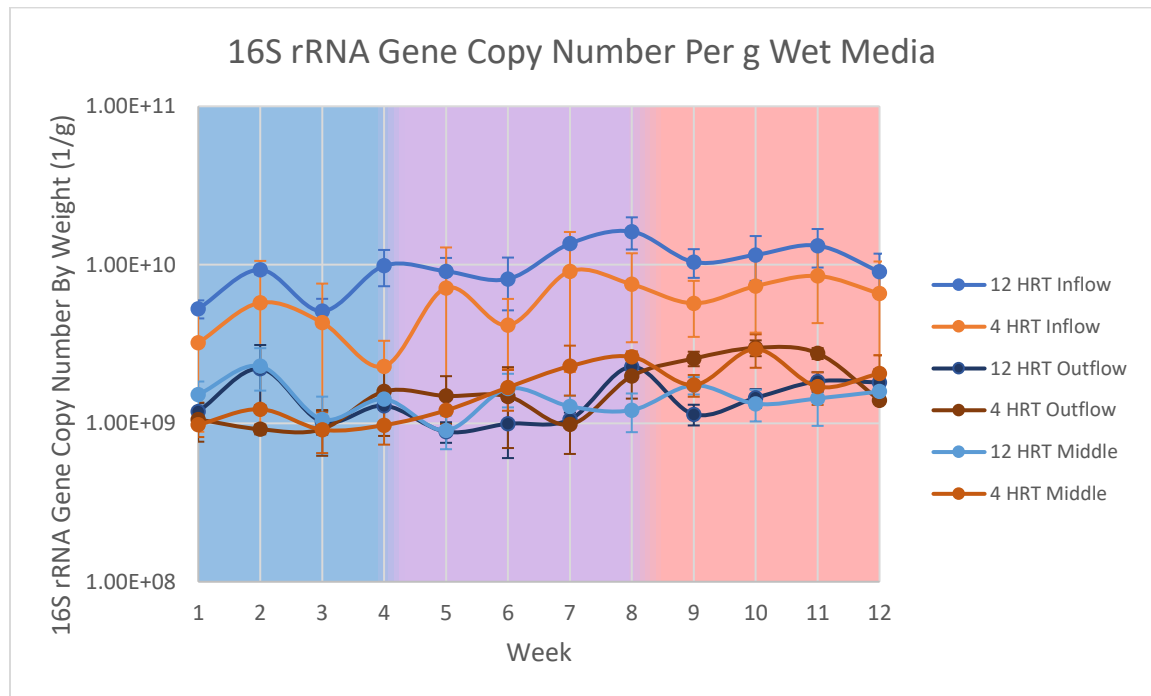


Figure 19: 16S rRNA gene copy number per gram of wet bioreactor media over time for 12-hour hydraulic residence time (HRT) and 4-hour HRT inflow, middle and outflow sampling locations. Temperature regime is indicated by background color. Blue indicates

cool (6°C weeks 1-4), purple designates warming (+2.1°C each week, weeks 5-8) and red denotes warm (14.5°C, weeks 9-12) temperature regime.

Over the course of the experiment, the gene copy number for the total bacteria 16S rRNA for the middle and outflow sampling points for both the 12-hour and 4-hour HRT remained between 1.00 E+09 and 1.50 E+09 (Figure 19). A slight increase in the gene copy numbers for these locations is noted during the warming (+2.1°C each week, weeks 5-8) and warm (14.5°C, weeks 9-12) temperature regimes. The inflow sampling locations for both the 12-hour and 4-hour HRT had higher 16S rRNA gene copy numbers than the middle and outflow sampling points, with both exhibiting over 1.50 E+09 gene copy numbers for the majority of the experiment. A slight increase during the warming and warm temperature regime is also noted for the inflow sampling points for both HRT (Figure 19).

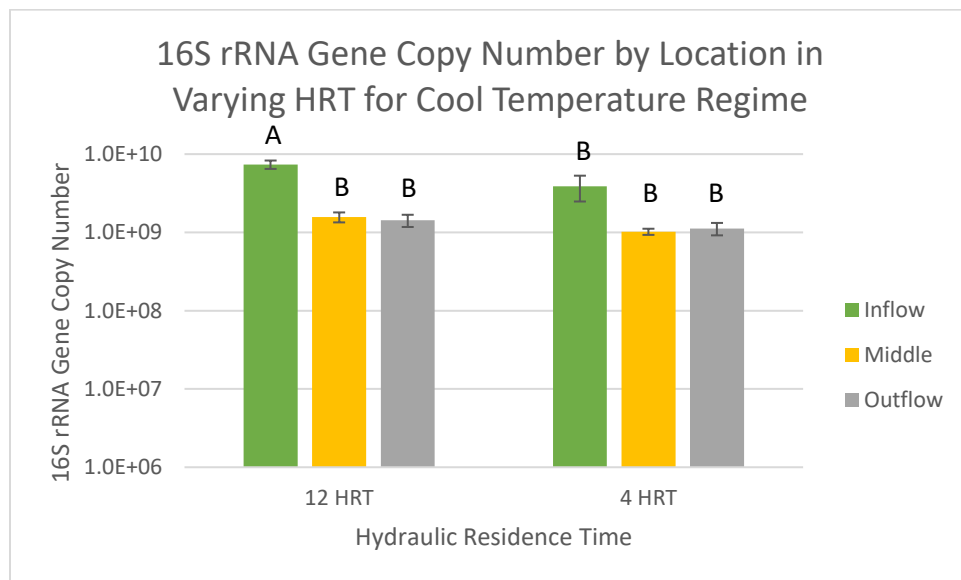


Figure 20: Effect of location and hydraulic residence time (HRT) on 16S rRNA gene copy numbers during the cool (6°C, weeks 1-4) temperature regime for 12-hour and 4-hour HRT and for inflow, middle and outflow sampling locations. Identical letters indicate no statistically significant difference, different letters denote statistical significance (two-way ANOVA; $p < 0.05$).

While higher 16S rRNA gene copy numbers were found at the inflow location than the middle and outflow, no significant difference was observed between inflow, middle and outflow sampling locations during the 4-hour HRT under the cool (6°C, weeks 1-4) temperature regime. Nevertheless, there were significantly higher 16S rRNA gene copy numbers at the inflow sampling location than the middle and outflow for the 12-hour HRT under the cool temperature regime (Figure 20; $p < 0.001$). Accordingly, there were also significantly higher 16S rRNA gene copy numbers for the 12-hour HRT than the 4-hour HRT at the inflow, however this significant effect of HRT was not found between the other sampling locations (Figure 20; $p < 0.010$).

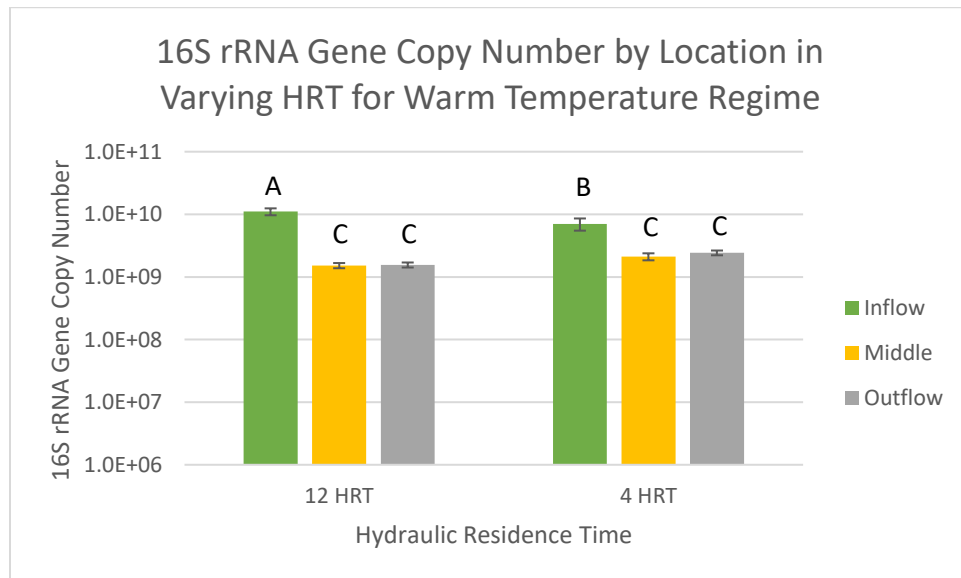


Figure 21: Effect of location and hydraulic residence time (HRT) on 16S rRNA gene copy numbers during the warm (14.5°C, weeks 9-12) temperature regime for 12-hour and 4-hour HRT and for inflow, middle and outflow sampling locations. Identical letters indicate no statistically significant difference, different letters denote statistical significance (two-way ANOVA; $p < 0.05$).

Significantly higher 16S rRNA gene copy numbers were found for the inflow than the middle and outflow sampling locations for both the 12-hour and 4-hour HRT under the warm temperature regime (14.5°C, weeks 9-12) (Figure 21; $p < 0.001$ for 12-hour HRT

inflow vs middle and outflow; $p < 0.002$ for 4-hour HRT inflow vs middle; and $p < 0.005$ 4-hour HRT inflow vs outflow). There were also significantly higher 16S rRNA gene copy numbers discovered for the 12-hour HRT than the 4-hour HRT at the inflow sampling location, this finding was not noted between the two hydraulic residence times at the other sampling locations (Figure 21; $p < 0.001$).

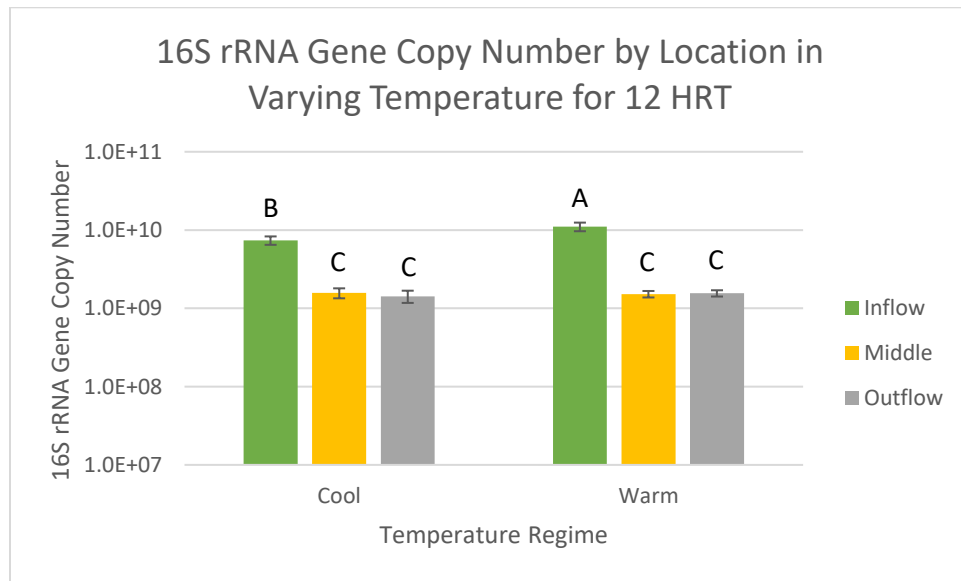


Figure 22: Effect of location and temperature regime on 16S rRNA gene copy numbers during 12-hour hydraulic residence time (HRT) for cool (6°C, weeks 1-4) and warm (14.5°C, weeks 9-12) temperature regimes and for inflow, middle and outflow sampling locations. Identical letters indicate no statistically significant difference, different letters denote statistical significance (two-way ANOVA; $p < 0.05$).

No significant difference was discovered between the cool (6°C, weeks 1-4) and warm (14.5°C, weeks 9-12) temperature regimes for 16S rRNA gene copy numbers at the middle and outflow sampling locations at 12-hour HRT (Figure 22). However, the 16S rRNA gene copy numbers at the inflow location for the warm temperature regime and 12-hour HRT were significantly higher than those at the inflow of the cool temperature regime (Figure 22; $p < 0.005$). There were also significantly higher 16S rRNA gene copy numbers

at the inflow locations for both cool and warm temperature regimes than their respective middle and outflow sampling locations (Figure 22; $p < 0.001$).

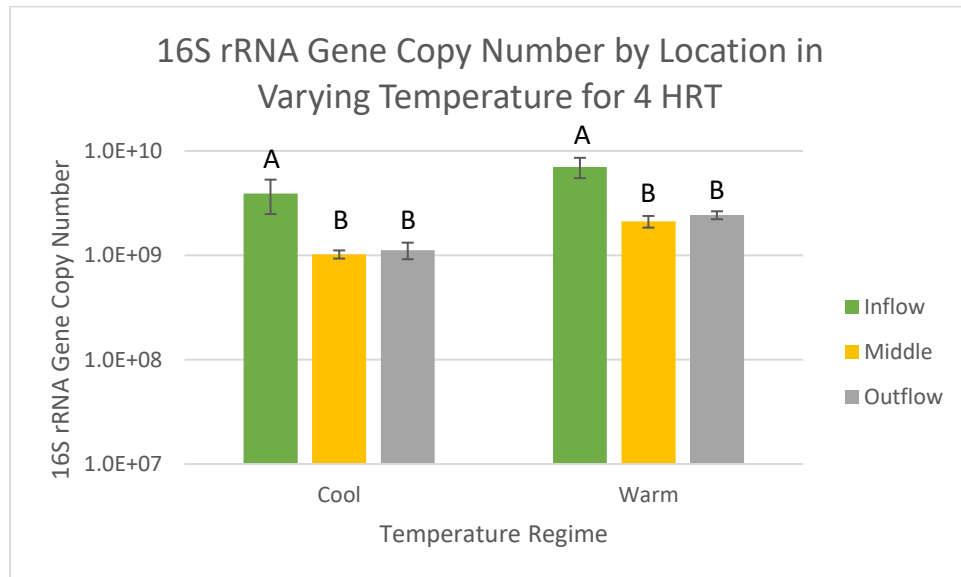


Figure 23: Effect of location and temperature regime on 16S rRNA gene copy numbers during 4-hour hydraulic residence time (HRT) for cool (6°C, weeks 1-4) and warm (14.5°C, weeks 9-12) temperature regimes and for inflow, middle and outflow sampling locations. Identical letters indicate no statistically significant difference, different letters denote statistical significance (two-way ANOVA; $p < 0.05$).

Significantly higher 16S rRNA gene copy numbers were found at the inflow locations than both middle and outflow for both cool (6°C, weeks 1-4) and warm (14.5°C, weeks 9-12) temperature regimes under 4-hour HRT (Figure 23; $p < 0.002$ for warm; $p < 0.005$ for cool). No significant differences were observed between the two temperature regimes when comparing corresponding locations.

nirK (Nitrite Reductase)

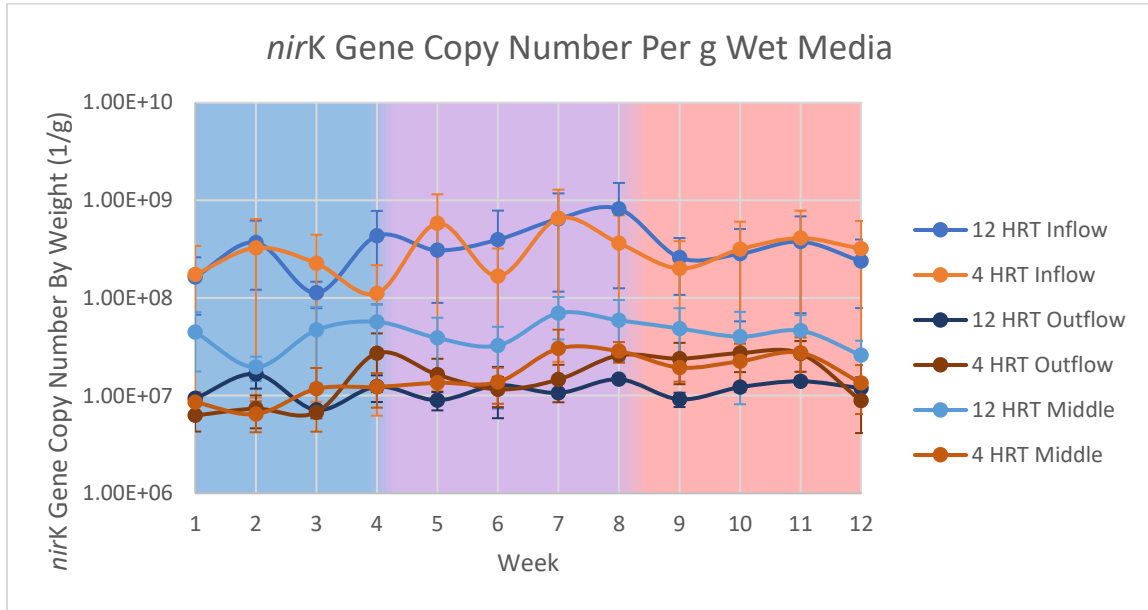


Figure 24: *nirK* gene copy number per gram of wet bioreactor media over time for 12-hour hydraulic residence time (HRT) and 4-hour HRT inflow, middle and outflow sampling locations. Temperature regime is indicated by background color. Blue indicates cool (6°C weeks 1-4), purple designates warming (+2.1°C each week, weeks 5-8) and red denotes warm (14.5°C, weeks 9-12) temperature regime.

During the length of the experiment the inflow gene copy numbers of *nirK* for both the 12-hour and 4-hour HRT remained higher than those from the middle and outflow locations of both residence times (Figure 24). The inflow sampling locations maintained *nirK* gene copy numbers above 1.00 E+08 throughout the entire experiment, while the other sampling locations never exceeded that amount. The *nirK* gene copy numbers for the middle sampling location with 12-hour HRT also remained above those of the middle and outflow locations of the 4-HRT, as well as the outflow of the 12-hour HRT. No increase or decrease during certain temperature regimes was noticeable.

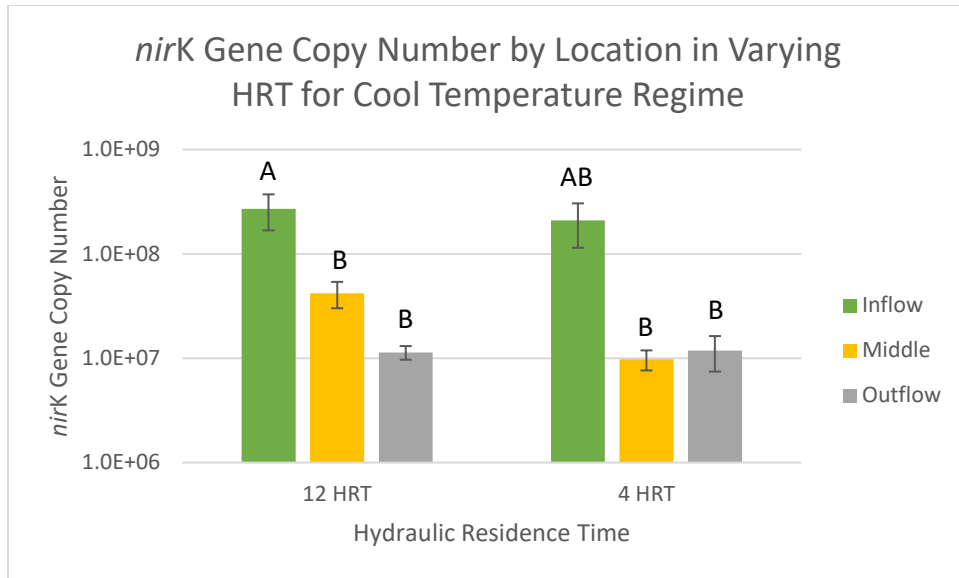


Figure 25: Effect of location and hydraulic residence time (HRT) on *nirK* gene copy numbers during the cool temperature regime (6°C, weeks 1-4) for 12-hour and 4-hour HRT and for inflow, middle and outflow sampling locations. Identical letters indicate no statistically significant difference, different letters denote statistical significance (two-way ANOVA; $p < 0.05$).

While no significant difference between *nirK* gene copy numbers between middle and outflow locations for 12-hour HRT were found, there were significantly higher *nirK* gene copy numbers at the inflow sampling locations than both the middle and the outflow under the cool temperature regime (6°C, weeks 1-4) (Figure 25; $p < 0.025$). No significant differences were found between the three sampling locations in the 4-hour HRT for the cool temperature regime. There were also no significant differences observed between the two hydraulic residence times and their corresponding sampling locations.

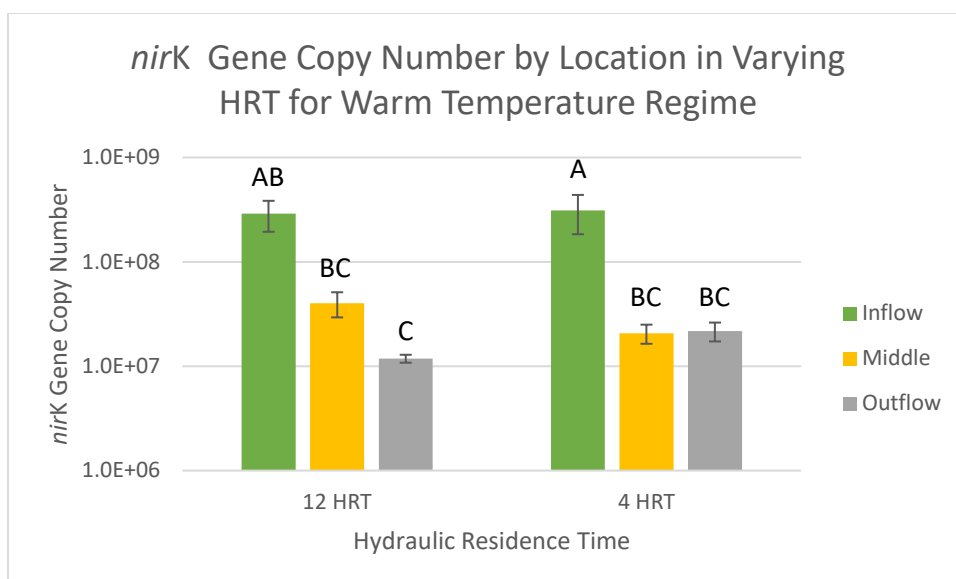


Figure 26: Effect of location and hydraulic residence time (HRT) on *nirK* gene copy numbers during the warm temperature regime (14.5°C, weeks 9-12) for 12-hour and 4-hour HRT and for inflow, middle and outflow sampling locations. Identical letters indicate no statistically significant difference, different letters denote statistical significance (two-way ANOVA; $p < 0.05$).

Significantly higher *nirK* gene copy numbers at the inflow sampling location than the middle and outflow was noted for the 4-hour HRT reactors under the warm temperature treatment (14.5°C, weeks 9-12) (Figure 26; $p < 0.025$). Similarly, the 12-hour HRT had significantly higher *nirK* gene copy numbers at the inflow, however, this was only statistically significant between the inflow and outflow sampling locations under the warm temperature regime (Figure 26; $p < 0.040$). No significant differences in *nirK* gene copy numbers between the two HRT were noted when comparing corresponding sampling locations.

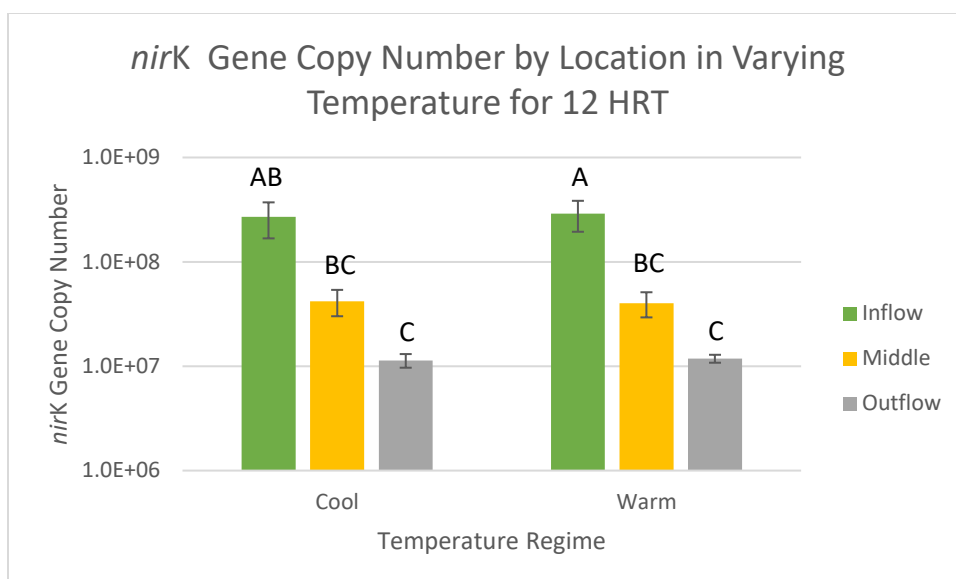


Figure 27: Effect of location and temperature regime on *nirK* gene copy numbers during 12-hour hydraulic residence time (HRT) for cool (6°C, weeks 1-4) and warm (14.5°C, weeks 9-12) temperature regimes and for inflow, middle and outflow sampling locations. Identical letters indicate no statistically significant difference, different letters denote statistical significance (two-way ANOVA; $p < 0.05$).

While no significant difference between the inflow and middle sampling locations for the cool temperature regime (6°C, weeks 1-4) was noted, there were significantly higher *nirK* gene copy numbers at the inflow than both the middle and outflow locations for the warm temperature regime (14.5°C, weeks 9-12) under 12-hour HRT (Figure 27; $p < 0.035$ and $p < 0.013$, respectively). Nevertheless, significantly higher *nirK* gene copy numbers were discerned at the inflow than the outflow sampling locations for the cool temperature regime under 12-hour HRT (Figure 27; $p < 0.026$). In contrast, no significant differences were discovered between the two temperature regimes when comparing *nirK* gene copy numbers between corresponding sampling locations.

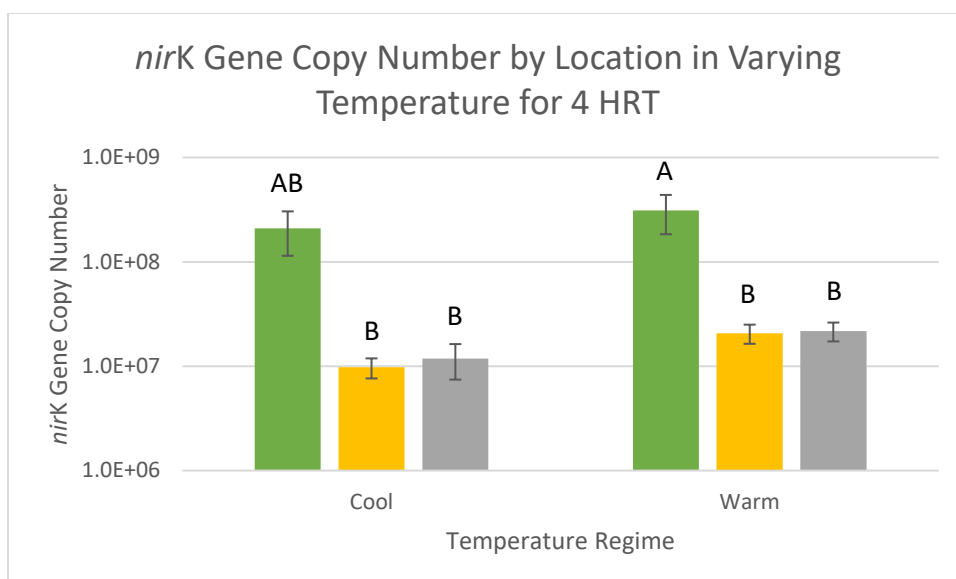


Figure 28: Effect of location and temperature regime on *nirK* gene copy numbers during 4-hour hydraulic residence time (HRT) for cool (6°C, weeks 1-4) and warm (14.5°C, weeks 9-12) temperature regimes and for inflow, middle and outflow sampling locations. Identical letters indicate no statistically significant difference, different letters denote statistical significance (two-way ANOVA; $p < 0.05$).

Significantly higher *nirK* gene copy numbers were found at the inflow location than the middle and outflow sampling locations for the warm temperature regime (14.5°C, weeks 9-12) at 4-hour HRT (Figure 28; $p < 0.027$ and $p < 0.028$, respectively). This trend was also exhibited for the *nirK* gene copy numbers at the varying locations for the cool temperature regime (6°C, weeks 1-4), however, this finding was not significant. Additionally, there were no significant differences discovered between the *nirK* gene copy numbers of the two temperature regimes at a 4-hour HRT when comparing the corresponding sampling locations.

nirS (Nitrite Reductase)

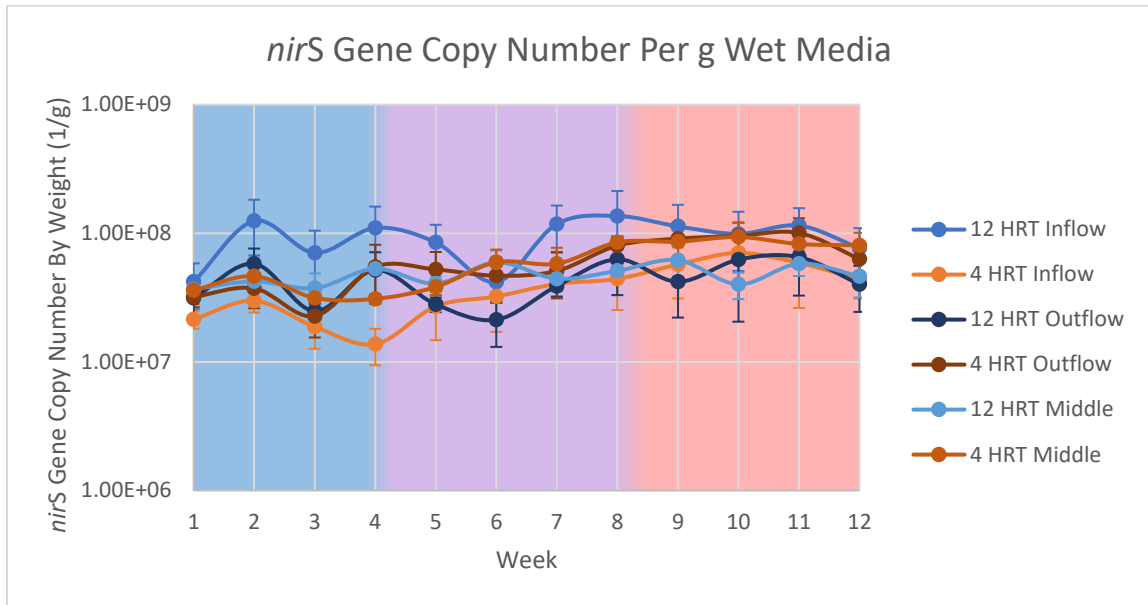


Figure 29: *nirS* gene copy number per gram of wet bioreactor media over time for 12-hour hydraulic residence time (HRT) and 4-hour HRT inflow, middle and outflow sampling locations. Temperature regime is indicated by background color. Blue indicates cool (6°C weeks 1-4), purple designates warming (+2.1°C each week, weeks 5-8) and red denotes warm (14.5°C, weeks 9-12) temperature regime.

During the length of the experiment there was some variation in *nirS* gene copy numbers, however, *nirS* gene copy numbers for all sampling locations for both 12-hour and 4-hour HRT did not vary greatly in comparison to each other, apart from the inflow *nirS* gene copy numbers for 12-hour HRT (Figure 29). Gene copy numbers of *nirS* for this treatment stayed higher than the other treatments except during week six, when it decreased. While there aren't any obvious trends in relation to *nirS* gene copy numbers during the varying temperature regimes, the gene copy numbers for all treatments, except for the 12-hour HRT inflow, see a general increase throughout the experiment.

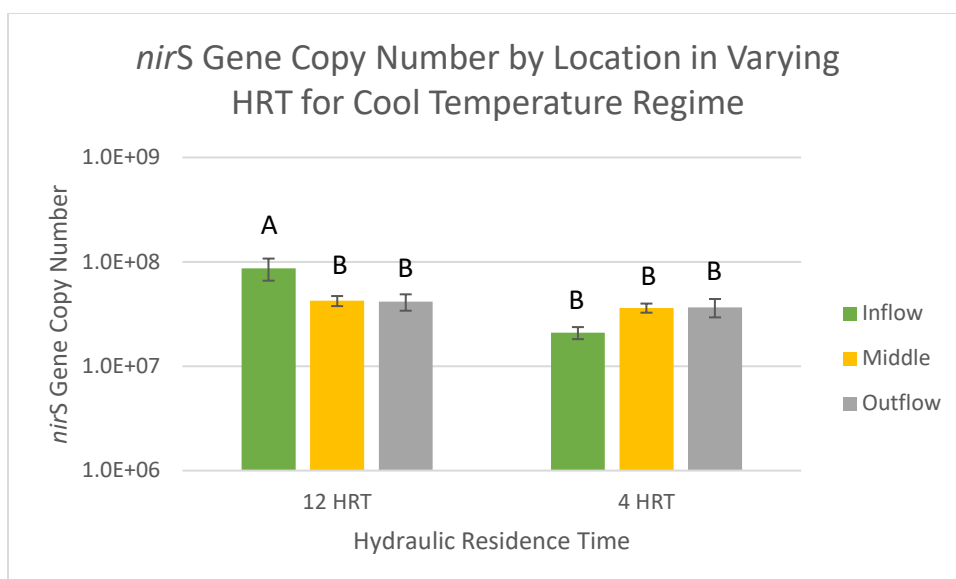


Figure 30: Effect of location and hydraulic residence time (HRT) on *nirS* gene copy numbers during the cool (6°C, weeks 1-4) temperature regime for 12-hour and 4-hour HRT and for inflow, middle and outflow sampling locations. Identical letters indicate no statistically significant difference, different letters denote statistical significance (two-way ANOVA; $p < 0.05$).

Significantly higher *nirS* gene copy numbers were found at the inflow sampling location than both the middle and outflow for 12-hour HRT under a cool temperature regime (6°C, weeks 1-4), however, this finding was not replicated in the 4-hour HRT reactors (Figure 30; $p < 0.026$ and $p < 0.022$, respectively). There were also significantly higher *nirS* gene copy numbers discovered for the 12-hour HRT than the 4-hour HRT at the inflow sampling location (Figure 30; $p < 0.001$). Conversely, there was no significant effect of HRT on the *nirS* gene copy numbers for the middle and outflow sampling locations.

No significant differences were found to occur between the varying locations under the same HRT, nor between the two HRT on corresponding sampling locations on *nirS* gene copy numbers at the warm temperature regime (14.5°C, weeks 9-12) (Appendix C: Additional Biological Data for Bioreactor Troughs; Figure 52).

No significant differences were found to occur between the varying locations under the same temperature regime, nor between the two temperature regimes on corresponding sampling locations on *nirS* gene copy numbers under 12-hour HRT (Appendix C: Additional Biological Data for Bioreactor Troughs; Figure 53).

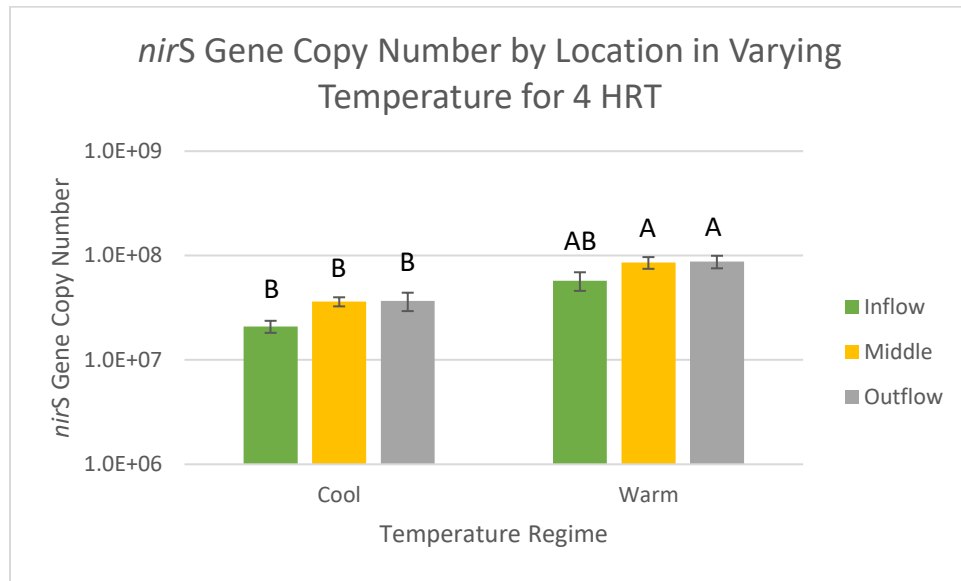


Figure 31: Effect of location and temperature regime on *nirS* gene copy numbers during 4-hour hydraulic residence time (HRT) for cool (6°C, weeks 1-4) and warm (14.5°C, weeks 9-12) temperature regimes and for inflow, middle and outflow sampling locations. Identical letters indicate no statistically significant difference, different letters denote statistical significance (two-way ANOVA; $p < 0.05$).

No statistically significant difference in *nirS* gene copy number was noted between varying locations during both the cool (6°C, weeks 1-4) and warm (14.5°C, weeks 9-12) temperature regime for 4-hour HRT (Figure 31). In contrast, there were significantly higher *nirS* gene copy numbers during the warm temperature regime than the cool temperature regime between the middle and outflow locations (Figure 31; $p < 0.003$ and $p < 0.002$, respectively). This significant difference was not observed at the inflow sampling locations between the two temperature regimes at 4-hour HRT.

nosZ Clade I (Typical Nitrous Oxide Reductase)

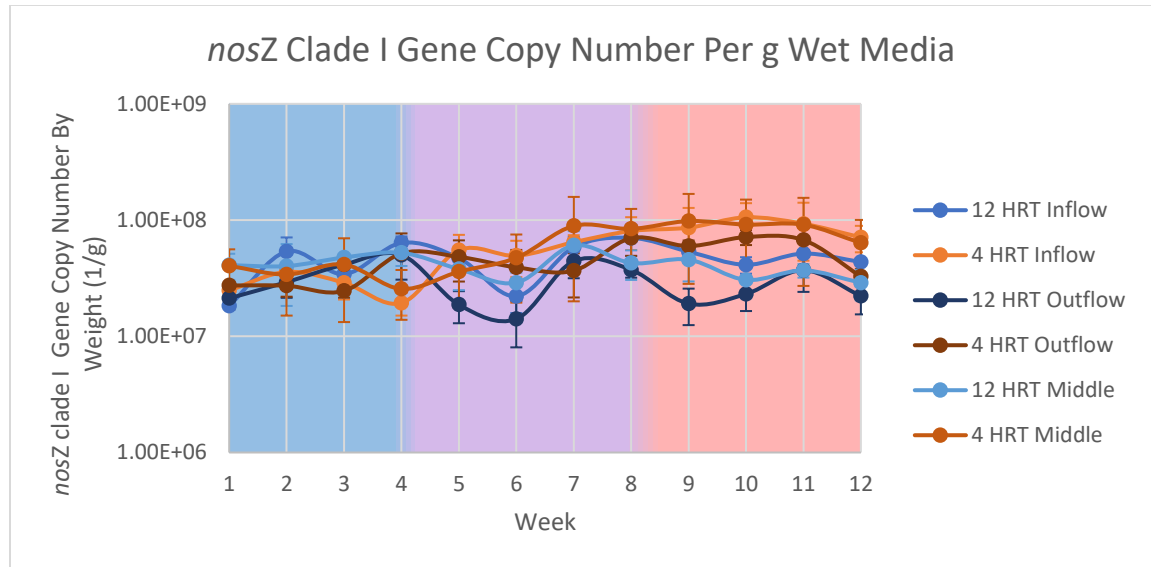


Figure 32: *nosZ* clade I gene copy number per gram of wet bioreactor media over time for 12-hour hydraulic residence time (HRT) and 4-hour HRT inflow, middle and outflow sampling locations. Temperature regime is indicated by background color. Blue indicates cool (6°C weeks 1-4), purple designates warming (+2.1°C each week, weeks 5-8) and red denotes warm (14.5°C, weeks 9-12) temperature regime.

Throughout the course of the experiment, *nosZ* clade I gene copy numbers varied slightly from week to week for each treatment, however, all treatments had similar gene copy numbers for the length of the experiment (Figure 32). A slight increase in *nosZ* clade I gene copy numbers during the warming (+2.1°C, weeks 5-8) and warm (14.5°C, weeks 9-12) months is noticeable for the 4-hour HRT inflow, middle and outflow sampling locations, but not for the 12-hour HRT reactors.

No significant differences were found to occur between the varying locations under the same HRT, nor between the two residence times on corresponding sampling locations on *nosZ* clade I gene copy numbers under the cool temperature regime (6°C, weeks 1-4) (Appendix C: Additional Biological Data for Bioreactor Troughs; Figure 54).

No significant differences were observed between the varying locations within each hydraulic residence, nor between the two HRT when comparing correlating sampling locations on *nosZ* clade I gene copy numbers under the warm temperature regime (14.5°C, weeks 9-12) (Appendix C: Additional Biological Data for Bioreactor Troughs; Figure 55).

No significant differences were found between the different sampling locations within each temperature regime, nor were any significant differences discovered between the two temperature regimes when comparing correlating sampling locations on *nosZ* clade I gene copy numbers under 12-hour HRT (Appendix C: Additional Biological Data for Bioreactor Troughs; Figure 56).

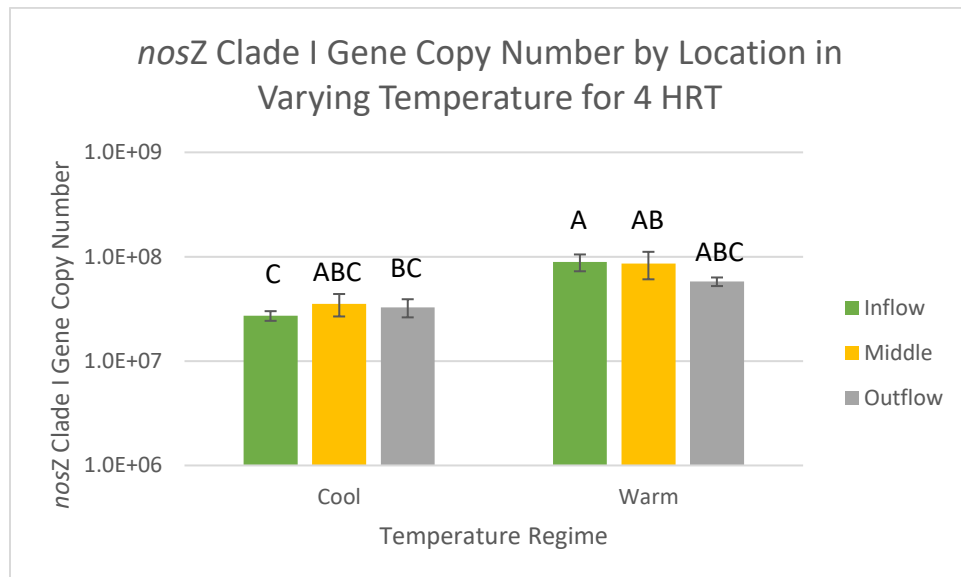


Figure 33: Effect of location and temperature regime on *nosZ* clade I gene copy numbers during 4-hour hydraulic residence time (HRT) for cool (6°C, weeks 1-4) and warm (14.5°C, weeks 9-12) temperature regimes and for inflow, middle and outflow sampling locations. Identical letters indicate no statistically significant difference, different letters denote statistical significance (two-way ANOVA; $p < 0.05$).

No significant differences were found between sampling locations within the cool (6°C, weeks 1-4) and warm (14.5°C, weeks 9-12) temperature regimes, however, there were significantly higher *nosZ* clade I gene copy numbers under the warm temperature

regime than the cool at the inflow sampling location under 4-hour HRT (Figure 33; $p < 0.020$). In contrast, significant differences were not found between the two temperature regimes for the other corresponding sampling locations.

nosZ Clade II (Atypical Nitrous Oxide Reductase)

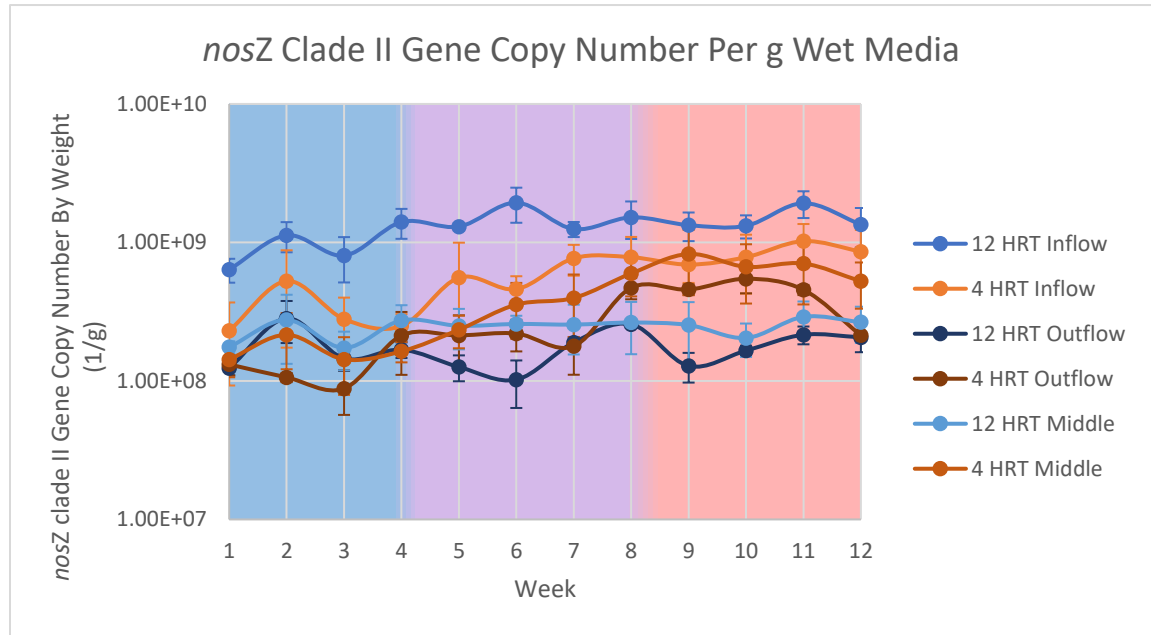


Figure 34: *nosZ* clade II gene copy number per gram of wet bioreactor media over time for 12-hour hydraulic residence time (HRT) and 4-hour HRT inflow, middle and outflow sampling locations. Temperature regime is indicated by background color. Blue indicates cool (6°C weeks 1-4), purple designates warming (+2.1°C each week, weeks 5-8) and red denotes warm (14.5°C, weeks 9-12) temperature regime.

The inflow sampling locations for both the 12-hour and 4-hour HRT maintained slightly higher *nosZ* clade II gene copy numbers than their respective HRT middle and outflow locations throughout the course of the experiment (Figure 34). While changes during the varying temperature regimes is difficult to discern, a gradual upward trend in *nosZ* clade II gene copy numbers during the warm (14.5°C, weeks 9-12) and warming (+2.1°C each week, weeks 5-8) temperature regimes appear to occur for the 12-hour HRT inflow, and the 4-hour inflow and middle sampling locations.

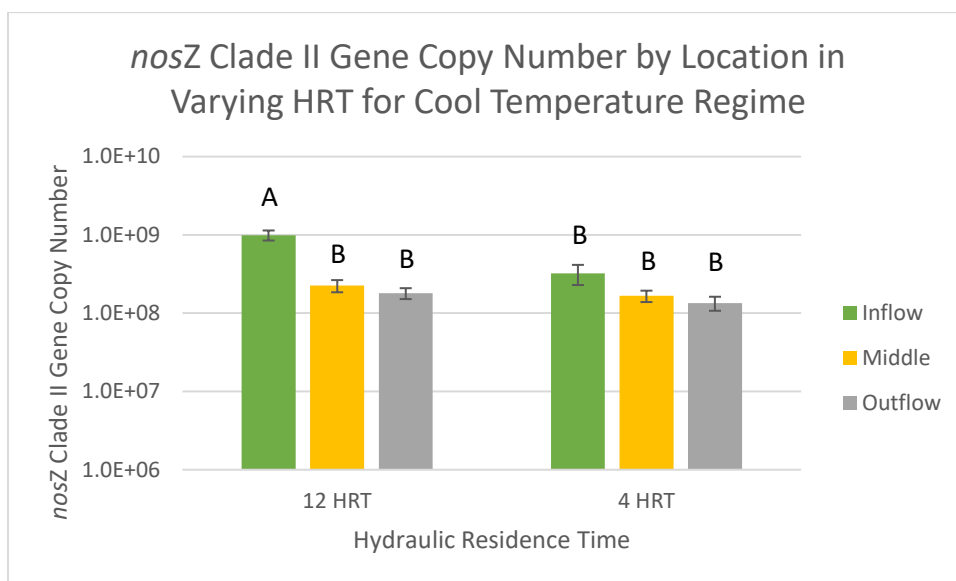


Figure 35: Effect of location and hydraulic residence time (HRT) on *nosZ* clade II gene copy numbers during the cool (6°C, weeks 1-4) temperature regime for 12-hour and 4-hour HRT and for inflow, middle and outflow sampling locations. Identical letters indicate no statistically significant difference, different letters denote statistical significance (two-way ANOVA; $p < 0.05$).

The 12-hour HRT reactors had significantly higher *nosZ* clade II gene copy numbers than the 4-hour HRT under the cool (6°C, weeks 1-4) temperature regime, however, this was only found to occur at the inflow sampling location (Figure 35; $p < 0.001$). The inflow sampling location for the 12-hour HRT also had significantly higher *nosZ* clade II gene copy numbers than the middle and outflow sampling locations for 12-hour HRT under the cool temperature regime (Figure 35; $p < 0.001$). This result was not found in the 4-hour HRT reactors under the cool temperature regime.

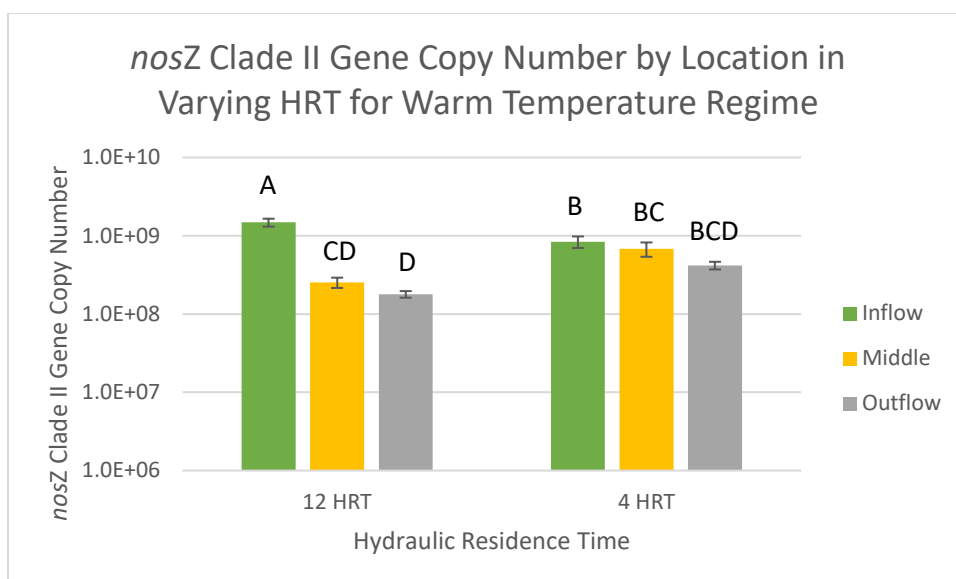


Figure 36: Effect of location and hydraulic residence time (HRT) on *nosZ* clade II gene copy numbers during the warm (14.5°C, weeks 9-12) temperature regime for 12-hour and 4-hour HRT and for inflow, middle and outflow sampling locations. Identical letters indicate no statistically significant difference, different letters denote statistical significance (two-way ANOVA; $p < 0.05$).

Significantly higher *nosZ* clade II gene copy numbers were discerned under the 12-hour HRT than the 4-hour HRT at the inflow sampling location during the warm temperature regime (14.5°C, weeks 9-12) (Figure 36; $p < 0.002$). This finding was not replicated between the middle and outflow sampling locations, which did not exhibit any significant differences between the two hydraulic residence times. Significantly higher *nosZ* clade II gene copy numbers at the inflow than the middle and outflow sampling locations for the 12-hour HRT reactors were also found under the warm temperature regime (Figure 36; $p < 0.001$). No significant differences between sampling locations in the 4-hour HRT reactors were discovered.

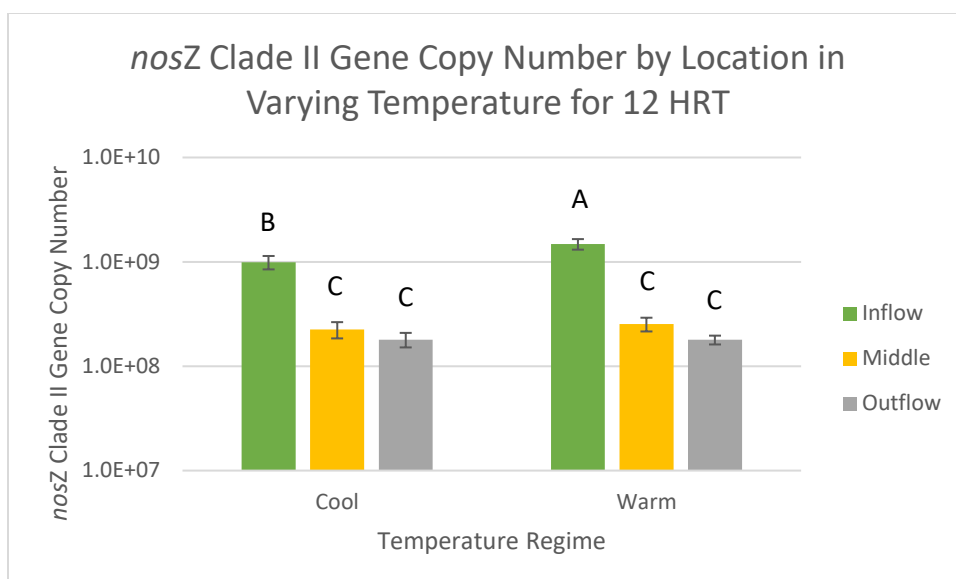


Figure 37: Effect of location and temperature regime on *nosZ* clade II gene copy numbers during 12-hour hydraulic residence time (HRT) for cool (6°C, weeks 1-4) and warm (14.5°C, weeks 9-12) temperature regimes and for inflow, middle and outflow sampling locations. Identical letters indicate no statistically significant difference, different letters denote statistical significance (two-way ANOVA; $p < 0.05$).

Significantly higher *nosZ* clade II gene copy numbers at the inflow than the middle and outflow sampling locations were noted for both the cool (6°C, weeks 1-4) and warm (14.5°C, weeks 9-12) temperature regimes under 12-hour HRT (Figure 37; $p < 0.001$). There were also significantly higher *nosZ* clade II gene copy numbers under the warm temperature regime than the cold temperature regime at the inflow sampling locations during the 12-hour HRT (Figure 37; $p < 0.008$). This significant difference between the two temperature regimes was not found at the middle and outflow sampling locations.

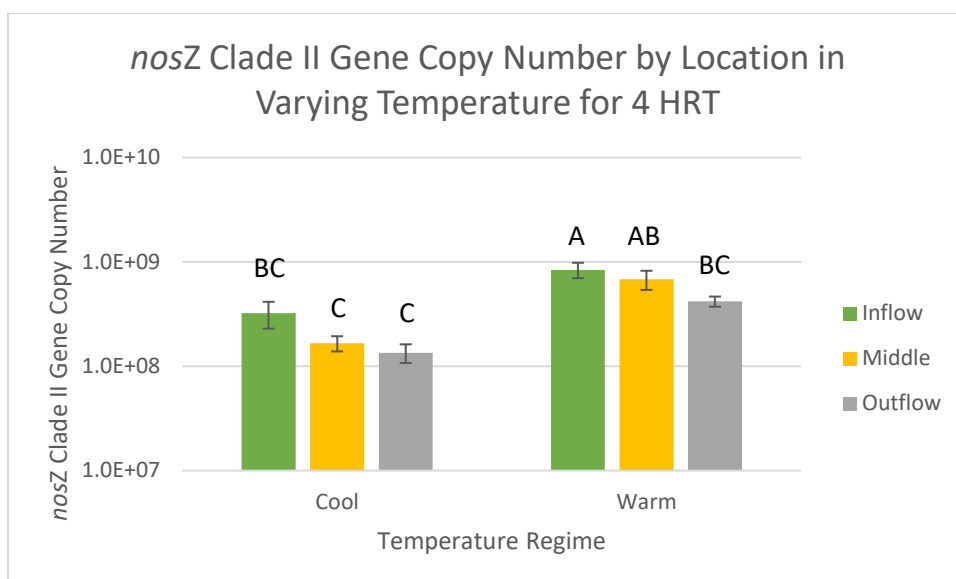


Figure 38: Effect of location and temperature regime on *nosZ* clade II gene copy numbers during 4-hour hydraulic residence time (HRT) for cool (6°C, weeks 1-4) and warm (14.5°C, weeks 9-12) temperature regimes and for inflow, middle and outflow sampling locations. Identical letters indicate no statistically significant difference, different letters denote statistical significance (two-way ANOVA; $p < 0.05$).

There were significantly higher *nosZ* clade II gene copy numbers during the warm temperature regime (14.5°C, weeks 9-12) than the cool temperature regime (6°C, weeks 1-4) at the inflow and middle sampling locations under the 4-hour HRT (Figure 38; $p < 0.003$). This finding was not replicated between the outflow sampling location of the two temperature regimes. There were also significantly higher *nosZ* clade II gene copy numbers at the inflow sampling location than the outflow sampling location during the warm temperature regime under the 4-hour HRT (Figure 38; $p < 0.026$). No other significant differences between sampling locations under the same temperature regime were discovered.

Multivariate Analysis

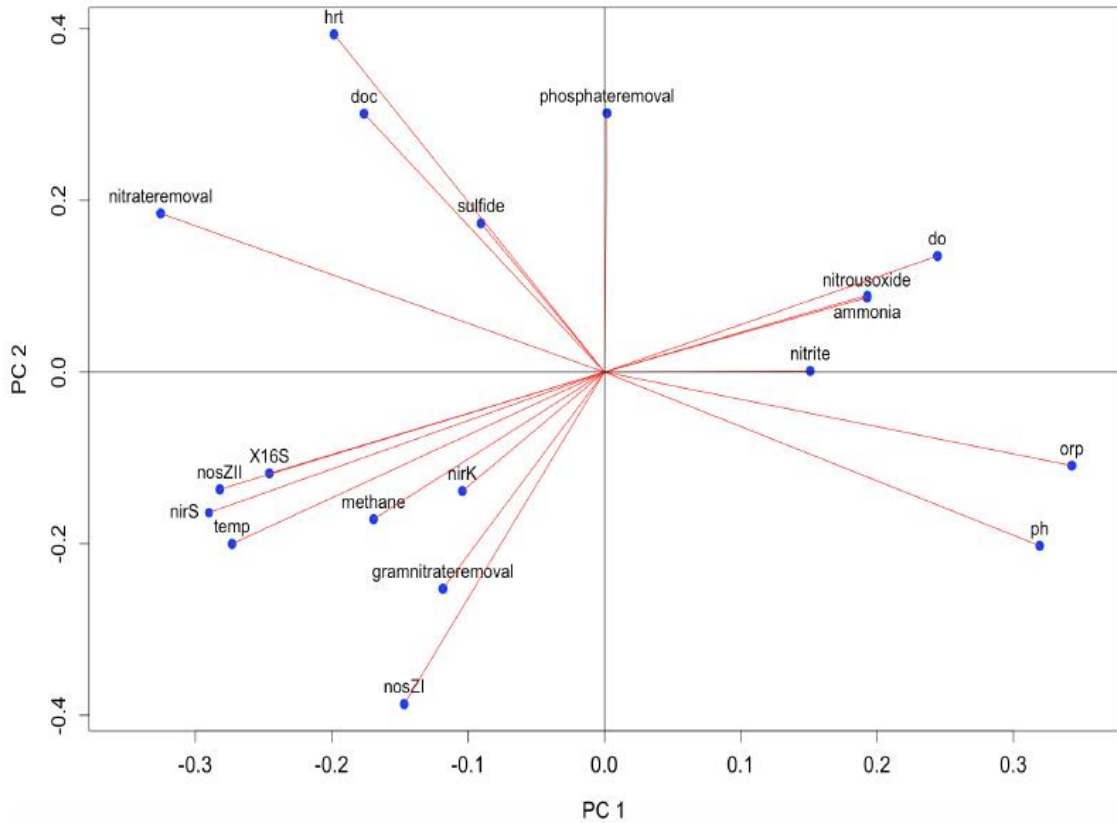


Figure 39: Principle component analysis (PCA) plot of the chemical and biological parameters measured in this study. Points in close proximity to one another indicate a strong correlation, points at a great distance from one another denote a low correlation.

The functional denitrifying genes (*nirK*, *nirS*, and *nosZI* and *nosZII*) and the total bacteria (X16S) gene copy numbers are all clustered closely together (Figure 39). Positioned closely with the functional and total bacteria gene copy numbers is both the nitrate removal efficiency (nitrate removal) and the nitrate removal rate (gramnitrate removal). Temperature (temp) and HRT are also situated adjacent to the nitrate removal efficiency, along with DOC, sulfide and methane. Percent phosphate removal (phosphateremoval) is positioned separately from all the other measured parameters, and is almost opposite of nitrate removal rate and *nosZ* clade II gene copy numbers. Located

opposite of the functional and total bacterial gene copy numbers are DO, nitrous oxide and ammonia. Opposite of nitrate removal efficiency are nitrite, ORP and pH (Figure 39).

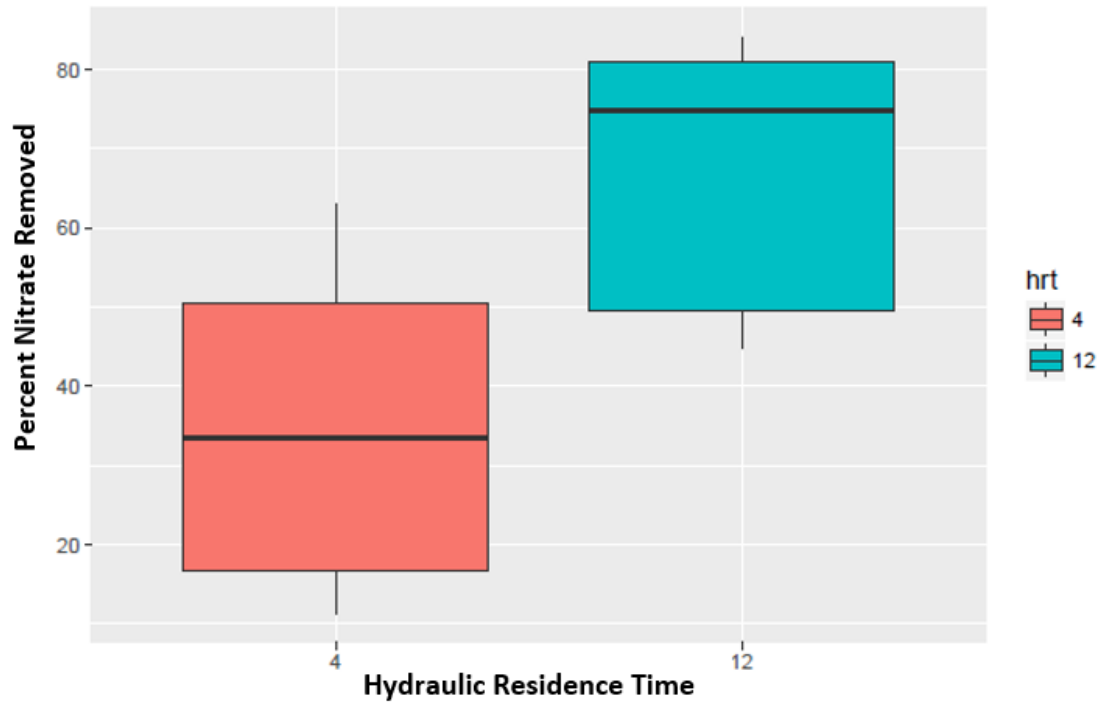


Figure 40: Whisker plot of percent nitrate removed by 12-hour and 4-hour hydraulic residence times (HRT).

The means and the ranges of percent nitrate removal between the two hydraulic residence times were considerably different (Figure 40). On average, the 12-hour HRT reactors removed 75% of the nitrate, while the 4-hour HRT reactors removed, on average, 34%. Similarly, the range of percent nitrate removal for the 12-hour HRT was from 81% to 49%, while it ranged from 51% to 17% for the 4-hour HRT reactors (Figure 40).

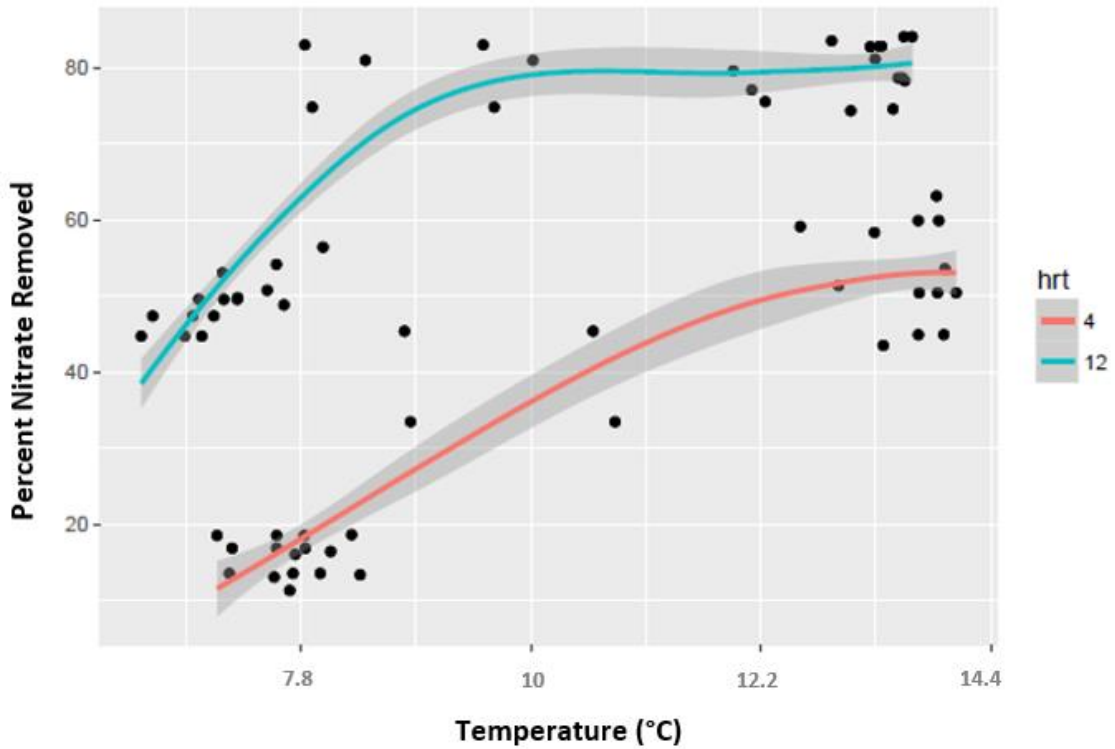


Figure 41: Effect of temperature (°C) on percent nitrate removal for 12-hour and 4-hour hydraulic residence times (HRT) using a linear mixed effects model ($p < 0.05$).

With increasing water temperatures, there was a significant increase in percent nitrate removed (Figure 41; $p < 0.001$). There was also significantly greater percent nitrate removed for the 12-hour HRT than the 4-hour HRT reactors regardless of water temperature (Figure 41; $p < 0.001$).

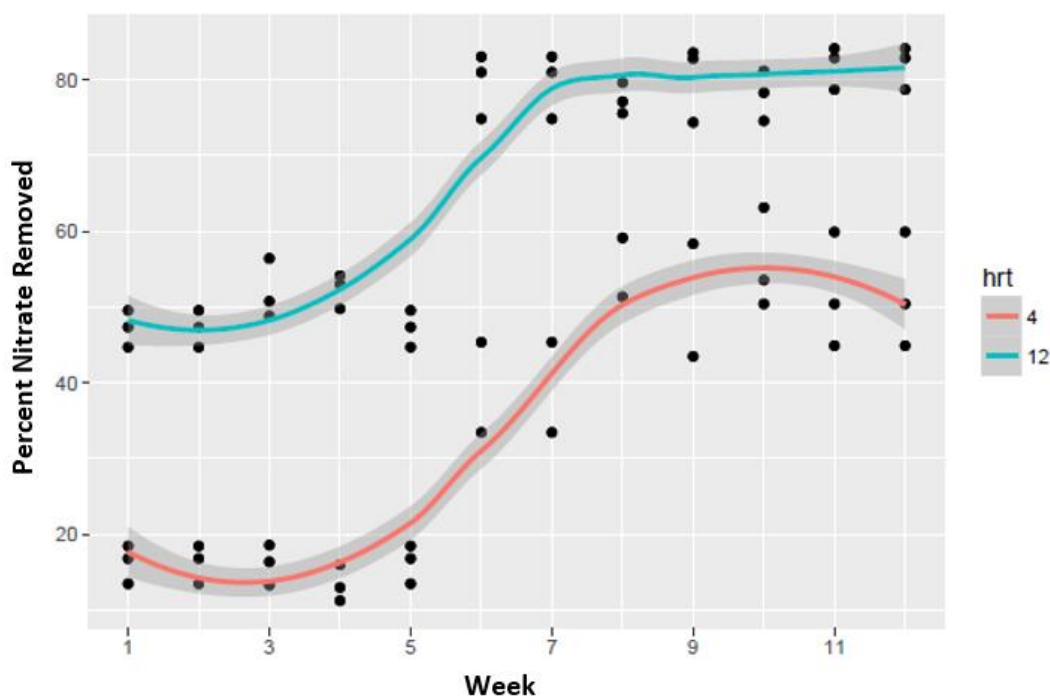


Figure 42: Percent nitrate removed over time for 12-hour and 4-hour hydraulic residence time (HRT) using a linear mixed effects model ($p < 0.05$).

A linear mixed effects model was utilized to model the percent nitrate removed to determine which experimental parameters had a significant influence on nitrate removal (Figure 42). An increase in nitrate removal over time and with increasing temperatures (Figure 41, Figure 42; $p < 0.001$) was noted, along with significantly higher percent nitrate removed with longer HRT (Figure 40, Figure 42; $p < 0.001$). It was found that temperature and HRT were the most significant variables in the experiment, followed by dissolved oxygen ($p < 0.001$) and dissolved organic carbon ($p < 0.0012$).

Discussion

Chemical Data

Percent Nitrate Removed (Nitrate Removal Efficiency)

We found that with an increase in temperature there was an increase in nitrate removal efficiency (*Figure 7; Figure 8*). This finding has been confirmed in a number of other studies that have also investigated the effect of temperature on nitrate removal efficiency (Christianson et al., 2012; Cameron & Schipper, 2010; Hoover et al., 2016; Lepine et al., 2016; Warneke, et al., 2011b). The lowest nitrate removal efficiencies were during the cool temperature regime (6°C, weeks 1-4) and 4-hour HRT and the highest efficiencies occurred during the warm temperature regime (14.5°C, weeks 9-12) and 12-hour HRT, with a minimum efficiency of 15% and a maximum removal efficiency of 81%. These values for nitrate removal efficiency are comparable to those of other studies, which have average nitrate removal efficiencies varying from 18% to 100%, with the lowest removal efficiencies occurring at colder temperatures (5.4-15°C) and higher, sometimes complete, nitrate removal efficiency occurring at warmer temperatures (16-30°C) (Bell et al., 2015; Hassanpour et al., 2017; Hoover et al., 2016). Studies that have succeeded in 100% nitrate removal efficiency were operating with temperatures that were warmer than those in this study (16-30°C) and might explain for their increased nitrate removal efficiency. One of these studies found that there was a temperature cutoff at 16°C; when temperatures were over this threshold nitrate removal efficiency was close to 100% and under this threshold nitrate removal efficiency averaged at 30% (Hassanpour et al., 2017). Despite this, our warm temperature regime, which was only 14.5°C, achieved a nitrate removal efficiency of 81% and 52% (12-hour and 4-hour HRT, respectively) suggesting

that this “temperature threshold” hypothesis of Hassanpour et al. (2017) might have been reactor-specific.

We also found that an increase in HRT led to increased nitrate removal efficiency, or, that with increasing flow rates there was a decrease in nitrate removal efficiency (Figure 7; Figure 8). This has also been suggested by a number of other studies which have tested a wide range of HRTs from 6 days to 2 hours (Addy et al., 2016; Gibert et al., 2008; Hoover et al., 2016; Pluer et al., 2016; Lepine et al., 2016; Greenan et al., 2009). Due to the wide range of HRTs tested in the previous studies, drawing direct comparisons can be difficult, however, one study that tested reactors with 2, 4, 6 and 8-hour HRTs showed an average nitrate removal efficiency of 63%, ranging from 20% to 98%, with the higher efficiency corresponding to the longer HRT and the lower efficiency correlating to the shorter HRT (Bell et al., 2015). These values are comparable to the nitrate efficiencies of our reactors under the warm temperature regime, which exhibited an average nitrate removal efficiency of 81% during the 12-hour HRT and 52% during the 4-hour HRT. Another study with similar HRT also found that with increasing HRT there was increasing nitrate removal efficiency, with average removal efficiencies ranging from 42% to 68%, suggesting that the nitrate removal efficiencies of our reactors were higher than might be expected given the temperatures and HRTs that our reactors were operated at (Hassanpour et al., 2017).

Nitrate Removal Rate ($\text{g-N m}^{-3}\text{d}^{-1}$)

Similar to nitrate removal efficiency, nitrate removal rates were found to increase with increasing temperatures, with a maximum average rate of $7.8 \text{ g N m}^{-3}\text{d}^{-1}$ and a minimum average rate of $3 \text{ g N m}^{-3}\text{d}^{-1}$ (Figure 9; Figure 10). This finding has been confirmed in a number of other studies that have also showed a positive interaction of

temperature on nitrate removal rates (Bell et al., 2015; Bock et al., 2016; David et al., 2016; Hassanpour et al., 2017; Feyereisen et al., 2016; Lepine et al., 2016). The nitrate removal rates in this study are comparable to those in other studies with similar HRT that have demonstrated removal rates ranging from 2 to 30 g N m⁻³d⁻¹, with lower rates corresponding to cooler temperatures (5.4-15°C) (Addy et al., 2016; Bell et al., 2015). As mentioned earlier, one study found a temperature threshold at 16°C; when temperatures were over this threshold nitrate removal rates were greater (reaching 73 g N m⁻³d⁻¹) and under this threshold nitrate removal rates were much less (dropping to 0 g N m⁻³d⁻¹) (Hassanpour et al., 2017). The study performed by Hassanpour et al. (2017) exhibited a much wider range in removal rates than demonstrated in our study, which might be due to the wider range of temperatures that was tested in their research. Despite our temperatures remaining under the 16°C threshold, a significant amount of nitrate was still removed. This, again, suggests that this temperature threshold might be reactor-specific.

Unlike nitrate removal efficiency, nitrate removal rates were shown to decrease with increasing HRT, or, in other terms, nitrate removal rates increased with increasing flow rate (Figure 9; Figure 10). During the warm temperature regime (14.5°C, weeks 9-12), nitrate removal ranged from 4.5 g N m⁻³d⁻¹ with 12-hour HRT to 7.8 g N m⁻³d⁻¹ with 4-hour HRT. A number of other studies have also found increasing nitrate removal rates with decreased HRT (Lepine et al., 2016; Greenan et al., 2009; David et al., 2016). These studies have also found that while decreasing HRT increases nitrate removal rates, it also decreases the nitrate removal efficiency, corroborating the findings in this study. Conversely, a number of other studies have shown no change in nitrate removal rates with changes in HRT (Hoover et al., 2016; Bell et al., 2015). It is suggested that the increase in

nitrate removal rate with decreasing HRT is most likely due to larger amounts of nitrate being passed per unit of time through the system, which would easily explain higher removal rates with shorter HRT. As the flow rate increases, more nitrate is passed through the bioreactors, thus leading to greater removal rates. It should be noted that even during the cool temperature regime (6°C, weeks 1-4) and at a 4-hour HRT, nitrate removal rates were at least 3 g N m⁻³d⁻¹, indicating that substantial nitrate removal occurred even at cold temperatures and short HRT.

Dissolved Organic Carbon (DOC)

Higher DOC concentrations in the effluent were noted with increasing HRT (Figure 11; Figure 12), which was also found in another study that investigated the effect of HRT on bioreactor performance using various carbon substrates (Krause Camilo et al., 2013). Conversely, another study observed no effect of HRT on DOC concentration in the effluent (Bell et al., 2015). We also found that with increasing temperatures, the 4-hour HRT bioreactors had higher DOC concentrations in the effluent, but the 12-hour HRT bioreactors exhibited similar average DOC concentrations during both temperature regimes (Figure 11; Figure 12). Other studies have also demonstrated differences on the effect of temperature on carbon availability in denitrifying bioreactors. One study noted higher effluent biological oxygen demand (BOD) with increasing temperatures (Cameron & Schipper, 2010), while another documented that there were no significant changes in DOC concentrations with increasing temperatures (Bell et al., 2015). A third study found that after high DOC concentrations (200 mg/L) in the effluent during the startup period (10 months after initiating bioreactor operation), average DOC varied seasonally from 0.5 to 22 mg/L with the higher effluent concentrations occurring during warmer weather (16-

20°C) (Hassanpour et al., 2017). The authors proposed a possible explanation for the high initial concentrations of DOC that could also explain the high DOC concentrations that we observed during the first four weeks of our experiment for the 12-hour HRT reactors: leaching of DOC from bioreactor media during the startup phase. Higher DOC concentrations in other studies only during the start-up phase (ranging from 1-12 months after bioreactor startup) of woodchip denitrifying bioreactors have been documented before (Christianson & Schipper, 2016; Greenan et al., 2009). While these other studies have an initial range from 300 to 900 mg/L during the startup phase, our reactors had DOC concentrations that never exceeded 10 mg/L. After startup, these other reactors typically had DOC concentrations ranging from 10 to 40 mg/L, which were still higher than the DOC concentrations exhibited in our study. This leads us to postulate that our initial higher concentrations of DOC might have been due to the addition of acetate before reactor startup which might not have been completely flushed out of the 12-hour HRT reactors at the beginning of the experimental phase.

The low DOC concentrations in the effluent of our bioreactors have both positive and negative connotations. Typically, DOC is viewed as a possible pollutant, a concern that has hindered the widespread application of denitrifying bioreactors, however, our reactors demonstrated that this was not an issue (Addy et al., 2016; Schipper et al., 2010). Despite this, DOC is also considered a possible limiting factor, since organic carbon serves as the electron donor for microbial denitrification, which is likely to be the case for bioreactors, such as ours, that have very low DOC concentrations in the effluent (Warneke et al., 2011c; Feyereisen et al., 2016). Subsequently, ascertaining how to design and

maintain bioreactors that can provide just enough DOC to promote denitrification while not exceeding effluent limits is an area of growing interest.

Dissolved Oxygen (DO)

Dissolved oxygen (DO) concentrations in the effluent were lower at higher temperatures (14.5°C, weeks 9-12); however, no differences were noted between the short and long HRT (Figure 13). This is consistent with the findings of several other studies that have also shown an increase in effluent DO concentrations with decreasing temperatures and no significant impact of varying HRTs (Bock et al., 2016; Lepine et al., 2016). Nevertheless, another study demonstrated that while influent DO concentrations increased with decreasing temperatures, there was no effect of temperature on the effluent DO concentrations, which remained consistently just below 3 mg/L for various temperatures (5.4-16.5 °C) (Bell et al., 2015). The values of effluent DO concentrations reported in other studies have been <2 mg/L, or even <1 mg/L throughout varying water temperatures (7-20°C) (Bock et al., 2016; Lepine et al., 2016). In contrast, the effluent DO concentrations in this study were not as low since they remained between 3 to 5 mg/L (31% to 41% saturation, respectively) for the entirety of the experiment (Figure 13). This supports Warneke et al.'s (2011c) conclusion that there is a range of concentrations (0.5 to 4.5 mg/L DO is suggested) where DO is not limiting to denitrification. The large variability in limiting DO concentrations is likely due to the formation and presence of anaerobic microsites not only in the woodchips, but also in the biochar, which has been noted to promote the creation of distinct microsites that allow anaerobic microbial processes to occur at a range of pore water DO concentrations (Lehmann et al., 2011; Harter et al., 2016). Because there were no significant changes in DO concentrations throughout the

length of the experiment and values remained at relatively low and consistent concentrations, DO is not considered to have a great influence on the performance of our system (Warneke et al., 2011c).

Nitrous Oxide Emissions

Because nitrous oxide is a highly potent greenhouse gas, it is considered a pollutant. Nitrous oxide is known to be a common intermediate byproduct during denitrification when nitrate is not completely reduced to nitrogen gas. Subsequently, there is great concern that the introduction of denitrifying bioreactors might elevate greenhouse gas emissions by incomplete nitrate reduction to nitrous oxide (Addy et al., 2016). During the course of our study, nitrous oxide emissions did not exceed 600 ppb (Figure 14), remaining low enough to be considered negligible (Warneke et al., 2011c). Under the cool temperature regime (6°C, weeks 1-4), nitrous oxide emissions were higher for the shorter HRT, but under the warm temperature regime (14.5°C, weeks 9-12), nitrous oxide emissions were higher for the longer HRT (Figure 14; Figure 15). Thus, our study demonstrated that with a 4-hour HRT there was a decrease in nitrous oxide emissions as temperature increased and with a 12-hour HRT there were no significant changes in nitrous oxide emissions between operation in 6°C and 14.5°C temperatures. An increase in nitrous oxide production with increasing temperature was observed in another study as well, however, the authors only measured the dissolved nitrous oxide produced, while our study only quantified the gaseous nitrous oxide produced (Warneke et al., 2011b). Another study that utilized 12-hour HRT columns demonstrated increasing nitrous oxide production in colder temperatures (Feyereisen et al., 2016). However, the study by Feyereisen et al. (2016) included the production of both gaseous nitrous oxide emissions as well as the dissolved nitrous oxide

produced in the effluent, whereas our study only accounted for gaseous nitrous oxide emissions. It is possible that there were higher cumulative nitrous oxide emissions released in our bioreactors if dissolved nitrous oxide had been included. This must be taken into account when assessing the risk of implementing denitrifying bioreactors into the field. While our study, along with a number of others (David et al., 2016; Greenan et al., 2009; Moorman et al., 2010), would suggest that only a small amount of nitrous oxide is released by denitrifying bioreactors, other studies that have either quantified gaseous or dissolved nitrous oxide have reported significantly higher amounts (Warneke et al., 2011c). Nevertheless, values of nitrous oxide emissions in control agricultural field plots that did not utilize denitrifying bioreactors were found to be similar to those produced by field plots with denitrifying bioreactors, ranging from 2.6 to 73.2 N₂O-N/L (Moorman et al., 2010). The emissions found in our study are below the lower end of this range (<2.6 N₂O-N/L), indicating that our bioreactors are not likely to be producing nitrous oxide emissions that would be a cause for concern, particularly because it is comparable to the emissions produced by a typical agricultural field. It is possible that the biochar included in our bioreactors could be responsible for the low values of nitrous oxide produced, since it has been demonstrated to greatly reduce nitrous oxide emissions when amended to agricultural fields (Cornelissen et al., 2013; Hagemann et al., 2017a; Hagemann et al., 2017b; Harter et al., 2016).

Phosphate Removal Efficiency

Very few, if any, studies have investigated the ability of woodchip denitrifying bioreactors to remove other pollutants even though numerous studies have called for the need to analyze this as an additional benefit to the field application of denitrifying

bioreactors (Addy et al., 2016; Christianson & Schipper, 2016; Schipper et al., 2010). Because of the recent push to include other pollutants into denitrifying bioreactors' scope of treatment, phosphate was included in our experimental design. While the influent concentration of phosphate was only 0.5 mg/L, this concentration is typical in tile drainage in southern Minnesota (Krider, 2018). Phosphate removal was found to occur at both temperature regimes (6°C and 14.5°C) and at both short and long HRT, demonstrating that denitrifying bioreactors are capable of treating tile drainage for phosphate (Figure 16; Figure 17). This differs from a study done by Bell et al. (2015) which observed that denitrifying bioreactors actually produced phosphorous, as the effluent concentrations of dissolved reactive phosphorous were higher than those in the influent. Clearly, further research into the capacity of denitrifying woodchip bioreactors removing phosphate is necessary, particularly to assess this ability at varying concentrations and conditions. We did discover that there were some effects of temperature and HRT on phosphate removal, with shorter HRT there was less phosphate removal, but with varying temperatures there were mixed effects for the different HRTs, leading us to conclude that this needs to be studied in greater depth in future experiments.

pH

Typically, pH increases during denitrification due to the release of hydroxyl anions during the sequential reduction of nitrate to nitrite, nitrite to nitrous oxide, and nitrous oxide to nitrogen gas (Christianson et al., 2012). This increase in pH from the influent to the effluent has been observed in other studies (Bock et al., 2016; Warneke et al., 2011c). In contrast, the pH was shown to decrease as it passed through our bioreactor troughs (Appendix B: Additional Chemical Parameters of Bioreactor Troughs; Figure 46), which

has also been observed in other studies (Lepine et al., 2016; Bell et al., 2015). It is unclear why certain denitrifying bioreactors exhibit an increase in pH and others have a decrease, however, we postulate that the decrease in pH observed in our reactors might be due to the slightly acidic nature of the walnut shell biochar added to our bioreactor media mix (Appendix A: Walnut Shell Biochar Characterization; Table 7). Regardless of the change in pH from the influent to the effluent, the effluent pH remained constant across all treatments under varying temperatures and HRT, with an average range of 6.8 to 7.1 (Appendix B: Additional Chemical Parameters of Bioreactor Troughs; Figure 46). This is within the expected and optimal pH range for denitrification and is similar to those in other studies which have reported pH ranges from 6.5 to 8.5 (Bock et al., 2016; Lepine et al., 2016; Gibert et al., 2008). Because the pH remained fairly constant during our experiment, it is not considered to substantially influence the system performance (Warneke et al., 2011c).

Ammonia and Nitrite

Ammonia and nitrite concentrations remained constant and at negligible concentrations (<0.9 mg/L and <0.5 mg/L, respectively) for the duration of the experiment (Appendix B: Additional Chemical Parameters of Bioreactor Troughs; Figure 48; Figure 49). Average range values for both ammonia and nitrite did decrease as temperature increased, however, this finding was not significant. Likewise, no significant differences were observed between the varying HRTs. The lack of effect of both temperature and HRT on ammonia and nitrite concentrations has been established in several other studies (Schipper et al., 2010; Warneke et al., 2011a). The negligible concentrations of nitrite and ammonia indicate that nitrogen removal from the system is not likely to be due to

dissimilatory nitrate reduction to ammonia (DNRA) nor anaerobic ammonia oxidation (Anammox) (Schipper et al., 2010).

Sulfide and Methane

The production of hydrogen sulfide and methane are a concern when utilizing denitrifying woodchip bioreactors because both are considered a potential adverse byproduct during highly reduced operating conditions (Addy et al., 2016; Christianson & Schipper, 2016; Schipper et al., 2010; Warneke et al., 2011c; Warneke et al., 2011b). While a distinct sulfide smell was noted in the effluent water throughout the experiment, the concentration of sulfide varied only over small increments during the experiment and remained at negligible concentrations (<0.6 mM) (Appendix B: Additional Chemical Parameters of Bioreactor Troughs; Figure 50), indicating that denitrifiers were not likely to be competing with sulfate reducing bacteria (Schipper et al., 2010). Similarly, since our reactors never exceeded 82 ppm of methane emissions (Appendix B: Additional Chemical Parameters of Bioreactor Troughs; Figure 51), it can be concluded that methane production was negligible and that competition with methanogens did not limit denitrification (Schipper et al., 2010; Warneke et al., 2011b). Other studies have found higher concentrations of sulfide in the effluent (up to 1mM) and that sulfate reduction occurred significantly more with increasing HRT (up to 13 mg/L sulfate reduced to sulfide) (Lepine et al., 2016; Bell et al., 2015). The authors noted that higher sulfide concentrations in the effluent occurred during extended periods of nitrate limiting conditions in the bioreactors, leading them to believe that this was the cause for excess sulfate reduction (Lepine et al., 2016). A study done by Robertson (2010) demonstrated that when nitrate concentrations

were less than 1 mg/L sulfate reduction occurred. Thus, we postulate that because our reactors never underwent nitrate limiting conditions, sulfide production was limited.

Nitrate Concentrations Along Bioreactor Length

Decreasing nitrate concentrations were predicted along the length of the replicate bioreactor troughs, which was confirmed using the hydraulic flow model designed by Krider (2018) (Figure 18). A decrease in nitrate concentrations along the length of denitrifying bioreactors has also been noted in a few other studies (Warneke et al., 2011c; Gibert et al., 2008). Besides being confirmed by these other studies, it also makes logical sense that as nitrate laden water is passed through the reactor, nitrate concentrations should decrease because it is being removed. We also found that the decrease in nitrate concentrations along the length of the replicate troughs was much more significant for the 12-hour HRT than the 4-hour HRT (Figure 18). A study looking at much longer HRT (6.6 d and 1.7 d) also noted a significant drop in the first 42 cm of their bioreactor column for the longer HRT, but an even amount of nitrate removal along the entire column length for the shorter HRT (Gibert et al., 2008). After completing biological sampling of the replicate troughs, we inserted a nitrate probe in the sampling ports along the length of the bioreactor. We found that 50% of nitrate removal had occurred within the first 50 cm of our 12-hour HRT, while 25% had occurred in our 4-hour HRT. These findings have some interesting implications not only for the operation and management of denitrifying woodchip bioreactors, but also in terms of the availability of electron acceptors and selective pressure on the microbial community along the length of the bioreactor bed.

Biological Data

16S rRNA

Higher 16S rRNA gene copy numbers were found during the warm temperature regime (14.5°C, weeks 9-12) for both HRT, however, this effect was only observed at the inflow locations of the bioreactor troughs (Figure 19; Figure 22; Figure 23). Similarly, higher 16S rRNA gene copy numbers were observed with the 12-hour HRT than the 4-hour HRT, but this only occurred at the inflow locations of the bioreactor troughs (Figure 20; Figure 21). There are no other studies that have investigated the effect of HRT and temperature on 16S rRNA gene copy numbers in denitrifying bioreactors, but these results are plausible. It is widely known that at warmer temperatures bacterial activity and populations generally increase, thus, an increase in 16S rRNA gene copy numbers would be expected with increasing temperatures. Why 16S rRNA gene copy numbers increased with increasing HRT is unclear and could be due to several factors. It is important to note that the effect of HRT and temperature are significant only at the inflow locations of the bioreactor troughs. Moreover, inflow locations also had significantly higher 16S rRNA gene copy numbers than the middle and outflow locations for a variety of conditions (12-hour HRT under the warm temperature regime (14.5°C) and the 4-hour HRT under both the warm and cool (6°C) temperature regimes).

The effect of location on 16S rRNA gene copy numbers is not only significant when considering it by itself, but also in regard to the impact it holds on the effect of temperature and HRT. Not only were there significantly higher 16S rRNA gene copy numbers at the inflow location, but under the warm temperature regime and 12-hour HRT a significant increase in 16S rRNA gene copy numbers was also discerned, although only at the inflow

locations (Figure 20; Figure 22). This suggests that the location along the length of the bioreactor has a greater influence on the gene copy number of 16S rRNA in denitrifying bioreactors than temperature and HRT. This does not necessarily indicate that it is the physical property of the location itself that influences the abundance of total bacteria, but that it is more likely due to the presence or absence of other chemical or physical properties at the inflow location that are limiting to the total bacteria at the other locations along the bioreactor trough (i.e.: nitrate, DO, DOC, etc.). A study performed on agricultural soils concluded that a significant decrease in 16S rRNA gene copy numbers with increasing soil depth was attributable to decreasing oxygen concentrations (Mergel et al., 2001a). Thus, it is possible that higher 16S rRNA gene copy numbers were present at the inflow locations because of higher DO concentrations at the inlet. As the water passed along the length of the bioreactor, conditions became more reduced, which could explain a drop in 16S rRNA gene copy numbers. A similar line of reasoning could be applied to argue that DOC concentrations are limiting 16S rRNA gene copy numbers at the middle and outflow locations of the bioreactor troughs, however, speculating on the DOC concentrations along the length of the bioreactor troughs is much more complex because both production and consumption of carbon must be considered. Regardless, we can conclude that location along the length of the bioreactor has a significant impact on 16S rRNA gene copy numbers, which could be attributable to the presence, or absence, of chemical or physical properties at those locations.

Location having a significant control over the abundance and diversity of total bacteria in denitrifying bioreactors has also been demonstrated in other studies (Andrus et al., 2014; Feyereisen et al., 2016). While the difference was not statistically significant,

Feyereisen et al. (2016) did find higher 16S rRNA gene copy numbers at the outlet locations than the inlet of a corn cob denitrifying bioreactor under a warm temperature regime (15.5°C). This is the opposite of our findings, which had significantly higher 16S rRNA gene copy numbers at the inflow than both the middle and outflow locations. This discrepancy could be due to a number of factors, including the use of different solid carbon substrates in the reactors and the scale of the experimental setup. Another study found a significant variation in bacterial community that was related to the distance from the inlet, not the depth nor the placement along the width of the reactor, corroborating the significance of location along the length of the bioreactors on total bacteria that was found in our study (Andrus et al., 2014).

Nitrite Reductase (nirK and nirS)

The second step of denitrification is the reduction of nitrite to nitric oxide by nitrite reductase. There are two genes that are used to quantify this enzyme, *nirK* and *nirS*. Although both *nirK* and *nirS* code for nitrite reductase, the structure of the enzyme is determined by which gene is encoded (Henry et al., 2004). Nitrite reductase that is encoded by the *nirK* gene contains copper, while those encoded by *nirS* do not. Some studies have indicated that there is niche differentiation between organisms carrying *nirK* and *nirS*, thus both target genes were included in the scope of this study (Hallin et al., 2009).

Although higher *nirK* gene copy numbers were observed in warmer temperatures (14.5°C, weeks 9-12), this finding was only significant at the inflow locations and at 4-hour HRT (Figure 27; Figure 28). Similarly, higher *nirS* gene copy numbers were also observed under the warm temperature regime, but this was only significant at the middle and outflow locations and at 4-hour HRT (Figure 31). An increase in *nirK* gene copy

numbers with increasing temperatures has been documented in previous research performed on microbial communities in agricultural soils (Wolsing & Prieme, 2004). In denitrifying bioreactors, both *nirK* and *nirS* gene copy numbers have been found to decline with decreasing temperatures and to have a greater relative abundance with increasing temperatures, verifying the general trends observed in our study (Smith et al., 2010; Warneke et al., 2011b). While one study found that with decreasing flow rates there were lower *nirK* and *nirS* gene copy numbers in agricultural soils, we found no significant effect of HRT on *nirK* gene copy numbers (Figure 25; Figure 26) and significantly higher *nirS* gene copy numbers with longer HRT while under the cool temperature regime (6°C, weeks 1-4) (Figure 30) (Smith et al., 2010). This discrepancy could be due to differences in microbial community structures between agricultural soils and bioreactors, however, as no other study has investigated the effect of HRT on *nirK* and *nirS* gene copy numbers in denitrifying bioreactors we are unable to corroborate our findings.

We also found, as expected, around two orders of magnitude less *nirK* and *nirS* gene copy numbers than 16S rRNA (Figure 19; Figure 24; Figure 29). This is anticipated, as denitrifiers do not typically comprise of more than 7% of the total bacterial population, and have usually been found to be two orders of magnitude less than 16S rRNA gene copy numbers (Henry et al., 2006). Much like our results for 16S rRNA gene copy numbers, higher *nirK* gene copy numbers were observed at the inflow locations than at the middle and outflow (Figure 25; Figure 26; Figure 27; Figure 28). However, these differences were only significant at warmer temperatures and at 4-hour HRT. Likewise, higher *nirS* gene copy numbers were found at inflow locations than at the middle and outflow, but these findings were only significant at cooler temperatures and at 12-hour HRT (Figure 30;

Figure 31). Interestingly, under 4-hour HRT and warm temperatures (14.5°C), *nirS* gene copy numbers were higher at the middle and outflow than inflow location, although these differences were not statistically significant. No studies have been performed on the effect of location specifically on *nirK* and *nirS* gene copy numbers in denitrifying bioreactors, making it difficult to compare our results. Nevertheless, one study found that there was a decrease in both *nirK* and *nirS* gene copy numbers in soil as soil depth increased (Mergel et al., 2001b). The authors concluded that this was due to decreasing DO concentrations, even though denitrifiers are typically facultative anaerobes. It is possible that the decrease in *nirS* and *nirK* gene copy numbers in the middle and outflow locations of the bioreactor troughs could be due to decreased DO concentrations, although, it could just as likely be due to decreasing concentrations of DOC and nitrate.

In nature, *nirS* is typically found to be more abundant than *nirK*, however, in our study, higher gene copy numbers of *nirK* than *nirS* were observed. Not many studies have investigated the abundance of *nirK* and *nirS* in denitrifying bioreactors, but studies performed on soils and ditches have had contradictory results. A study looking at weirs in agricultural ditches found higher *nirS* gene abundances than *nirK* (Baker et al., 2015), whereas other studies performed on soils found higher abundances of *nirK* than *nirS* carrying organisms (Mergel et al., 2001a; Mergel et al., 2001b). In general, it has been noted that *nirK* abundances are higher in agricultural soils than in other soils, where *nirS* is more abundant (Henry et al., 2006). Hallin et al. (2009) suggested that there is niche differentiation between *nirK* and *nirS* carrying organisms, so that these genes are not ecologically redundant but fulfill separate niches. This suggestion could explain the disparity of results regarding *nirK* and *nirS* abundances. Our results indicate that HRT and

temperature have a limited effect on *nirK* and *nirS* gene copy numbers, but that location along the length of the bioreactors has a greater effect. Similar to our conclusions on the effect of location on 16S rRNA gene copy numbers, it is most likely the presence or absence of a chemical at the inflow location, and not the physical location itself, that promotes higher *nirS* and *nirK* gene copy numbers. Thus, while Hallin et al. (2009) concluded niche differentiation for *nirK* and *nirS* to be due to the presence or absence of plants, it is likely that a more complex set of factors are influencing the selection of *nirK* or *nirS* in our study; possibly the concentration of nitrate, DOC, DO, or some combination of all three.

Nitrous Oxide Reductase (nosZ clade I and clade II)

The fourth and final step in denitrification is the reduction of nitrous oxide to nitrogen gas (N₂). The enzyme responsible for performing this step is called nitrous oxide reductase and is of particular interest because it indicates the genetic potential in the bacterial community to perform complete denitrification. Nitrous oxide reductase is encoded by two different genes, *nosZ* clade I and *nosZ* clade II, or, typical *nosZ* and atypical *nosZ*, respectively. Organisms that carry the *nosZ* clade I gene are considered “classical” denitrifiers, belong to the Proteobacteria and have the genetic capability to perform the other steps in denitrification (Harter et al., 2016). Clade II carrying organisms are from a variety of Phyla and about half of the organisms in this clade do not have the genetic potential to perform the other steps in denitrification, thus, these organisms are frequently dubbed “incomplete” denitrifiers as they only have the genetic potential to reduce nitrous oxide to nitrogen gas (Jones et al., 2013). In other studies, *nosZ* clade II has been noted to have at least the same abundance as *nosZ* clade I. However, varying ratios of *nosZ* clade II

and *nosZ* clade I have also been observed across various environments, and in our study we discovered a higher abundance of *nosZ* clade II than *nosZ* clade I, by about one order of magnitude (Figure 32; Figure 34) (Jones et al., 2013)

Higher gene copy numbers of *nir* than *nosZ* were also observed during the course of the study (Figure 24; Figure 29; Figure 32; Figure 34). This agrees with the findings in another study, which also demonstrated higher abundances of *nir* than *nosZ* in agricultural drainage ditches (Veraart et al., 2017). Similar gene abundances for *nirS* and *nosZ* clade I was also found in a study looking at the use of weirs in agricultural ditches, demonstrating that the general trends and abundances in our study are within an expected range (Baker et al., 2015). Because there was a higher number of *nir* gene copy numbers than *nosZ*, there was a great genetic potential for high nitrous oxide emissions. With greater *nir* gene copy numbers, more organisms have the genetic capability to reduce nitrite to nitric oxide and then to nitrous oxide (utilizing nitric oxide reductase) than they do to reduce nitrous oxide to nitrogen gas. Despite this, our nitrous oxide emissions remained low throughout the experiment (Figure 14).

Temperature has been demonstrated to have a significant effect on determining the *nosZ* clade I microbial community, which has been shown to have seasonal cycling that can be attributed, in part, to temperature fluctuation (Porter et al., 2015). Thus, we expected to see changes in *nosZ* clade I gene copy numbers with changes in temperature. With warmer temperatures (14.5°C) there were higher *nosZ* clade I gene copy numbers, but this was only significant at inflow locations and at the 4-hour HRT (Figure 33; Appendix C: Additional Biological Data for Bioreactor Troughs; Figure 56). Higher *nosZ* clade II gene copy numbers with warmer temperatures were also found, with significantly higher

numbers only at inflow locations (Figure 37; Figure 38). Feyereisen et al. (2016) also found an increase in *nosZ* clade II gene copy numbers with warmer temperatures (15.5°C), however, these findings were not significant and were noted to only occur in the treatments containing corn cobs as the carbon substrate.

Very little is known about the effect of HRT on the *nosZ* functional community and abundance. One study has investigated seasonal cycling in denitrifying bioreactors and has linked two distinct seasonal flow patterns and flow rates to altering *nosZ* microbial distribution (Porter et al., 2015). While this study informs us that there is a shift within the *nosZ* community distribution, it does not address whether there are any changes in functional community size. We found no significant effect of HRT on *nosZ* clade I gene copy numbers (Appendix C: Additional Biological Data for Bioreactor Troughs; Figure 54; Figure 55) but did observe higher *nosZ* clade II gene copy numbers with longer HRT, with significantly higher numbers only at the inflow locations (Figure 35; Figure 36). This indicates that HRT has a significant effect on *nosZ* clade II functional gene copy numbers at inflow locations, but, interestingly, not on *nosZ* clade I functional gene copy numbers, regardless of location. Why there is a discrepancy on the effect of HRT between the two clades of nitrous oxide reductase carrying organisms is uncertain, but might be due to an abundance of organisms capable of nitrate reduction to nitrous oxide, thus selecting for organisms that are only capable of nitrous oxide reduction. It is also possible that nitrous oxide was entrapped in the walnut shell biochar, as found in a study by (Harter et al., 2016), promoting the abundance of incomplete denitrifiers.

Similar to our findings on the effect of HRT on *nosZ* gene copy numbers, no significant effect of location on *nosZ* clade I gene copy numbers was observed (Figure 33; Appendix

C: Additional Biological Data for Bioreactor Troughs; Figure 54; Figure 55; Figure 56), but significantly higher *nosZ* clade II gene copy numbers at the inflow than the middle and outflow locations were found (Figure 35; Figure 36; Figure 37; Figure 38). Again, the cause for the divergence of effect of location between clade I and clade II is unclear, but could be due to several factors. Other studies have found that *nosZ* clade I gene copy numbers are strongly affected by location. The study performed by Andrus et al. (2014) concluded that the change in gene copy numbers of *nosZ* clade I was due to the distance from the reactor inlet and not due to depth or location along a transect. Interestingly, Feyereisen et al. (2016) found that *nosZ* clade II functional gene abundance was not altered by location in reactors, but *nosZ* clade I was. The authors found that there were higher *nosZ* clade I gene copy numbers at the outlet than the inlet in their corn cob reactors, however, these findings were not significant. The difference in our findings and those of Feyereisen et al. (2016) could be due to the different carbon substrates used, particularly since other studies have indicated that biochar can significantly alter the *nosZ* community (Lehmann et al., 2011; Harter et al., 2016a; Harter et al., 2016b). Regardless, our results indicate that HRT and temperature have a limited effect on *nosZ* clade II gene copy numbers, but that location along the length of the bioreactors has a significant effect. Like our conclusions on the effect of location on total bacterial and *nir* gene copy numbers, it is most likely the abundance, or lack of one, of a chemical at the inflow location, and not the physical location itself, that promotes higher *nosZ* clade II gene copy numbers. In contrast to this, HRT, temperature and location had little effect on *nosZ* clade I gene copy numbers, implying that the *nosZ* clade I functional community is relatively stable throughout the length of the reactor as well as through various temperatures and flow rates.

Linking the Bacterial Community and Bioreactor Performance

Nitrate Removal Efficiency and Nitrate Removal Rate

Utilizing a multivariate approach, it is demonstrated that functional denitrifying and 16S rRNA gene copy numbers in the bioreactor troughs closely correlate to both nitrate removal efficiency and nitrate removal rates (Figure 39). Also closely correlated to nitrate removal efficiency and nitrate removal rates are temperature, HRT and DOC. During the warm temperature regime there was significantly higher nitrate removal efficiency as well as nitrate removal rates (Figure 8; Figure 10). This corresponded to a general increase in gene copy numbers during the warm temperature regime (statistical significances only noted for 16S, *nosZ* clade I and *nosZ* clade II, see previous sections for further clarification) (Figure 19; Figure 24; Figure 29; Figure 32; Figure 34). This trend was most prominent at the inflow locations of the bioreactor troughs, which was also where statistically significant differences were found. While nitrate removal efficiency and nitrate removal rates were more significantly altered by changes in HRT, the bacterial community demonstrated less of an effect of HRT on gene copy numbers than temperature. Nitrate removal efficiency increased with increasing HRT, while nitrate removal rate decreased (Figure 8; Figure 10). Gene copy numbers of 16S rRNA and *nosZ* clade II were observed to increase with increasing HRT, however this trend was only present at the inflow locations (Figure 20; Figure 35; Figure 36). The greater influence of location on the bacterial community implies that temperature and HRT were not the only limiting variables in the bioreactor troughs. It is possible that at the inflow location HRT and temperature were what significantly influenced bioreactor performance and gene copy numbers, however, throughout the

remainder of the bioreactor troughs another factor was likely limiting performance and gene copy numbers.

Nitrate Concentration

We found that with decreasing nitrate concentrations along the length of the bioreactor troughs (Figure 18) there was a decrease in 16S rRNA and certain denitrification functional genes, most consistently 16S, *nirK* and *nosZ* clade II (Figure 22; Figure 23; Figure 27; Figure 28; Figure 37; Figure 38). The gene copy numbers of these 16S rRNA and functional denitrifying genes were only significantly higher at the locations nearest the inlet of the bioreactor troughs, where nitrate concentrations were at their highest. This could indicate that high nitrate concentrations induced the growth of total bacteria as well as organisms carrying *nirK* and *nosZ* clade II genes. A study examining the effect of nitrate loads on transcripts per million (TPM) found that during high nitrate loading events, there were higher numbers of *nirK*, *nirS* and *nosZ* TPM, leading the authors to conclude that the higher nitrate concentrations induced the expression of these genes (Grießmeier et al., 2017). Another study showed that an increase in denitrification rates correlated to an increase in nitrate concentration (Mergel et al., 2001b). Nonetheless, the finding by Mergel et al. (2001b) does not necessarily correlate to higher abundance of denitrification functional genes. Two studies observed that an increase in nitrate concentration led to an increase in denitrification rates, but did not alter denitrifier abundance, subsequently suggesting that denitrification rates do not correlate to denitrifier abundance (Veraart et al., 2017; Wallenstein et al., 2006).

In contrast to the trends noted for 16S rRNA, *nirK* and *nosZ* clade II gene copy numbers, neither *nosZ* clade I nor *nirS* consistently nor significantly exhibited decreasing

gene copy numbers along the length of the bioreactor troughs. Both *nirS* and *nosZ* clade I were not substantially affected by changes in temperature, HRT and location (Figure 30; Figure 31; Figure 33; Appendix C: Additional Biological Data for Bioreactor Troughs; Figure 52; Figure 53; Figure 54; Figure 55; Figure 56). Interestingly, with decreasing nitrate concentrations along the length of the bioreactor troughs, *nirS* exhibited an increase in gene copy numbers (Figure 30; Figure 31), the opposite of what was noted for *nirK* (Figure 25; Figure 26; Figure 27; Figure 28). This could be further indication that there are distinct niches for *nirK* and *nirS* carrying organisms, possibly relating to the availability of nitrate.

If nitrate concentration was wholly responsible for driving gene abundance we would expect that when there were higher nitrate concentrations there would be higher gene copy numbers. Subsequently, at times and locations when there was higher nitrate we should have seen higher gene copy numbers, such as at the inflow location, and at 4-hour HRT and during the cool temperature (6°C, weeks 1-4) regime (when less nitrate removal occurred). While we see the first example occurring for 16S rRNA, *nirK* and *nosZ* clade II, it does not hold true for other instances when nitrate concentrations throughout the bioreactor troughs were relatively higher. Instead, the 12-hour HRT and warm temperature regime (14.5°C, weeks 9-12) most consistently had similar or higher gene abundances for 16S rRNA, *nirK* and *nosZ* clade II (Figure 20; Figure 22; Figure 25; Figure 27; Figure 35; Figure 37). One simple explanation for an increase in gene abundance during the warm temperature regime is that increasing temperatures have been documented to increase bacterial growth. Thus, with increasing temperatures, regardless of nitrate concentrations, there would be an increase in gene copy numbers. An increase in higher gene abundances

during longer HRT could be due to slower flow rates retaining electron donors (DOC) and e-acceptors (nitrate) in the system for longer. This would give the bacteria more time to utilize them for energy generation, which would result in higher energy yields per organisms and, thus, more growth.

Since we did not have 100% nitrate removal, nitrate was not likely to be limiting in our system (Schipper et al., 2010; Warneke et al., 2011c). Thus, it is just as possible that other chemical parameters were limiting functional denitrifying and 16S rRNA gene copy numbers and bioreactor performance. Our results suggest that the temperature, HRT and concentration of nitrate are not the only factors that are influencing functional and total bacterial gene copy numbers in the bioreactor troughs, but that other factors, such as DOC or DO might be further limiting the system.

DOC/C Availability

Carbon availability has been proposed to be one of the factors influencing bioreactor performance, along with nitrate concentration, temperature, HRT and DO (Christianson et al., 2012; Schipper et al., 2010). A study by Hassanpour et al. (2017) found that nitrate removal efficiency was determined by both temperature and DOC concentrations, which were also demonstrated to interact with one another (i.e.: higher temperatures led to higher decomposition rates, which subsequently led to higher DOC). It is likely that carbon was limiting in our system, particularly in the middle and outflow portions of the bioreactor troughs, as this was where a lack of effect of temperature and HRT were noted for 16S rRNA and *nosZ* clade II (Figure 20; Figure 22; Figure 35; Figure 37). Carbon availability has been noted to be one of the most important factors that shape and alter denitrification communities and affect bioreactor performance (Drenovsky et al.,

2004; Wallenstein et al., 2006; Fierer, 2017; Tiedje et al., 1983; Hassanpour et al., 2017). It has even been suggested to cause seasonal shifts in the microbial community (Porter et al., 2015). More specifically, a study performed by Veraart et al (2017) correlated *nirK* gene abundance to the amount of organic matter. Similarly, a study investigating bacterial gene abundances in agricultural ditches observed a positive correlation between 16S rRNA, *nirS* and *nosZ* clade I gene abundances and soil carbon (Baker et al., 2015). The latter study is of particular interest, as it demonstrates a correlation between carbon availability and two functional genes that were discovered to have lower abundances and exhibited less effect of temperature, HRT and location in our study (*nirS* and *nosZ* clade I) (Figure 30; Figure 31; Figure 33; Appendix C: Additional Biological Data for Bioreactor Troughs; Figure 52; Figure 53; Figure 54; Figure 55; Figure 56). This could indicate that *nosZ* clade I and *nirS* carrying organisms require much higher organic carbon than *nosZ* clade II carrying organisms. If carbon availability was limiting throughout the length of the bioreactor troughs we would expect to see little to no effect of other potential limiting factors, such as temperature, HRT and nitrate concentration, which was what was noted for *nirS* and *nosZ* clade II gene copy numbers. Furthermore, our PCA analysis indicates that DOC is not only correlated to nitrate removal efficiency, but also to our 16S rRNA and certain functional denitrifying gene copy numbers (Figure 39).

Nevertheless, our study does not include a hydraulic flow model that predicts DOC concentrations along the length of the bioreactor troughs, thus we are unable to draw direct comparisons between DOC concentrations and denitrifying functional and 16S rRNA gene copy numbers. Furthermore, we did not include an analysis of decomposing organisms, thus we are also unable to draw comparisons or interactions between denitrifiers and

heterotrophic organisms that are capable of degrading complex organic matter such as cellulose and lignocellulose. Because organic carbon has been demonstrated to substantially effect denitrifying communities, further investigation, not only on DOC concentrations throughout the length of the bioreactor troughs, but also on decomposing organisms at each sampling point would provide crucial insight into the complex interplay of biological and chemical factors that determine bioreactor performance. A study has shown an increase in methanogens under high nitrate loading events (Grießmeier et al., 2017). The authors also found that genes encoding cellulose degrading enzymes and *nir* and *nosZ* transcripts increased with increasing nitrate concentrations. This study, along with the results of our study, suggest an interesting interplay between nitrogen and carbon cycling organisms that warrants further research.

Dissolved Oxygen (DO)

The concentration of DO has also been postulated to be a potential limiting factor in denitrifying woodchip bioreactors (Schipper et al., 2010; Christianson et al., 2012). Because nitrate reduction is favored when oxygen is absent or in low concentrations, it seems logical that the less oxygen present in the bioreactors, the better the bioreactor performance and the greater the numbers of denitrifying functional genes. This, however, is not necessarily the case. A study has demonstrated a decrease in 16S rRNA, *nirK*, *nirS* and *nosZ* clade I gene copy numbers with decreasing DO availability in soil (Mergel et al., 2001b). While it might sound counter-intuitive, the authors explain that there is no selective advantage for denitrifiers in less oxygenated habitats because of the presence of anoxic microsites in the soil (Mergel et al., 2001a; Mergel et al., 2001b). With these anoxic microsites, denitrifying organisms, which require an organic carbon source, can be situated

in areas with a higher oxygen concentration which will promote the degradation of more complex carbon forms to simple monomer sugars and short chain fatty acid that are more readily utilized by denitrifiers. Thus, it is quite possible that denitrifier growth will be promoted in areas of slightly higher DO due to the degradation of recalcitrant carbon sources into more labile carbon forms by aerobic organisms. This is applicable to both soils and denitrifying bioreactors, particularly those containing biochar, as biochar has been demonstrated to provide not only a plethora of surface area for microorganism attachment, but also promotes the creation of microhabitats (Lehmann et al., 2011).

While we found that with increasing temperatures and increasing nitrate removal efficiency there was decreased DO, there was no significant change in DO. Because DO remained at low and consistent values throughout the length of the experiment it is not considered to have a great influence on the system (Warneke et al., 2011c). Furthermore, in our PCA analysis, DO was located opposite of denitrifying gene copy numbers and nitrate removal rate (Figure 39). Thus, it is unlikely that DO had a direct effect on denitrifying functional gene copy numbers or on the bioreactor performance. It is more likely that it had an indirect effect on the bioreactor community and performance by promoting or limiting carbon production.

Biochar

Biochar is a term that refers to many different forms of pyrolyzed feedstock. It has been described as charcoal, activated carbon, black carbon, as well as numerous other terms. While there are many different labels and qualities of pyrolyzed material that are considered a part of the biochar spectrum, the defining feature that qualifies charred, or pyrolyzed, feedstock as biochar is that the finished material is utilized as a soil amendment

(Cayuela et al., 2013; Gul et al., 2015). Biochar is typically made by pyrolysis, which is the thermal degradation of organic feedstock without the presence of oxygen at high temperatures (Lehmann et al., 2011). Recently, the incorporation of biochar into agricultural soil as a means to reduce nitrogen leachate and nitrous oxide emissions while increasing microbial activity, has caused a surge of interest on the possibility of incorporating biochar in denitrifying bioreactors (Bock et al., 2016; Pluer et al., 2016; Hassanpour et al., 2017).

Walnut shell biochar was included in all of our bioreactor troughs, thus the effect of biochar on our microbial community and on bioreactor performance cannot be determined. However, we can postulate some possible effects that the biochar might have incurred based on trends we observed and on other's research, particularly in regard to nitrous oxide emissions and denitrifying functional genes. An increase in relative abundance of *nosZ* clade I and clade II were noted over time with the presence of biochar in a study performed on agricultural soils amended with biochar (Harter, et al., 2016). The results in this study indicate that biochar can lead to a shift in the microbial community of soils. However, as discussed previously, the gene copy numbers for *nosZ* clade I and clade II in our bioreactor troughs were found to be within the typical range that other studies without biochar amendment have found. An increase in *nosZ* clade I and II was noted over time, however, whether this can be linked to the presence of biochar is doubtful as the temperature was increasing over time. Biochar has also been demonstrated to reduce the amount of nitrous oxide emissions from agricultural soils (Harter et al., 2016; Hagemann et al., 2017a; Cayuela et al., 2013; Lehmann et al., 2011). Harter et al. (2016) concluded this to be due to the biochar retaining more nitrous oxide than soils, which allowed for

increased microbial nitrous oxide reduction. Our bioreactors exhibited relatively low nitrous oxide emissions (Figure 14), which could be due to the retention of nitrous oxide to the biochar. With the nitrous oxide captured on the biochar there might be more opportunity for complete denitrification to take place, reducing nitrous oxide emissions and promoting the growth of organisms capable of nitrous oxide reduction (i.e.: *nosZ* clade I and II carrying organisms). This might also explain the greater abundance of *nosZ* clade II than clade I; with nitrous oxide entrapped on the biochar, organisms only capable of nitrous oxide reduction might have a distinct advantage.

Recently, several studies have incorporated biochar into denitrifying bioreactors to ascertain the effect it has on bioreactor performance. These studies have found that nitrate removal increases in the presence of biochar (Bock et al., 2016; Plier et al., 2016). This could be a consequence of nitrate sorption to the biochar or stimulation of the microorganisms within the bioreactor (Hagemann et al., 2017b; Lehmann et al., 2011). The removal rates in our study were within the expected range, but were on the high end of this range. This is notable considering that there was substantial removal even during our 4-hour HRT and cool temperature regime (6°C, weeks 1-4). Other studies that have maintained warmer temperatures (16-30°C) throughout the course of their experiments have frequently exhibited much lower nitrate removal rates (less than 2 g N m⁻³d⁻¹) (Addy et al., 2016; Schipper et al., 2010). This could be attributed to the biochar, as a study by Hassanpour et al. (2017) noted that field sites that had the highest influent nitrate concentrations showed a greater effect of biochar in removal rates than those with lower nitrate concentrations. Thus, with higher nitrate loading rates the presence or absence of biochar was observed to have a greater effect on bioreactor performance. This could

explain why nitrate removal was still considerable for the bioreactor troughs operated under 4-hour HRT and cool temperature regime. Nevertheless, the exact extent that the walnut shell biochar affected bioreactor performance and the denitrifying functional community cannot be determined because it was not included as an experimental condition. Further research into utilizing biochar, not only as a means to reduce nitrous oxide emissions, but also to reduce leachate from the reactors and retain organic carbon in the system is promising.

Outlook

While denitrifying bioreactors are being implemented in pollution reduction strategies in the United States, particularly in the Midwest (IL EPA, 2015; Iowa Nutrient Reduction Strategy, 2016; MPCA, 2014; USDA-NRCS, 2015), there is still a significant lack of understanding of the microbial processes that control and drive bioreactor performance. Our study sought to establish basic trends of 16S rRNA and denitrifying functional gene copy numbers and bioreactor performance and how these respond to changes in temperature and HRT. Further research should expand on our findings and seek to further elucidate not only the role of the denitrifying functional guild, but also carbon cycling organisms. Investigating the role of decomposing communities and what environmental factors influence them is an area of particular interest, as our study, along with others, have indicated that carbon might be a significant limiting factor in these reactors (Christianson et al., 2012; Feyereisen et al., 2016; Warneke et al., 2011c).

Future research on microbial communities in denitrifying bioreactors should investigate not only shifts within the functional communities, but should also investigate a possible relationship between nitrogen and carbon cycling organisms. One study found that during high nitrate loading events there were higher transcript numbers of *nirK*, *nirS* and *nosZ* clade I, along with an increase in methanogens and an increase in genes encoding cellulose degrading enzymes (Grießmeier et al., 2017). The authors concluded that there is a complex network of organisms that are involved in removing nitrate from agricultural runoff and that both denitrification and cellulose degradation are influenced by nitrate concentrations. Determining the existence and nature of a possible relationship between nitrogen and carbon cycling organisms in denitrifying bioreactors could greatly alter how

we approach the design and maintenance of these bioreactors as well as greatly enhance bioreactor performance.

Another area of future research is in utilizing compartment designs, such as those employed in Feyereisen et al. (2016). We suggest that the compartments include a combination of wood chips, a labile carbon source, such as corn cobs, and biochar. Using this combination could increase carbon availability, while also reducing the amount of carbon leachate. The labile carbon source would provide greater carbon availability, the woodchips would provide a longer-term source of carbon and the biochar would reduce carbon leaching by sorption of carbon onto its surface. Ideally, the biochar would be placed after the labile carbon source, not only to retain more carbon, but also to increase nitrate sorption, as biochar has been shown to have increased nitrate sorption when it is covered in a layer of organic carbon (Kammann et al., 2015).

The inclusion of biochar in denitrifying bioreactors has been demonstrated to reduce adverse conditions and increase bioreactor performance (Bock et al., 2016; Pluer et al., 2016; Hassanpour et al., 2017). While these studies indicate that biochar amendment in denitrifying bioreactors is beneficial to performance, they only consider the short-term effects. Studies done on biochar amendments in agricultural soils have indicated that biochar aging can significantly alter the effect it has (Spokas, 2013; Cayuela et al., 2013). Incorporating biochar into denitrifying bioreactor designs could alter the long-term performance, thus, investigating the longevity and long-term performance of biochar amended denitrifying bioreactors is imperative before full-scale application begins.

Further research on the application of these reactors in the field is also recommended. This is not only to ascertain if field applications are similar to laboratory applications in

terms of nitrate removal, but also whether the microbial community in the field is comparable to those of laboratory experiments. The potential for significantly different microbial communities between laboratory setups and in-field experiments is substantial, considering that laboratory experiments do not take into account the use of pesticides and varying forms of fertilizers. Studies on microbial communities in agricultural fields have shown to be significantly different based on the type of fertilizer used; more organic fertilizers usually show increased denitrification rates (Enwall et al., 2005) and higher 16S rRNA, *nirK*, *nirS* and *nosZ* clade I gene copy numbers (Hallin et al., 2009) than inorganic fertilizers. Subsequently, studying the effect that different types of fertilizer and pesticides might have and how they could alter microbial communities and influence bioreactor performance is another opportunity for future research.

Most recently there has been a push for having a more holistic approach in designing and maintaining denitrifying bioreactors. This includes considering the effect that highly reduced waters being released from denitrifying bioreactors might have on receiving waters (Christianson & Schipper, 2016), as well as utilizing denitrifying bioreactors in the field along with other nitrate mitigation strategies, such as constructed wetlands or drainage ditches with weirs (Baker et al., 2015). While this holistic approach is appealing to many researchers, the amount of land and money required to have an entire suite of nitrate mitigation strategies installed could act as a severe deterrent to many farmers.

Many authors have also called for the need to explore the ability of denitrifying bioreactors to remove other pollutants (Addy et al., 2016; Christianson & Schipper, 2016). Our reactors indicated the ability of denitrifying bioreactors to remove phosphate, consequently, expanding the uses of denitrifying bioreactors to include other pollutants

such as phosphate, pharmaceuticals and *E. coli* (fecal matter indicators) is recommended. Broadening the application of denitrifying bioreactors to include these other pollutants may lead to many exciting opportunities for further research and application of woodchip bioreactors into other fields.

Conclusion

It was found that higher temperatures (14.5°C) led to increased bioreactor performance, with an increase in nitrate removal efficiency and nitrate removal rate. Higher temperatures also resulted in higher 16S rRNA, and *nosZ* clade II gene copy numbers, however, this finding was only significant at the inflow locations of the bioreactor troughs. No significant effect of temperature was observed on *nirK*, *nirS* or *nosZ* clade I gene copy numbers. Increasing HRT led to increased nitrate removal efficiency, but also to a decrease in nitrate removal rate. The decrease in nitrate removal rate with longer HRT is most likely due to more nitrate being passed through the system at higher flow rates (shorter HRT). It was also found that HRT had a greater effect on nitrate removal efficiency than temperature, thus at cool temperatures (6°C) and short HRT, increasing HRT would increase bioreactor performance significantly more than by increasing the temperature. Conversely, temperature had a greater effect on bacterial communities than HRT, however both were observed to influence gene copy numbers at the inflow locations. Increased HRT led to higher gene copy numbers for 16S rRNA and *nosZ* clade II, but only at the inflow locations of the bioreactor troughs. No significant effect of HRT was observed on *nirK*, *nirS* or *nosZ* clade I gene copy numbers. Because no significant effect of both temperature and HRT were found on *nirK*, *nirS* and *nosZ* clade I gene copy numbers, it is concluded that these functional communities remain relatively stable through varying temperatures and HRTs, while total bacteria and *nosZ* clade II carrying organisms do not.

Utilizing a hydraulic flow model, decreasing nitrate concentrations along the length of the bioreactor troughs were predicted, correlating to decreasing 16S rRNA, *nirK* and *nosZ* clade II gene copy numbers, all of which were demonstrated to have a significant effect of

location. The highest values for nitrate and gene copy numbers were found at the inflow locations, while the lowest values were observed at the outflow locations. Conversely, no significant effect of location on *nirS* or *nosZ* clade I gene copy numbers was found. We postulate that we may be seeing niche differentiation between *nirK* and *nirS* along the length of the bioreactor, with *nirK* carrying organisms dominating the location nearest the inlet and *nirS* dominating the locations nearest the outlet. Because these two regions of the bioreactor correspond to higher and lower nitrate concentrations, respectively, it is possible that niche differentiation between the two nitrite reductase functional genes might be regulated by nitrate concentration. Location is concluded to have a greater effect on denitrifying functional gene copy numbers than HRT and temperature. Because 16S rRNA, *nirK* and *nosZ* clade II gene copy numbers only show a significant effect of temperature and HRT at the inflow location, it is suggested that there is another limiting factor at the middle and outflow portions of the bioreactor troughs. These gene copy numbers are most likely being limited by the presence or absence of a chemical parameter that is present in abundance or entirely absent at the inflow, particularly during the warm temperature regime and 12-hour HRT.

While nitrate concentrations have been considered to be the limiting factor in many other studies, our results indicate that this might not be the case. Nitrate is still present in abundance in the latter half of the bioreactor troughs when HRT and temperature are no longer limiting the removal of nitrate. Thus, it is possible that there is another factor that is limiting in the middle and outflow portions of the bioreactor troughs. Results from our PCA plot demonstrate that functional denitrifying gene copy numbers, HRT, temperature and DOC are all closely correlated to bioreactor performance. More recent studies have

also proposed that DOC might be a limiting factor in denitrifying woodchip bioreactors. This other limiting factor in our bioreactor troughs might be DOC based on the elimination of other factors, the close correlation of DOC in our PCA analysis and on the low concentrations of DOC observed in the effluent during our study. Future studies should investigate the interplay between nitrogen and carbon cycling microorganisms. We expect that decomposing organisms, not just denitrifiers, play a pivotal role in denitrifying bioreactors. Understanding the relationship between these two microbial communities could greatly enhance bioreactor performance.

References

- Addy, K., Gold, A. J., Christianson, L. E., David, M. B., Schipper, L. A., & Ratigan, N. A. (2016). Denitrifying bioreactors for nitrate removal: A meta-analysis. *Journal of Environmental Quality*, 45(3), 873-881.
- Andrus, J. M., Porter, M. D., Rodriguez, L. F., Kuehlhorn, T., Cooke, R. A., Zhang, Y., . . . Zilles, J. L. (2014). Spatial variation in the bacterial and denitrifying bacterial community in a biofilter treating subsurface agricultural drainage. *Microbial Ecology*, 67(2), 265-272.
- Baker, B., Kroger, R., Brooks, J., Smith, R., & Prince Czarnecki, J. (2015). Investigation of denitrifying microbial communities within an agricultural drainage system fitted with low-grade weirs. *Water Research*, 87, 193-201.
- Bell, N., Cooke, R. A., Olsen, T., David, M. B., & Hudson, R. (2015). Characterizing the performance of denitrifying bioreactors during simulated subsurface drainage events. *Journal of Environmental Quality*, 44(5), 1647-1656.
- Bock, E. M., Coleman, B., & Easton, Z. M. (2016). Effect of biochar on nitrate removal in a pilot-scale denitrifying bioreactor. *Journal of Environmental Quality*, 45(3), 762-771.
- Cameron, S. G., & Schipper, L. A. (2010). Nitrate removal and hydraulic performance of organic carbon for use in denitrification beds. *Ecological Engineering*, 36(11), 1588-1595.
- Cayuela, M. L., Sanchez-Monedero, M. A., Roig, A., Hanley, K., Enders, A., & Lehmann, J. (2013). Biochar and denitrification in soils: when, how much and why does biochar reduce N₂O emissions? *Scientific Reports*, 3, 1732.
- Christianson, L. E., & Schipper, L. A. (2016). Moving denitrifying bioreactors beyond proof of concept: Introduction to the special section. *Journal of Environmental Quality*, 45(3), 757-761.
- Christianson, L. E., Bhandari, A., & Helmers, M. J. (2012). A practice-oriented review of woodchip bioreactors for subsurface agricultural drainage. *Applied Engineering in Agriculture*, 28(6), 861-874.
- Cord-Ruwisch, R. (1985). A quick method for the determination of dissolved and precipitated sulfides in cultures of sulfate-reducing bacteria. *Journal of Microbiological Methods*, 4(1), 33-36.
- Cornelissen, G., Rutherford, D. W., Arp, H. H., Dorsch, P., Kelly, C. N., & Rostad, C. E. (2013). Sorption of pure N₂O to biochars and other organic and inorganics materials under anhydrous conditions. *Environmental Science and Technology*, 47(14), 7704-7712.
- David, M. B., Gentry, L. E., Cooke, R. A., & Herbstritt, S. M. (2016). Temperature and substrate control woodchip bioreactor performance in reducing tile nitrate loads in east-central Illinois. *Journal of Environmental Quality*, 45(3), 822-829.
- Drenovsky, R. E., Vo, D., Graham, J., & Scow, K. M. (2004). Soil and water content and organic carbon availability are major determinants of soil microbial community composition. *Microbial Ecology*, 48(3), 424-430.
- Ennis, C. J., Evans, A. G., Islam, M., Ralebitso-Senior, T. K., & Senior, E. (2012). Biochar: Carbon sequestration, land remediation, and impacts on soil microbiology. *Critical Reviews in Environmental Science and Technology*, 42(22), 2311-2364.

- Enwall, K., Philippot, L., & Hallin, S. (2005). Activity and composition of the denitrifying bacterial community respond differently to long-term fertilization. *Applied and Environmental Microbiology*, 71(12), 8335-8343.
- Feyereisen, G. W., Moorman, T. B., Christianson, L. E., Venterea, R. T., Coulter, J. A., & Tschirner, U. W. (2016). Performance of agricultural residue media in laboratory denitrifying bioreactors at low temperatures. *Journal of Environmental Quality*, 45(3), 779-787.
- Fierer, N. (2017). Embracing the unknown: Disentangling the complexities of the soil microbiome. *Nature Reviews Microbiology*, 15(10), 579.
- Galloway, J. N., Townsend, A. R., Erismann, J. W., Bekunda, M., Cai, Z., Freney, J. R., . . . Sutton, M. A. (2008). Transformation of the nitrogen cycle: Recent trends, questions, and potential solutions. *Science*, 320(5878), 889-892.
- Gibert, O., Pomierny, S., Rowe, I., & Kalin, R. M. (2008). Selection of organic substrates as potential reactive materials for use in a denitrification permeable reactive barrier (PRB). *Bioresource Technology*, 99(16), 7587-7596.
- Greenan, C. M., Moorman, T. B., Parkin, T. B., Kaspar, T. C., & Jaynes, D. B. (2009). Denitrification in wood chip bioreactors at different water flows. *Journal of environmental quality*, 38(4), 1664-1671.
- Greenan, C. M., Moormans, T. B., Kaspar, T. C., Parkin, T. B., & Jaynes, D. B. (2006). Comparing carbon substrates for denitrification of subsurface drainage water. *Journal of Environmental Quality*, 35(3), 824-829.
- Grießmeier, V., Bremges, A., McHardy, A. C., & Gescher, J. (2017). Investigation of different nitrogen reduction routes and their key microbial players in wood chip-driven denitrification beds. *Scientific Reports*, 7(1), 17028.
- Gul, S., Whalen, J. K., Thomas, B. W., Sachdeva, V., & Deng, H. (2015). Physico-chemical properties and microbial responses in biochar-amended soils: Mechanisms and future directions. *Agriculture Ecosystems and Environment*, 206, 46-59.
- Hagemann, N., Harter, J., Kaldamukova, R., Guzman-Bastante, I., Ruser, R., Graeff, S., . . . Behrens, S. (2017). Does soil aging affect the N₂O mitigation potential of biochar? a combined microcosm and field study. *GCB Bioenergy*, 9(5), 953-964.
- Hagemann, N., Kammann, C. I., Schmidt, H.-P., Kappler, A., & Behrens, S. (2017). Nitrate capture and slow release in biochar amended compost and soil. *PloS One*, 12(2), e0171214.
- Hallin, S., Jones, C. M., Schlöter, M., & Philippot, L. (2009). Relationship between N-cycling communities and ecosystem functioning in a 50-year-old fertilization experiment. *ISME Journal*, 3(5), 597-605.
- Harter, J., Guzman-Bustamante, I., Kuehfuss, S., Ruser, R., Well, R., Spott, O., . . . Behrens, B. (2016). Gas entrapment and microbial N₂O reduction reduce N₂O emissions from a biochar-amended sandy clay loam soil. *Scientific Reports*, 6, 39574.
- Harter, J., Weigold, P., El-Hadidi, M., Huson, D. H., Kappler, A., & Behrens, S. (2016). Soil biochar amendment shapes the composition of N₂O-reducing microbial communities. *Science of the Total Environment*, 562, 379-390.

- Hassanpour, B., Giri, S., Plier, W. T., Steenhuis, T. S., & Geohring, L. D. (2017). Seasonal performance of denitrifying bioreactors in the Northeastern United States: Field trials. *Journal of Environmental Management*, 202, 242-253.
- Hathaway, S. K., Porter, M. D., Rodriguez, L. F., Kent, A. D., & Zilles, J. L. (2015). Impact of the contemporary environment on denitrifying bacterial communities. *Ecological Engineering*, 82, 469-473.
- Henry, S., Baudoin, E., Lopez-Gutierrez, J. C., Martin-Laurent, F., Brauman, A., & Philippot, L. (2004). Quantification of denitrifying bacteria in soils by nirK gene targeted real-time PCR. *Journal of Microbiological Methods*, 59(3), 327-335.
- Henry, S., Bru, D., Stres, S., Hallet, S., & Philippot, L. (2006). Quantitative detection of the nosZ gene, encoding nitrous oxide reductase, and comparison of the abundances of 16S rRNA, narG, nirK, and nosZ genes in soils. *Applied and Environmental Microbiology*, 72(8), 5181-5189.
- Hoover, N. L., Bhandari, A., Soupir, M. L., & Moorman, T. B. (2016). Woodchip denitrification bioreactors: Impact of temperature and hydraulic retention time on nitrate removal. *Journal of Environmental Quality*, 45(3), 803-812.
- IL EPA. (2015). *Illinois Nutrient Reduction Strategy*. Chicago: Illinois Environmental Protection Agency. Retrieved November 12, 2017, from www.epa.illinois.gov/topics/water-quality/watershed-management/excess-nutrients/index
- Iowa Nutrient Reduction Strategy. (2016). *A science and technology-based framework to assess and reduce nutrients to Iowa waters and the Gulf of Mexico*. Ames, Iowa: Iowa Department of Agriculture and Land Stewardship, Iowa Department of Natural Resources, Iowa State University College of Agriculture and Life Sciences. Retrieved November 12, 2017, from <http://www.nutrientstrategy.iastate.edu/documents>
- Jones, C. M., Graf, D. D., Bru, D., Philippot, L., & Hallin, S. (2013). The unaccounted yet abundant nitrous oxide-reducing microbial community: A potential nitrous oxide sink. *ISME Journal*, 7(2), 417-426.
- Kammann, C. I., Schmidt, H.-P., Messerschmidt, N., Linsel, S., Steffens, D., Muller, C., . . . Joseph, S. (2015). Plant growth improvement mediated by nitrate capture in co-composted biochar. *Scientific Reports*, 5, srep11080.
- Kandeler, E., Deiglmayr, K., Tschirko, D., Bru, D., & Philippot, L. (2006). Abundance of narG, nirS, nirK, and nosZ genes of denitrifying bacteria during primary successions of a glacier foreland. *Applied and Environmental Microbiology*, 72(9), 5957-5962.
- Knobeloch, L., Salna, B., Hogan, A., & Anderson, H. (2000). Blue babies and nitrate-contaminated well water. *Environmental Health Perspectives*, 108(7), 675-678.
- Kraft, B., Tegetmeyer, H. E., Sharma, R., Klotz, M. G., Ferdelman, T. G., Hettich, R. L., . . . Strous, M. (2014). The environmental controls that govern the end product of bacterial nitrate respiration. *Science*, 345(6197), 676-679.
- Krause Camilo, B., Matzinger, A., Litz, N., Tedesco, L. P., & Wessolek, G. (2013). Concurrent nitrate and atrazine retention in bioreactors of straw and bark mulch at short hydraulic residence times. *Ecological Engineering*, 55, 101-113.

- Krider, L. A. (2018). Novel best management practices for improving water quality in midwestern agricultural settings: field and lab applications. St. Paul, Minnesota: The University of Minnesota.
- Lehmann, J., Rillig, M. C., Thies, J., Masiello, C. A., Hockaday, W. C., & Crowley, D. (2011). Biochar effects on soil biota - A review. *Soil Biology and Biochemistry*, 43(9), 1812-1836.
- Lepine, C., Christianson, L., Sharrer, K., & Summerfelt, S. (2016). Optimizing hydraulic retention times in denitrifying woodchip bioreactors treating recirculating aquaculture system wastewater. *Journal of Environmental Quality*, 45(3), 813-8221.
- Mergel, A., Kloos, K., & Bothe, H. (2001a). Seasonal fluctuations in the population of denitrifying and N₂-fixing bacteria in an acid soil of a Norway spruce forest. *Plant and Soil*, 230(1), 145-160.
- Mergel, A., Schmitz, O., Mallmann, T., & Bothe, H. (2001b). relative abundance of denitrifying and dinitrogen-fixing bacteria in layers of a forest soil. *FEMS Microbiology Ecology*, 36(1), 33-42.
- Moorman, T. B., Parkin, T. B., Kaspar, T. C., & Jaynes, D. B. (2010). Denitrification activity, wood loss, and N₂O emissions over 9 years from a wood chip bioreactor. *Ecological Engineering*, 36(11), 1567-1574.
- MPCA. (2010, November 12). *Aquatic life water quality standards technical support document for nitrate. Triennial water quality standard amendments to Minn. R. chs 7050 and 7052 DRAFT for external review*. Retrieved March 6, 2018, from Minnesota Pollution Control Agency: <https://www.pca.state.mn.us/sites/default/files/wq-s6-13.pdf>
- MPCA. (2013). *Nitrogen in Minnesota Surface Waters*. Retrieved November 17, 2017, from Minnesota Pollution Control Agency: <http://www.pca.state.mn.us/index.php/viewdocument.html?gid=19623>
- MPCA. (2014). The Minnesota nutrient reduction strategy. Saint Paul, Minnesota: Minnesota Pollution Control Agency. Retrieved November 12, 2017, from <https://www.pca.state.mn.us/sites/default/files/wq-s1-80.pdf>
- Muyzer, G., De Waal, E. C., & Uitterlinden, A. G. (1993). Profiling of complex microbial populations by denaturing gradient gel electrophoresis analysis of polymerase chain reaction-amplified genes coding for 16S rRNA. *Applied and Environmental Microbiology*, 59(3), 695-700.
- Office of the Revisor of Statutes. (2017, December 14). *Specific water quality standards for class 2 waters of the state; aquatic life and recreation*. Retrieved March 6, 2018, from Minnesota Administrative Rules: <https://www.revisor.mn.gov/rules/?id=7050.0222>
- Philippot, L., Hallin, S., & Schlöter, M. (2007). Ecology of denitrifying prokaryotes in agricultural soil. *Advances in Agronomy*, 96, 249-305.
- Pluer, W. T., Geohring, L. D., Steenhuis, T. S., & Walter, M. T. (2016). Controls influencing the treatment of excess agricultural nitrate with denitrifying bioreactors. *Journal of Environmental Quality*, 45(3), 772-778.
- Porter, M. D., Andrus, M. J., Bartolero, N. A., Rodriguez, L. F., Zhang, Y., Zilles, J. L., & Kent, A. D. (2015). Seasonal patterns in microbial community composition in denitrifying bioreactors treating subsurface agricultural drainage. *Microbial Ecology*, 70(3), 710-723.

- Randall, G. W., & Sawyer, J. E. (2008). Chapter 6: Nitrogen Application Timing, Forms, and Additives Final Report. In *Gulf Hypoxia and Local Water Quality Concerns Workshop*. St. Joseph, MI: ASABE.
- Robertson, W. D. (2010). Nitrate removal rates in woodchip media of varying age. *Ecological Engineering*, 36(11), 1581-1587.
- Schindler, D. W. (1974). Eutrophication and recovery in experimental lakes: implications for lake management. *Science*, 184(4139), 897-899.
- Schipper, L. A., Robertson, W. D., Gold, A. J., Jaynes, D. B., & Cameron, S. C. (2010). Denitrifying bioreactors - an approach for reducing nitrate loads to receiving waters. *Ecological Engineering*, 36(11), 1532-1543.
- Smith, J., Wagner-Riddle, C., & Dunfield, K. (2010). Season and management related changes in the diversity of nitrifying and denitrifying bacteria over winter and spring. *Applied Soil and Ecology*, 44(2), 138-146.
- Spokas, K. A. (2013). Impact of field aging on laboratory greenhouse gas production potentials. *GCB Bioenergy*, 5(2), 165-176.
- Thomson, A. J., Giannopoulos, G., Pretty, J., Baggs, E. M., & Richardson, D. J. (2012). Biological sources and sinks of nitrous oxide and strategies to mitigate emissions. *Philosophical Transactions of the Royal Society B*, 367, 1157-1168.
- Tiedje, J. M., Sextstone, A. J., Myrold, D. D., & Robinson, J. A. (1983). Denitrification: Ecological niches, competition and survival. *Antonie van Leeuwenhoek*, 48(6), 569-583.
- U.S. Environmental Protection Agency. (1982). Methods of Preservation. In *Sampling and Sampling Preservation of Water and Wastewater* (pp. 368-393). Cincinnati, Ohio: U.S. E.P.A.
- US EPA. (2017, November 12). *National Primary Drinking Water Regulations*. Retrieved from United States Environmental Protection Agency: <https://www.epa.gov/ground-water-and-drinking-water/national-primary-drinking-water-regulations>
- USDA-NRCS. (2015). *Conservation practice standard denitrifying bioreactor code 605*. Washington DC: United States Department of Agriculture - Natural Resources Conservation Strategy.
- Veraart, A. J., Dimitrov, M. R., Schrier-Uijl, A. P., Smidt, H., & de Klein, J. J. (2017). Abundance, activity and community structure of denitrifiers in drainage ditches in relation to sediment characteristics, vegetation and land-use. *Ecosystems*, 20(5), 928-943.
- Wallenstein, M. D., Myrold, D. D., Firestone, M., & Voytek, M. (2006). Environmental controls on denitrifying communities and denitrification rates: Insights from molecular methods. *Ecological Applications*, 16(6), 2143-2152.
- Warneke, S., Schipper, L. A., Bruesewitz, D. A., & Baisden, W. T. (2011). A comparison of different approaches for measuring denitrification rates in a nitrate removing bioreactor. *Water Research*, 45(14), 4141-4151.
- Warneke, S., Schipper, L. A., Bruesewitz, D. A., McDonald, I., & Cameron, S. (2011c). Rates, controls and potential adverse effects of nitrate removal in a denitrification bed. *Ecological Engineering*, 37(3), 511-522.

- Warneke, S., Schipper, L. A., Matiassek, M. G., Scow, K. M., Cameron, S., Bruesewitz, D. A., & McDonald, I. R. (2011b). Nitrate removal, communities of denitrifiers and adverse effects in different carbon substrates for use in denitrification beds. *Water Research*, 45(17), 5463-5475.
- Wolsing, M., & Prieme, A. (2004). Observation of high seasonal variation in community structure of denitrifying bacteria in arable soil receiving artificial fertilizer and cattle manure by determining T-RFLP of nir gene fragments. *FEMS Microbiology Ecology*, 48(2), 261-271.

Appendix A: Walnut Shell Biochar Characterization

Table 7: Walnut shell biochar physical and chemical properties along with recommendations from the International Biochar Initiative (IBI) and the European Biochar Certificate (EBC).

Property	Unit	Walnut shell biochar	IBI	EBC
pH _{CaCl2} *		6.6		≤10
C _{total}	%	87.6		>50
C _{org}	%	87.6	≥10	
C _{inorg}	%	<0.1		
C _{fixed}	%	83.5		
N _{total}	%	0.44		
C _{org} /N	%	199		
H	%	2.85		
O	%	7.5		
H:C _{org}		0.39	<0.7	<0.7
O:C		0.064		<0.4
Ash ₅₅₀	%	1.9		
Ash ₈₁₅	%	1.6		
EC*	μS/cm	116		
SA	m ² /g	0.6264		
Ca	mg/kg	1400		
Fe	mg/kg	1700		
K	mg/kg	5000		
Mg	mg/kg	360		
B	mg/kg	5		
Cd	mg/kg	<0.2	1.4-39	<1.5
Cr	mg/kg	2	64-1200	<90
Cu	mg/kg	11	63-1500	<100
Hg	mg/kg	<0.07	1-17	<1
Mn	mg/kg	27		
As	mg/kg	<0.8	12-100	<13
Na	mg/kg	65		
Ni	mg/kg	1	47-600	<50
P	mg/kg	480		
Pb	mg/kg	3	70-500	<150
S	mg/kg	110		
Si	mg/kg	270		
Zn	mg/kg	5	200-7000	<400
PAHs	mg/kg	162	6-300	<12

all measurements are taken from dry basis unless otherwise noted

*measured using samples as received

IBI: International Biochar Initiative. Maximum threshold range is determined by the soil tolerance level of application.

EBC: European Biochar Certificate

SA: specific surface area (BET)

EC: electrical conductivity

PAHs: sum of EPA's 16 listed PAHs

Appendix B: Additional Chemical Parameters of Bioreactor Troughs

DO

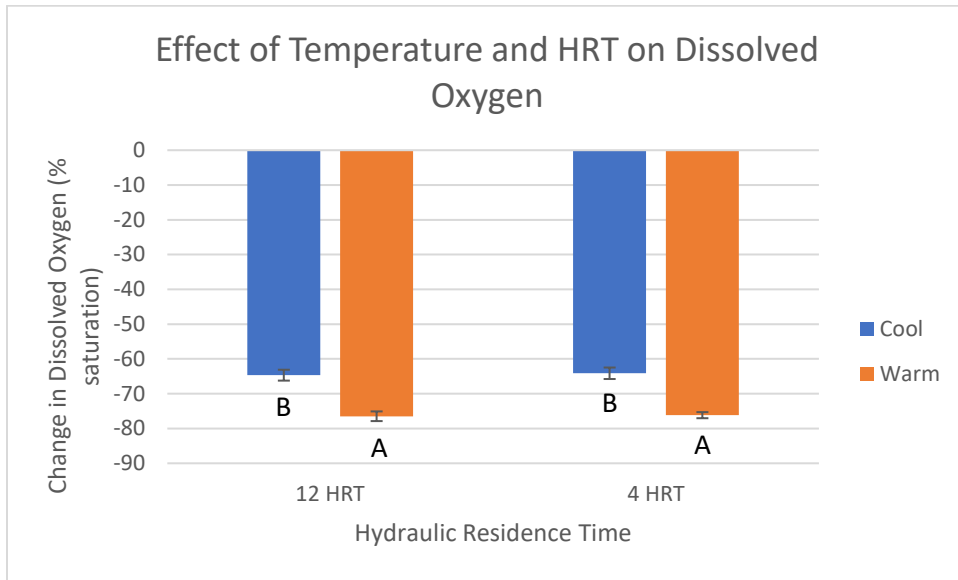


Figure 43: Effect of temperature and hydraulic residence time (HRT) on the change in dissolved oxygen (DO). Change in DO saturation was calculated by subtracting daily influent values from daily effluent values for each bioreactor trough and obtaining the average of these values across the different temperature and HRT treatments. Identical letters indicate no significant difference, while different letters denote a significant difference (two-way ANOVA; $p < 0.05$).

ORP

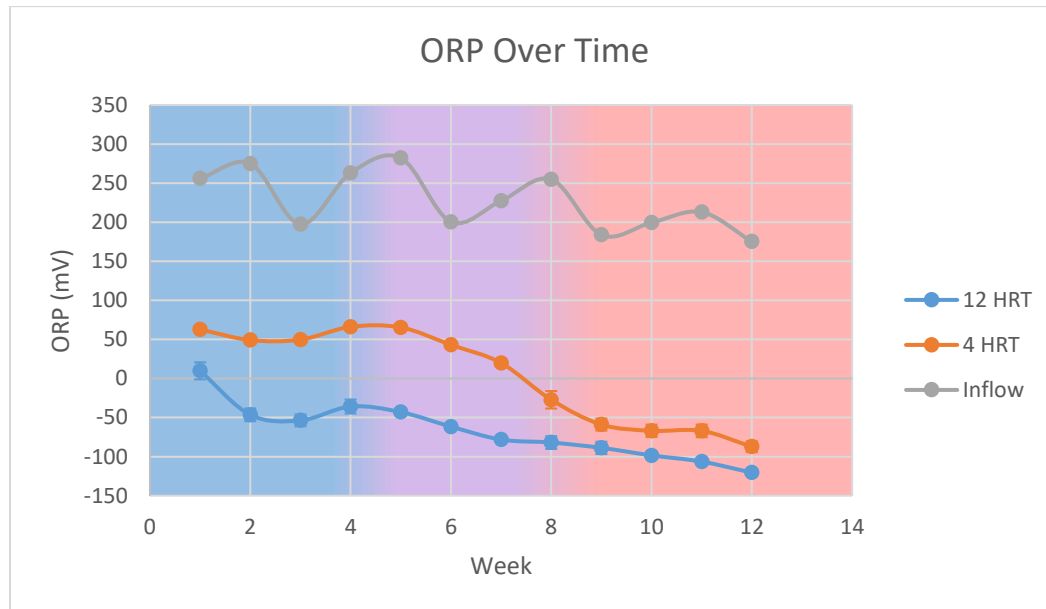


Figure 44: Oxidative-reductive potential (ORP) over time for inflow, 12-hour and 4-hour hydraulic residence time (HRT). Temperature regime is indicated by background color. Blue indicates cool (6°C weeks 1-4), purple designates warming (+2.1°C each week, weeks 5-8) and red denotes warm (14.5°C, weeks 9-12) temperature regime.

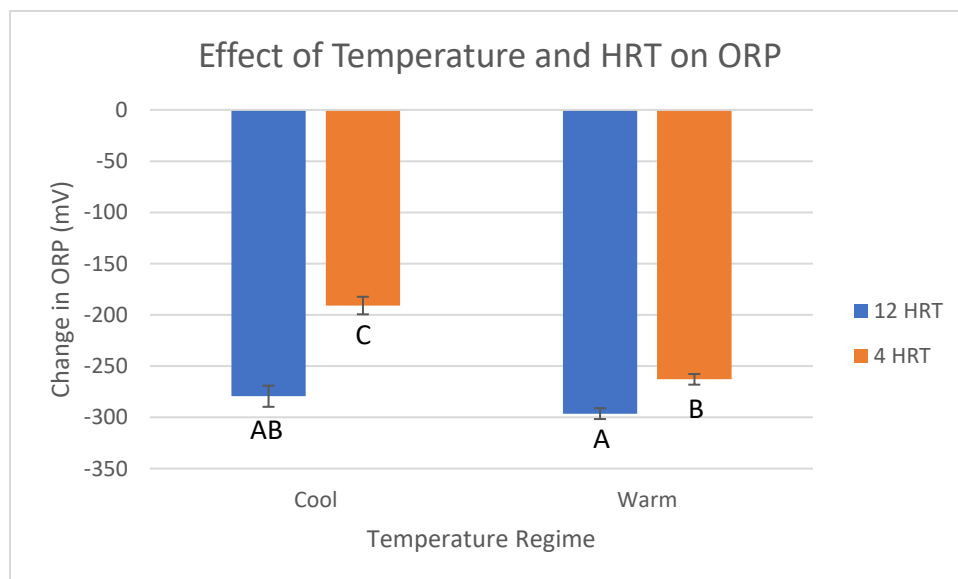


Figure 45: Effect of temperature and hydraulic residence time (HRT) on the change in oxidative-reductive potential (ORP) for 12-hour and 4-hour HRT for both cool (6°C, weeks 1-4) and warm (14.5°C, weeks 9-12) temperature regimes. Change in ORP was calculated by subtracting daily influent values from daily effluent values for each bioreactor trough and obtaining the average of these values across the different temperature and HRT

treatments. Identical letters indicate no statistically significant difference, different letters denote statistical significance (two-way ANOVA; $p < 0.05$).

pH

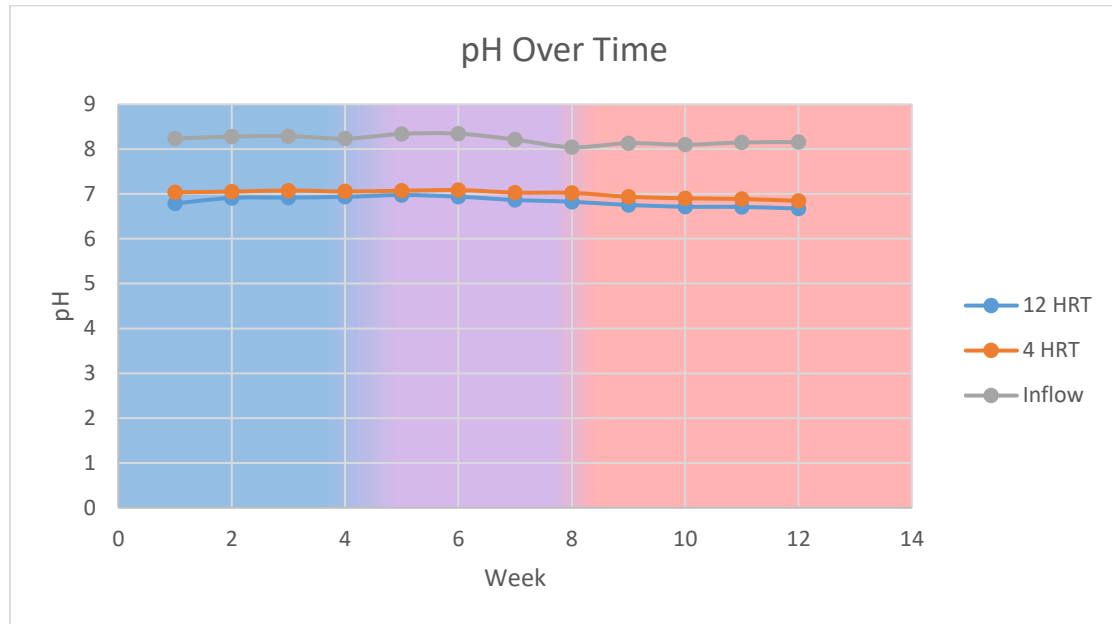


Figure 46: pH over time for 12-hour and 4-hour hydraulic residence time (HRT) and influent. Temperature regime is indicated by background color. Blue indicates cool (6°C weeks 1-4), purple designates warming ($+2.1^{\circ}\text{C}$ each week, weeks 5-8) and red denotes warm (14.5°C , weeks 9-12) temperature regime.

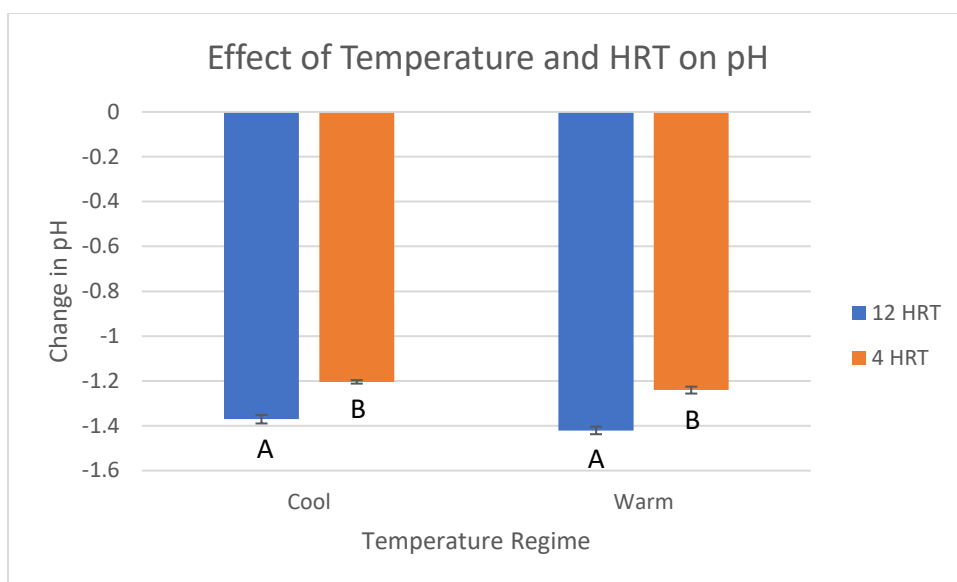


Figure 47: Effect of temperature and hydraulic residence time (HRT) on the change of pH for 12-hour and 4-hour HRT for cool (6°C, weeks 1-4) and warm (14.5°C, weeks 9-12) temperature regimes. Change in pH was calculated by subtracting daily influent values from daily effluent values for each bioreactor trough and obtaining the average of these values across the different temperature and HRT treatments. Different letters indicate a significant difference; identical letters do not (two-way ANOVA; $p < 0.05$).

Ammonia

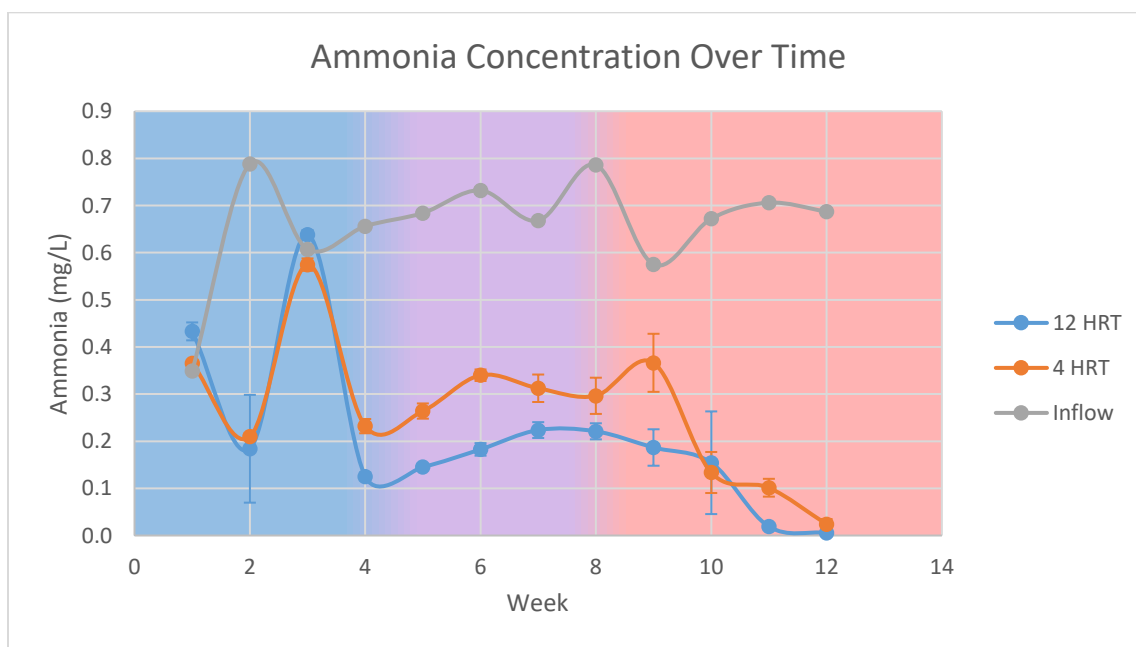


Figure 48: Ammonia concentration over time for inflow, 12-hour HRT and 4-hour hydraulic residence time (HRT). Temperature regime is indicated by background color.

Blue indicates cool (6°C weeks 1-4), purple designates warming ($+2.1^{\circ}\text{C}$ each week, weeks 5-8) and red denotes warm (14.5°C , weeks 9-12) temperature regime.

Nitrite

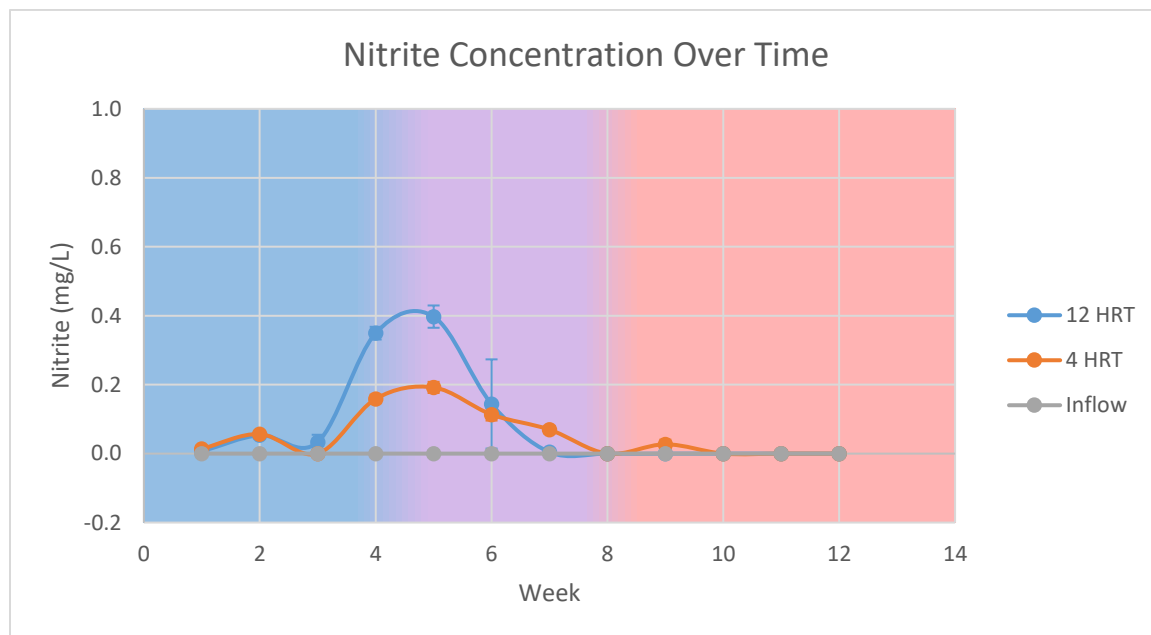


Figure 49: Nitrite concentration over time for inflow, 12-hour and 4-hour hydraulic residence time (HRT). Background color indicates temperature regime. Blue indicates cool (6°C weeks 1-4), purple designates warming ($+2.1^{\circ}\text{C}$ each week, weeks 5-8) and red denotes warm (14.5°C , weeks 9-12) temperature regime.

Sulfide

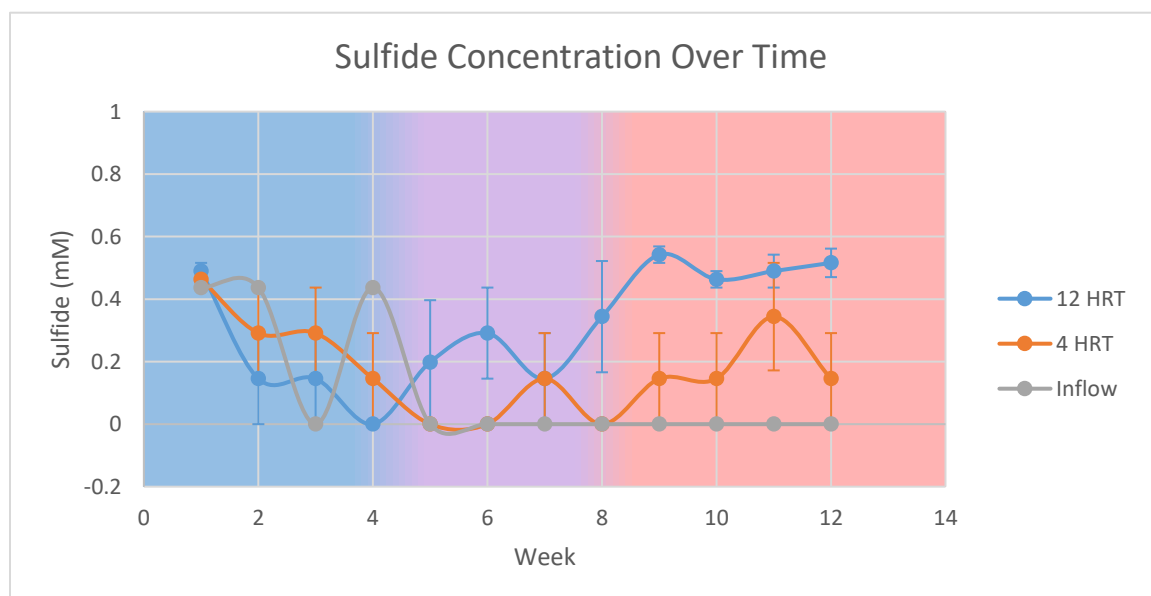


Figure 50: Sulfide concentration over time for inflow, 12-hour and 4-hour hydraulic residence time (HRT). Temperature regime is indicated by background color. Blue indicates cool (6°C weeks 1-4), purple designates warming (+2.1°C each week, weeks 5-8) and red denotes warm (14.5°C, weeks 9-12) temperature regime.

Methane

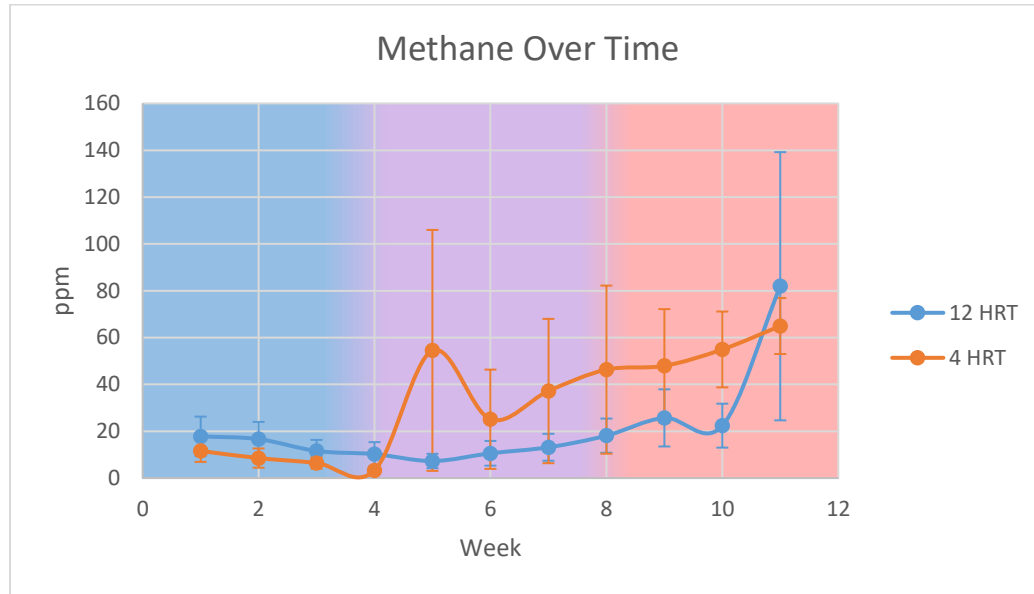


Figure 51: Methane concentration over time for 12-hour and 4-hour hydraulic residence time (HRT). Temperature regime is indicated by background color. Blue indicates cool (6°C weeks 1-4), purple designates warming (+2.1°C each week, weeks 5-8) and red denotes warm (14.5°C, weeks 9-12) temperature regime.

Appendix C: Additional Biological Data for Bioreactor Troughs

nirS

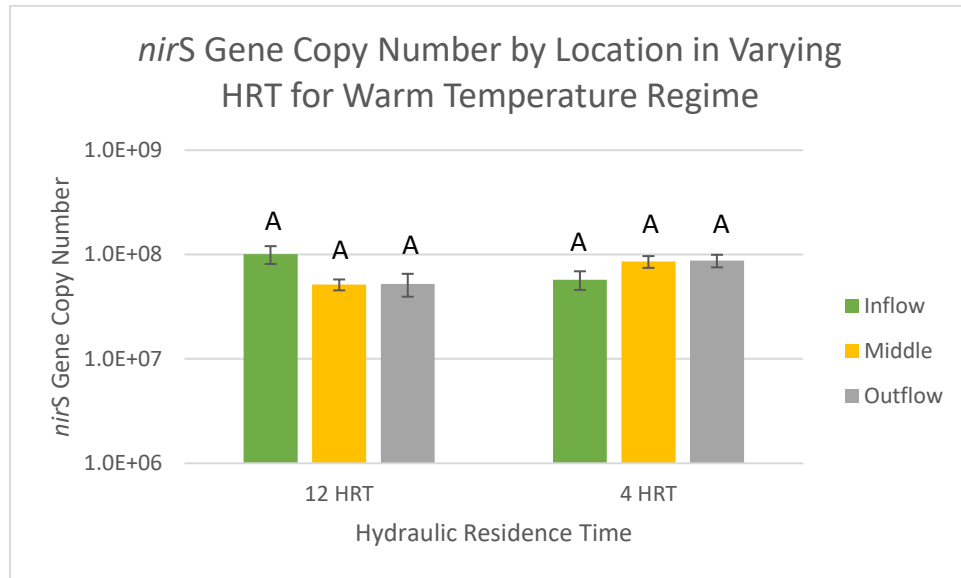


Figure 52: Effect of location and hydraulic residence time (HRT) on *nirS* gene copy numbers during the warm (14.5°C, weeks 9-12) temperature regime for 12-hour and 4-hour HRT and for inflow, middle and outflow sampling locations. Identical letters indicate no statistically significant difference, different letters denote statistical significance (two-way ANOVA; $p < 0.05$).

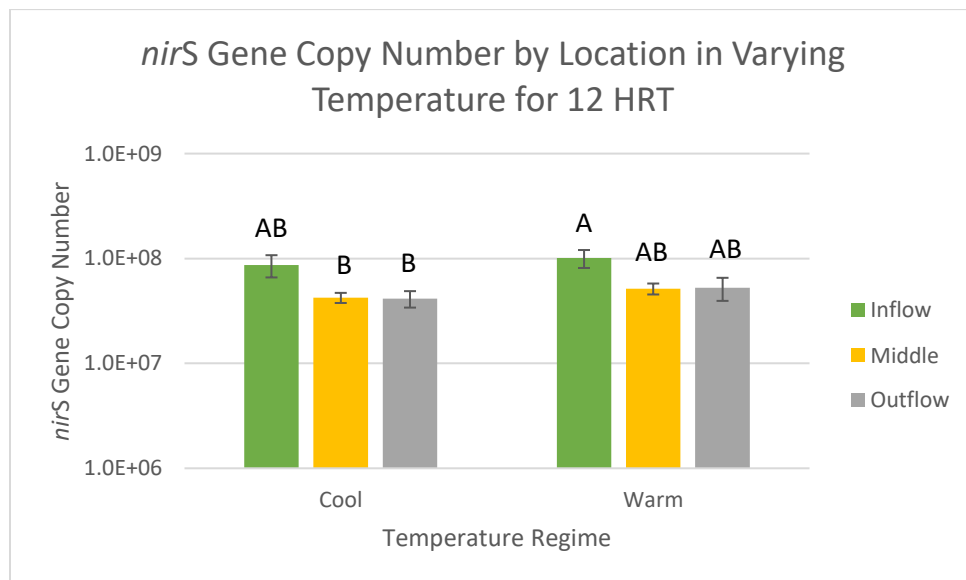


Figure 53: Effect of location and temperature regime on *nirS* gene copy numbers during 12-hour hydraulic residence time (HRT) for cool (6°C, weeks 1-4) and warm (14.5°C, weeks 9-12) temperature regimes and for inflow, middle and outflow sampling locations.

Identical letters indicate no statistically significant difference, different letters denote statistical significance (two-way ANOVA; $p < 0.05$).

nosZ Clade I

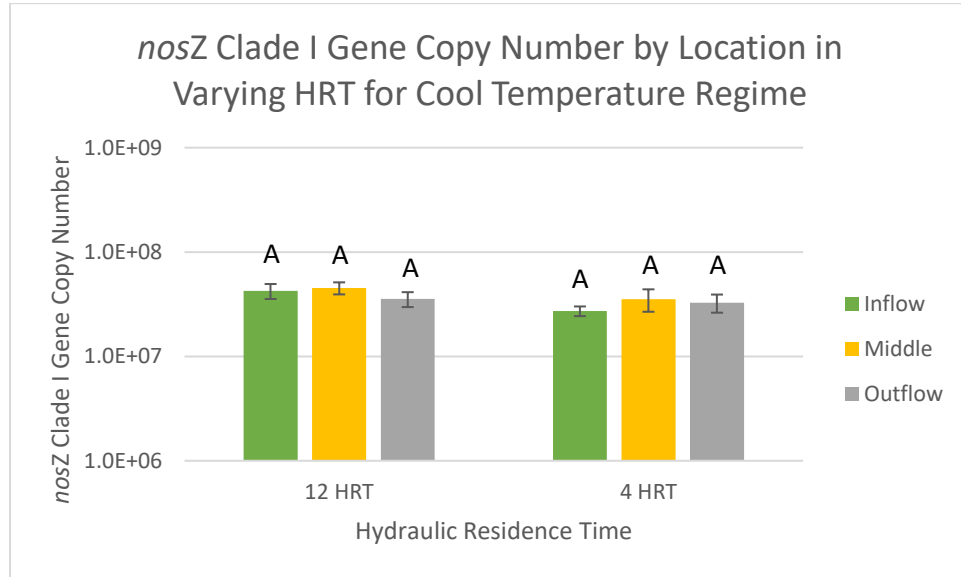


Figure 54: Effect of location and hydraulic residence time (HRT) on *nosZ* clade I gene copy numbers during the cool (6°C, weeks 1-4) temperature regime for 12-hour and 4-hour HRT and for inflow, middle and outflow sampling locations. Identical letters indicate no statistically significant difference, different letters denote statistical significance (two-way ANOVA; $p < 0.05$).

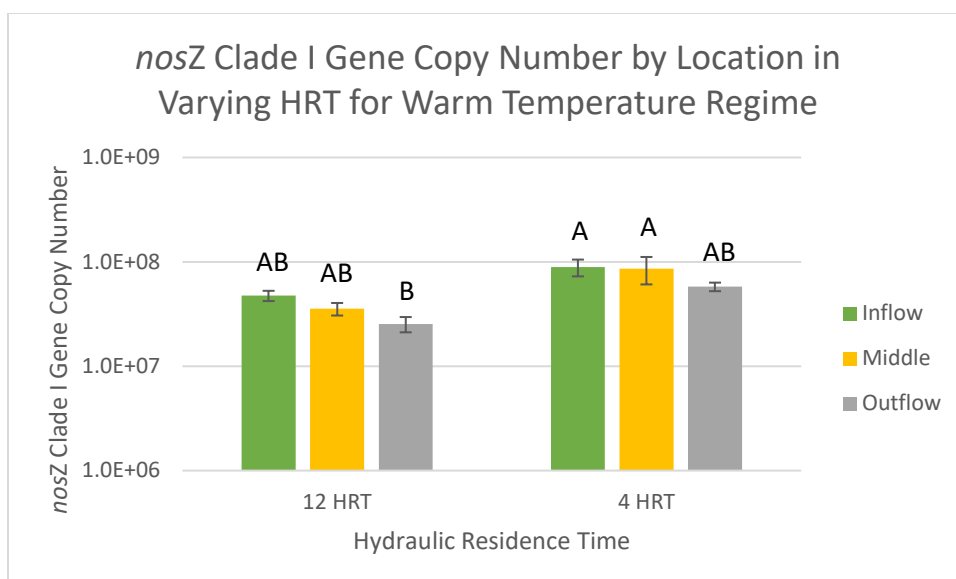


Figure 55: Effect of location and hydraulic residence time (HRT) on *nosZ* clade I gene copy numbers during the warm (14.5°C, weeks 9-12) temperature regime for 12-hour and 4-hour HRT and for inflow, middle and outflow sampling locations. Identical letters indicate no statistically significant difference, different letters denote statistical significance (two-way ANOVA; $p < 0.05$).

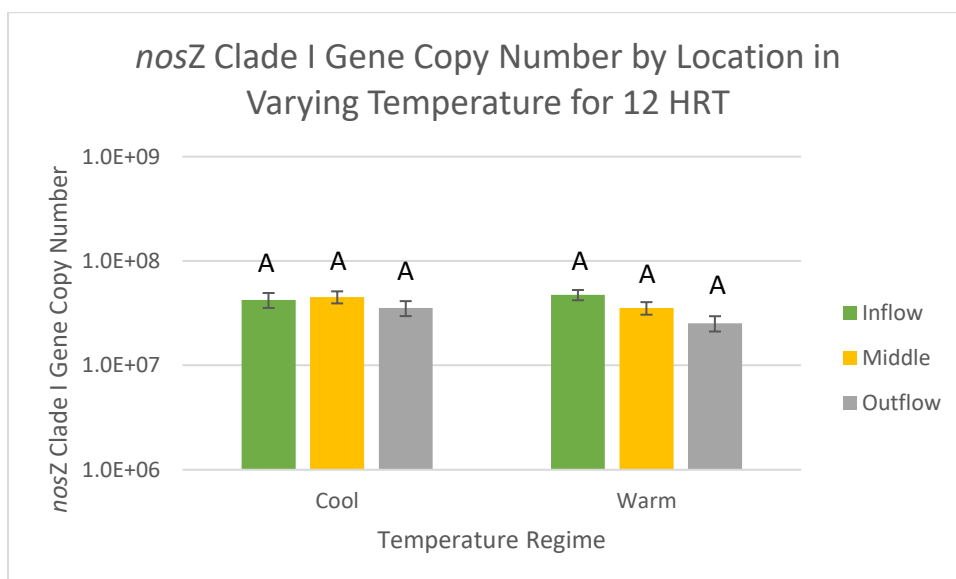


Figure 56: Effect of location and temperature regime on *nosZ* clade I gene copy numbers during 12-hour hydraulic residence time (HRT) for cool (6°C, weeks 1-4) and warm (14.5°C, weeks 9-12) temperature regimes and for inflow, middle and outflow sampling locations. Identical letters indicate no statistically significant difference, different letters denote statistical significance (two-way ANOVA; $p < 0.05$).